

UC Riverside

UC Riverside Electronic Theses and Dissertations

Title

Genome-Scale Investigation of Integrated Nuclear and Cytoplasmic Gene Regulatory Control in Arabidopsis

Permalink

<https://escholarship.org/uc/item/5t76q98p>

Author

Lee, Travis

Publication Date

2018

Copyright Information

This work is made available under the terms of a Creative Commons Attribution-NonCommercial-NoDerivatives License, available at <https://creativecommons.org/licenses/by-nc-nd/4.0/>

Peer reviewed|Thesis/dissertation

UNIVERSITY OF CALIFORNIA
RIVERSIDE

Genome-Scale Investigation of Integrated Nuclear and Cytoplasmic Gene
Regulatory Control in *Arabidopsis*

A Dissertation submitted in partial satisfaction
of the requirements for the degree of

Doctor of Philosophy

in

Plant Biology

by

Travis Andrew Lee

June 2018

Dissertation Committee:

Dr. Julia Bailey-Serres, Chairperson

Dr. Sean Cutler

Dr. Thomas Eulgem

Copyright by
Travis Andrew Lee
2018

The Dissertation of Travis Andrew Lee is approved:

Committee Chairperson

University of California, Riverside

Acknowledgements

I would like to thank my mentor Julia Bailey-Serres for her willingness to go out on a limb and accept a PhD student, a heavy commitment, directly into her laboratory with limited knowledge of the student. Without that generosity and faith in me as a student and researcher, my acceptance into UCR would not have been possible. Within her laboratory she has allowed me the creative freedom to grow as a scientist. She has supported me financially for my entire time within the laboratory, in addition to the substantial costs of my project, which would not be feasible elsewhere. Without her support and guidance as a mentor, I would certainly not be the scientist that I am today, nor would I have been presented the same career opportunities as a post-doc, and beyond.

I would like to thank the members of the Bailey-Serres lab for their continued support and encouragements. Without their guidance and discussions, my work in the lab may not have been possible. I would especially like to thank Lauren Dedow and Sonja Winte for their friendship within the lab and in life.

Finally, I would like to thank Melissa Jones for her continued support. Without her words of encouragement, attainment of my PhD would not have been possible.

Publications

1. Lee TA, Bailey-Serres J: **Lighting the shadows: methods that expose nuclear and cytoplasmic gene regulatory control.** *Current Opinion in Biotechnology* 2018, **49**:29-34.

ABSTRACT OF THE DISSERTATION

Genome-Scale Investigation of Integrated Nuclear and Cytoplasmic Gene
Regulatory Control in *Arabidopsis*

by

Travis Andrew Lee

Doctor of Philosophy, Graduate Program in Plant Biology
University of California, Riverside, June 2018
Dr. Julia Bailey-Serres, Chairperson

Plants are resilient to transient limitations in the availability of oxygen for efficient energy production. The highly reversible response to oxygen deprivation (hypoxia) is characterized by dynamics in accumulation and differential translation of a subset of genes in the model plant *Arabidopsis thaliana*. Transcriptional upregulation of genes associated with survival in response to hypoxia are mediated by group VII ETHYLENE RESPONSIVE FACTOR (ERFVII) transcription factors via binding to a conserved Hypoxia Responsive Promoter Element (HRPE) *cis*-element. Nonetheless, there is little knowledge of the effects of hypoxia on nuclear processes, including histone modification, chromatin accessibility, RNA polymerase II (RNAPII) elongation or RNA export. Additionally, *in vivo* ERFVII binding sites and dynamics are largely unexplored at the global scale.

In this dissertation, the modulation of chromatin features, RNAPII elongation and nascent transcripts were contrasted with the total polyadenylated

and ribosome-associated sub-populations of mRNA of seedlings exposed to non-stress, hypoxic, or re-oxygenation conditions. The technologies utilized in this study to generate datasets included Chromatin Immunoprecipitation (ChIP-seq), Isolation of Nuclei Tagged in Specific Cell Types (INTACT), Assay for Transposase Accessible Chromatin (ATAC-seq), RNA sequencing (RNA-seq), and Translating Ribosome Affinity Purification (TRAP-seq). *In vivo* binding sites were mapped for the *Arabidopsis* ERFVII HYPOXIA RESPONSIVE ERF2 (HRE2), and the rice (*Oryza sativa*) ERFVIIs SUBMERGENCE 1A and C (SUB1A/C).

Integrated bioinformatic analyses were performed to investigate coordination in regulation from chromatin to translation. This led to the identification of multiple nuclear-regulated processes that contribute to dynamics in gene activity. The ~50 hypoxia-responsive genes that display coordinate transcript accumulation and translation were characterized by increased chromatin accessibility, pronounced elevation of Histone 3-lysine 9 acetylation and depletion of Histone 2A.Z under hypoxic stress. HRE2 bound just 5' of the transcription start site for many of these genes. Universal stress response genes including those associated with heat stress displayed an early increase in RNAPII engagement along the transcription unit with elevation of mRNA only after the stress was prolonged. This study revealed genes and nascent transcripts poised for expression in anticipation of prolonged stress or

reoxygenation that were previously unrecognized in widely utilized whole-cellular RNA-seq analyses.

Contents	Page
List of tables.....	xiv
List of figures.....	xv
List of supplementary tables.....	xvii
1. Lighting the shadows: methods that expose nuclear and cytoplasmic gene regulatory control	
1.1. Introduction.....	1
1.2. Chromatin topology, interactions, and accessibility.....	2
1.3. Differentiation of RNA subpopulations by location and RNA binding protein partners.....	5
1.4. High resolution of translational activity.....	8
1.5. Nascent protein synthesis.....	9
1.6. Conclusions.....	10
1.7. Dissertation objectives.....	10
1.8. References and recommended reading.....	16
2. Integrated nuclear and cytoplasmic gene regulation defines dynamic responses to oxygen availability	
2.1. Abstract.....	21
2.1.1. Background.....	21
2.1.2. Results.....	21
2.1.3. Conclusions.....	23
2.1.4. Keywords.....	23

2.2. Background.....	24
2.3. Materials and methods.....	29
2.3.1. Genetic Material	29
2.3.2. Growth and Treatment Conditions.....	29
2.3.3. Seedling Treatments	30
2.3.4. Chromatin Immunopurification (ChIP)	30
2.3.5. CHIPmentation Library Preparation	33
2.3.6. Isolation of Nuclei Tagged in Specific Cell Types (INTACT).....	34
2.3.7. Assay for Transposase Accessible Chromatin (ATAC)	35
2.3.8. INTACT followed by Nuclear RNA Extraction.....	36
2.3.9. Total RNA Isolation and PolyA RNA Affinity Purification	36
2.3.10. Translating Ribosome Affinity Purification (TRAP-seq).....	37
2.3.11. Bioinformatic Analyses	39
2.3.12. Bioinformatic tools	39
2.4. Results.....	
2.4.1. Establishment of a multiscale dataset for evaluation of dynamics in gene regulatory control in response to hypoxic and reoxygenation stress	42
2.4.2. Histone modifications and chromatin accessibility near transcription start sites are reversibly regulated by hypoxic stress and reoxygenation	46

2.4.3. Survey of chromatin and RNA data for genes groups known to be oppositingly regulated by hypoxia.....	48
2.4.4. Distinct levels of gene regulation are observed for subsets of genes	51
2.4.5. Identification of chromatin features associated with distinctions in abundance and translation of individual mRNAs.....	53
2.4.6. ERFVII and Heat Shock Factor <i>cis</i> -elements are enriched in the coordinately upregulated and RNAPII paused gene promoters, respectively.....	56
2.4.7. Prolonged hypoxia reinforces H3 acetylation and perturbs circadian- regulated genes and prolonged stress.....	58
2.4.8. Hypoxia stress recovery includes mobilization of nuclear-retained transcripts to the polyA and translating ribosome pool.....	62
2.5. Discussion	63
2.6. Conclusions	73
2.7. Acknowledgements.....	74
2.8. References	75
3. Molecular characterization of SUBMERGENCE 1A and C stability and binding in <i>Arabidopsis</i>	
3.1. Abstract.....	116
3.2. Introduction	117
3.3. Materials and methods.....	126

3.3.1. Genetic material	126
3.3.2. Growth and treatment conditions.....	127
3.3.3. Seedling treatments.....	127
3.3.4. Immunopurification of protein	128
3.3.5. SDS-PAGE and immunoblot analysis.....	129
3.3.6. Chromatin immunopurification (ChIP).....	130
3.3.7. Library preparation	132
3.3.8. Bioinformatic analyses.....	133
3.4. Results.....	133
3.4.1. SUB1A accumulation is promoted in the <i>proteolysis 6</i> mutant that is deficient in oxygen-dependent N-end rule mediated degradation <i>in</i> <i>planta</i>	133
3.4.2. Genome-wide investigation of SUB1A and SUB1C binding sites.	135
3.5. Discussion	140
3.5.1. SUB1A accumulation is highly unstable and influence by the Cys- Arg/NERP and other factors when ectopically expressed in <i>Arabidopsis</i>	141
3.5.2. SUB1A and SUB1C have conserved targets of chromatin binding that can overlap with binding of the endogenous hypoxia-induced HRE2 in <i>Arabidopsis</i> seedlings.....	143
3.6. Acknowledgements.....	150
3.7. References	163

4. General conclusions	170
4.1. References	183

List of tables	Page
1.1. Multi-scale gene regulation assay multiplexing with nucleus-targeted and protein-targeted capture	15

List of figures	Page
1.1. Graphical abstract	12
1.2. Techniques that resolve specific aspects of gene regulation in the nucleus	13
1.3. Techniques to investigate multiple scales of RNA regulation, including translation, association with specific RNA-binding proteins and <i>de novo</i> protein synthesis	14
2.1. Multiscale chromatin and mRNA gene regulatory analyses of control (normoxic), hypoxic and re-oxygenated seedlings of Arabidopsis.....	84
2.2. Genome-wide survey of chromatin-level dynamics in response to hypoxic and reoxygenation treatments	86
2.3. Short term hypoxic stress promotes changes in chromatin, transcription and nascent transcripts that are not uniformly reflected in transcript steady-state abundance or translation	88
2.4. Multi-scale evaluation of differential regulation of subsets of protein-coding genes in response to hypoxic stress identifies coordination of chromatin, transcription and post-transcriptional upregulation in the most strongly upregulated genes.....	90
2.5. Prolonged but sublethal hypoxic stress promotes Histone 3 modifications, impacts nuclear RNA and polyA RNA abundance.....	92
2.6. Dynamic responses to reoxygenation include changes in chromatin and RNA populations	94

3.1.	Rice SUB1A and SUB1C are unstable proteins when constitutively expressed in <i>Arabidopsis</i>	151
3.2.	Global-scale evaluation of genomic regions bound by the ERFVII transcription factors SUB1A, SUB1C and HRE2 in <i>Arabidopsis</i> seedlings reveals a high similarity between the binding of SUB1s under non-stress (NS) and hypoxic stress (HS) conditions	153
3.3.	Scatterplot of reads (per kilobase per million reads; RPKM) values along gene bodies for SUB1A and SUB1C binding under a. non-stress (NS) and b. hypoxic stress (HS)	155
3.4.	Genome-wide distribution of SUB1A and SUB1C binding sites (peaks) and read distribution is influenced by oxygen availability	157
3.5.	Binding profile along genic regions of three ERFVIIs under non-stress (NS) and hypoxic stress conditions (HS) in <i>Arabidopsis</i> seedlings	159
3.6.	Genome browser view of normalized read coverage on selected genes for HRE2, SUB1A and SUB1C, as well as histone, RNAPII, and three distinct RNA outputs (Chapter 2) for 2NS and 2HS samples.....	161
4.1.	Overview of histone modifications and the histone variant H2A.Z in response to short term hypoxic stress in <i>Arabidopsis</i>	179
4.2.	Overview of H3K9Ac and H3K14Ac dynamics in response to short and long term hypoxic stress in <i>Arabidopsis</i>	181

List of supplemental figures	Page
2.1. Multiscale chromatin and mRNA gene regulatory analyses of control (normoxic), hypoxic and re-oxygenated seedlings of Arabidopsis.....	96
2.2. Comparison of change in nuclear- and ribosome-associated mRNA abundance relative to change in polyA RNA abundance reveals differential regulation of nuclear retention and translation in response to hypoxic stress and reoxygenation	98
2.3. Histones and chromatin accessibility of Hypoxia Responsive Genes (HRG) and cytosolic Ribosomal Protein (RP) genes are distinctly regulated by short term (2HS) and prolonged (9HS) hypoxic stress when compared to control samples (2NS and 9NS)	100
2.4. Distinctions in histones across genes that are co-regulated at the RNA level in response to hypoxic stress.....	102
2.5. Average signal of chromatin and RNA data for co-regulated gene clusters identified from the 2 h hypoxic stress comparison (2HS/2NS) in Fig. 4a in response to prolonged hypoxic stress (9HS/9NS).....	105
2.6. Average signal of chromatin and RNA data for co-regulated gene clusters identified from the 9 h hypoxic stress comparison (9HS/9NS) in Fig. 2.5.e	108
2.7. Average signal of chromatin and RNA data outputs for co-regulated gene clusters identified from the reoxygenation comparison (1R/2NS) shown in Fig. 2.6.d	111

2.8. Identification of genes with up or down-regulated transcripts under
reoxygenation..... 114

List of supplemental tables

- 2.1. Summary of information of expression datasets
- 2.2. ATAC-seq dataset
- 2.3. Chromatin and RNA dataset
- 2.4. GO enrichment of PAM clustered datasets
- 2.5. HRE2 ChIP-seq dataset

Supplemental datasets can be found at:

https://drive.google.com/open?id=1YAYYmHzDZy0XQrUxuo9wYTMUR_le9fFm

Chapter 1

Lighting the shadows: methods that expose nuclear and cytoplasmic gene regulatory control

1.1. Introduction

Dynamic regulation may occur at every step in the flow of genetic information from gene, to mRNA, and to protein in eukaryotes. Numerous genome-scale assays of chromatin state and gene activity have accelerated the recognition of coordinated gene regulation. These include the use of chromatin immunopurification-sequencing (ChIP-seq) to define histone modifications and transcription factor (TF) binding-sites, mRNA-seq to monitor poly-adenylated mRNAs, and mass spectrometry to quantify proteins. These powerful technologies have advanced functional analyses of regulatory networks but together do not fully capture the dynamics and nuances of gene expression control in multicellular organisms. For example, ChIP-seq does not expose simultaneous interactions between multiple regions of DNA and/or proteins, and RNA-seq does not yield information on the subcellular location or functional state of transcripts. Moreover, alterations in mRNA abundance do not correlate well with protein levels determined by steady-state proteomics [1]. In multicellular organisms a protein-coding gene active in one cell may be inactive in other cells of the same organ. Here, recent high-resolution technologies that empower

intricate dissection of gene regulation from the initiation of transcription to the de novo synthesis of a protein in plants are reviewed along with their multi-plexing with methods that resolve processes in cells of defined identity of multicellular organs (Table 1).

1.2. Chromatin topology, interactions, and accessibility

In the plant cell nucleus, interactions occur between DNA, proteins, and regulatory RNAs within the context of chromatin structure to enable RNA polymerase II (Pol II) to engage and commence pre-mRNA synthesis of a protein-coding gene (Figure 1). Determination of transcriptional initiation is modulated by an array of factors including higher-order chromatin structure, methylation of cytosine nucleotides, covalent modifications of the histones that form the octamer core of each nucleosome, the abundance, activity and interactions of TFs, and the core transcriptional apparatus, along with exposure of cis-regulatory DNA sequences (reviewed by [2]). At the highest order, the three-dimensional organization of chromosomes within the nucleus functions in gene activity [3,4]. Several inventive techniques provide perspective on the location of individual genes with respect to nuclear architecture, such as gene proximity to a nuclear pore or the juxtaposition of chromosomal regions. Fluorescence in situ hybridization (FISH) with 'padlock' probes, having termini complementary to a targeted DNA sequence, can detect a specific gene locus within a nucleus. In its recent application to plants, this method demonstrated the

repositioning of a gene to the periphery of the nucleus that was concomitant with elevation of the encoded transcript in response to a light signal [5]. At the genome-wide scale, chromatin conformation capture coupled with sequencing (nicknamed Hi-C) enables recognition of inter-chromosomal and intra-chromosomal interactions within nuclei. This approach provided evidence that proximity of distinct chromosomal regions can influence the activity of genes in plants [6,7].

ChIP-seq is routinely used to identify locations of TF residency, which is coupled with motif searches and other data to pair functional cis-elements and TFs to the genes they control. A challenge to concisely defining transcriptional regulatory networks is the disentanglement of the combinatorial roles of TFs, including factors that do and do not directly bind to DNA. Combinatorial indexed-ChIP (co-ChIP) allows for the identification of multiple protein interactors associated with single DNA fragments in a high throughput manner. Two sequential rounds of ChIP with antibodies that recognize specific DNA associated proteins coupled with unique indexing of the DNA fragments in each reaction allows for the identification of segments of chromatin associated with multiple histone marks [8]. Co-occurring interactions at the plant nuclear pore complex were resolved by pairing restriction enzyme-mediated ChIP-seq (RE-ChIP) with Hi-C [7]. This uncovered coordinated chromosomal-interactions, chromatin topology, and protein interactions. Cytosine methylation and covalent modifications of core histones, including, but not limited to methylation,

acetylation, and ubiquitination influence chromatin architecture by affecting DNA-nucleosome interactions, which in turn influence exposure of cis-elements via chromatin compaction and relaxation. Genome-wide, regions of relaxed chromatin typically lie just upstream of transcription start sites (TSS) and therefore demarcate actively transcribed regions. The methods DNase I hypersensitive-site sequencing (DNase-seq), formaldehyde-assisted isolation of regulatory elements with sequencing (FAIRE-seq), and micrococcal nuclease sensitive-site sequencing (MNase-seq) identify regions of accessible chromatin. Moreover, the fine-mapping of short unexposed regions within these accessibility sites can yield the precise positions occupied by TFs. The assay for transposase-accessible chromatin using sequencing (ATAC-seq) provides similar information [9]. In the ATAC procedure, isolated nuclei are incubated with an engineered recombinant Tn5 ‘transposome’ that inserts sequencing-compatible adapters into non-compacted regions of the chromatin. ATAC-seq has enabled modeling of environmentally-regulated gene networks in field-grown rice [10] as well as mapping of TF footprints in *Arabidopsis* [11]. Adaptation of ATAC-seq to single-cell systems (scATAC-seq) [12] may enable assay of DNA accessibility in individual cells. To assuage the challenge of defining processes that occur in specific cells of a multicellular organ, most of these chromatin survey methods can be coupled with technologies that enable the targeted capture of nuclei (Table 1). Fluorescence-activated cell sorting (FACS) can be used on transgenic plants with a sub-set of cells defined by a specific promoter driving a fluorescent

protein gene (reviewed by [13]). FACS requires the generation of protoplasts, whereas Fluorescence-activated nuclei sorting (FANS) [14] and isolation of nuclei tagged in specific cell types (INTACT) are performed on fresh or frozen tissue, respectively [15]. In FANS, DAPI (4,6-diamidino-2-phenylindole)-stained or fluorescently-marked nuclei are selectively isolated at high purity. In the case of INTACT, a synthetic biotinylable protein that is associated with the outer nuclear envelope enables isolation of nuclei marked by green fluorescent protein. FANS and INTACT provide a gateway to analyses of chromatin at the cell-specific and region-specific level of multicellular organs. The isolation of nuclei by these methods may also afford opportunity to investigate the diverse components of nucleoplasm and the nuclear envelope.

1.3. Differentiation of RNA subpopulations by location and RNA binding protein partners

Several mechanisms govern the processing of a nascent pre-mRNA into a mature mRNA (Figure 2). These include coordination of covalent addition of a 5'-7mG-cap to the 5' terminus, additional base modifications, splicing of introns, as well as the guided cleavage and polyadenylation at the 3' terminus. These steps in gene expression involve regulated interactions between Pol II and multi-subunit protein complexes, including the capping, splicing and polyadenylation machinery. Remarkably, little is known of pre-mRNA turnover in the nucleus and mRNA export through the nuclear pore to the cytoplasm in plants [16]. But

several new methods can provide information on the regulation of essential co-transcriptional and post-transcriptional nuclear processes. Genes undergoing transcription can be identified by ChIP with antisera recognizing specific phospho-isoforms of the highly repeated tandem heptapeptide carboxyl-terminal domain of the B1 subunit of Pol II. For example, phosphorylation at Ser5 is associated with initiation whereas Ser2 is associated with elongation of Pol II [17]. The global nuclear run-on sequencing (GRO-seq) and 50 GRO-seq methods are designed to monitor polymerase elongation. This entails inhibition of initiation and run-on elongation of transcription in a reaction incorporating 5-bromo UTP in isolated nuclei. GRO-seq profiles nascent transcripts, whereas 50 GRO-seq enriches for 50-7mG-cap regions of nascent transcripts for TSS determination. The use of these has exposed a marked difference between the abundance of nascent transcripts and routinely assayed poly(A)+ mRNAs [18,19], elevating awareness of RNA decay in plant gene regulation.

Nuclear RNA (nRNA), including nascent transcripts undergoing synthesis and maturation, as well as nucleus-retained mRNAs, can be evaluated with nuclei obtained by sedimentation, FANS, or INTACT followed by RNA-seq. The use of random primers after rRNA depletion or oligo-dT in the production of cDNA provides the flexibility to assay the full complement of nRNA versus polyadenylated mRNAs, respectively. Investigations of nRNA using array-based technology have reported marginal to widespread differences in the nRNA and poly(A)+ mRNA pool of plants [20–22]. We anticipate that systematic comparison

of nRNA-seq and poly(A)+ RNA-seq data that includes evaluation of sequencing read coverage across each transcription unit will shed light on regulation of pre-mRNA splicing and mRNA export. Additionally, nRNA-seq can be used to quantitate and explore regulatory non-coding RNAs involved in chromatin organization and transcription (ie. AUXIN REGULATED PROMOTER LOOP RNA and COOLAIR [reviewed by [23]]). Recently, in a powerful coupling of technologies, INTACT on root hair and non- hair epidermal cells identified protein-RNA interactions associated with cell identity [24]. INTACT was also used to profile shoot apical meristem nRNA [25] and parental-specific chromatin features in endosperm nuclei [26]. RNA binding proteins (RBPs) play diverse roles in mRNA processing, transport, turnover, sequestration and translational activity. These proteins can determine RNA localization within the nucleus or cytoplasm, or mediate cell-to-cell movement. Similar to ChIP, RNA immunoprecipitation (RIP) leverages antibodies against specific RBPs to capture associated transcripts that can be evaluated in targeted or global analyses of associated RNAs [27,28]. RIP-seq could be applied to epitope-tagged RBPs expressed in specific cell-types for targeted resolution of function. Refinements of RIP-seq include cross-linking followed by RNase to determine direct sites of protein-RNA interaction [24] and assay of RBPs associated with a range of regulatory RNAs.

1.4. High resolution of translational activity

Translation involves the recognition of the start codon and recruitment of the ribosome (initiation) to a 5'-7mG-capped and 30-polyadenylated mRNA. This is followed by sequential elongation of the nascent peptide until a termination codon provokes release of the polypeptide from the ribosome [29]. The isolation of mRNA associated with ribosomes enables monitoring of the translome (ribosome-associated poly(A)⁺ mRNAs; polysomal mRNA-seq) (Figure 2). Translation is conditionally and developmentally modulated in plants [30]. This can be gleaned by comparison of the translome to the complete poly(A)⁺ mRNA transcriptome. A high-resolution view of translation is obtained by mapping ribosome footprints (Ribo-seq), which define the positions of individual ribosomes on transcripts [31,32]. Ribo-seq is particularly useful for identifying open reading frames in the 5' leader region of mRNAs. These can modulate the translation of the main protein coding reading frame [30]. Both polysomal mRNA-seq and Ribo-seq can be accomplished with ribosomes obtained by centrifugation or translating ribosome affinity purification (TRAP) [33,34]. TRAP utilizes a functional epitope-tagged RIBOSOMAL PROTEIN L18 (RPL18) to capture ribosomes by affinity purification, avoiding other RNA-protein complexes that co-sediment with ribosomes. The use of cell-specific promoters to drive TRAP constructs enables capture of translomes of cells of defined identity [32,35] and has been translated to crops including *Medicago truncatula* [36], *Solanum lycopersicum* [37], and *Oryza sativa* [38].

1.5. Nascent protein synthesis

The sequencing of ribosome-associated mRNAs and ribosome footprints provides a proxy of protein synthesis; however, these methods do not confirm the active synthesis of proteins as achieved by co-translational labeling of de novo synthesized polypeptides. Mass spectrometry-based identification of trypsin-fragmented proteins (proteomics) is used routinely to investigate steady-state levels of cellular proteins; whereas, proteomic quantitation of nascent protein production requires a method such as Bioorthogonal noncanonical amino acid tagging (BONCAT) [39–42]. This technique utilizes the methionine surrogate azidohomoalanine (Aha) to pulse-label de novo synthesized proteins that can be captured from or monitored in total cell extracts (Figure 2). The azide moiety of Aha allows for an azide-alkyne cycloaddition reaction that enables selective processing of Aha containing peptides. Rapid dynamics in protein synthesis can be monitored with Aha pulse-labeling times as short as 30 min. By pairing BONCAT-enriched samples with proteomics, newly synthesized proteins were identified and quantified in response to various environmental stimuli in *Arabidopsis* [43].

1.6. Conclusions

Advances in imaging, RNA-sequencing and mass spectrometry based technologies combined with methods that sub-fractionate cellular components provide new opportunities for more refined dissection of transcriptional and post-transcriptional gene regulatory networks and recognition of new and nuanced regulatory mechanisms. Performing these with subcellular-type, cell-type or region-specific resolution within tissues or organs will enable a more holistic view of gene regulation, from chromatin to protein. Both prospecting and targeted analyses with these single and multiplexed technologies promise to provide clarity to the developmentally-programmed and environmentally-modulated gene activity that enable plants to thrive in highly dynamic environments. Moreover, the refined definition of multi-level gene regulatory processes of plants can provide new options for rational construction of biological systems and synthetic gene control circuits with diverse applications from agriculture to biotechnology.

1.7. Dissertation objectives

The aims of this dissertation research were:

- 1) To gain a global perspective of gene regulatory mechanisms within the nucleus that occur in response to hypoxic stress in *Arabidopsis*. Chapter 2 presents evidence of distinct regulation within the nucleus at the levels of chromatin organization, transcriptional activity, and nuclear transcript abundance in response to hypoxia. Comparative analyses were performed in response to

short term and prolonged hypoxic stress (2 and 9 h), and re-oxygenation (1 and 2 h re-oxygenation). The results reveal aspects of gene regulation not reflected in the poly(A)⁺ mRNA transcriptome.

2) To gain a greater understanding of the group VII ETHYLENE RESPONSE FACTORS (ERF-VII) *SUBMERGENCE 1A/C* (*SUB1A/C*) and *HYPOXIA RESPONSIVE ERF2* (*HRE2*). Chapter 3 evaluates *in planta* dynamics of SUB1A accumulation in response to hypoxia and in an N-end rule mutant background, which is known to affect ERF-VII stability. Genome wide *in planta* DNA binding profiles were also generated for SUB1A, SUB1C, and HRE2, revealing conserved ERF-VII binding dynamics between these transcription factors, and oxygen dependent regulation of SUB1A and SUB1C binding.

Figure 1.1. Graphical abstract. Within cells, myriad interconnected processes orchestrate the progression of gene expression from chromatin, to mRNA, and to protein. Assessment of DNA methylation, histone modification, transcript isoform abundance, and the proteome are frequently performed to examine this progression, but do not resolve many intermediary steps in the coordinated regulation of gene expression. Here, we consider single and multiplexed technologies that yield genome-wide assessment of gene and mRNA activity, from transcription factor access to DNA to de novo synthesis of protein. An emphasis is placed on methods that can resolve gene regulatory processes in cells of defined identity within multicellular organs at spatial and temporal scales, leading to more effective design of gene regulatory cassettes for biotechnology.

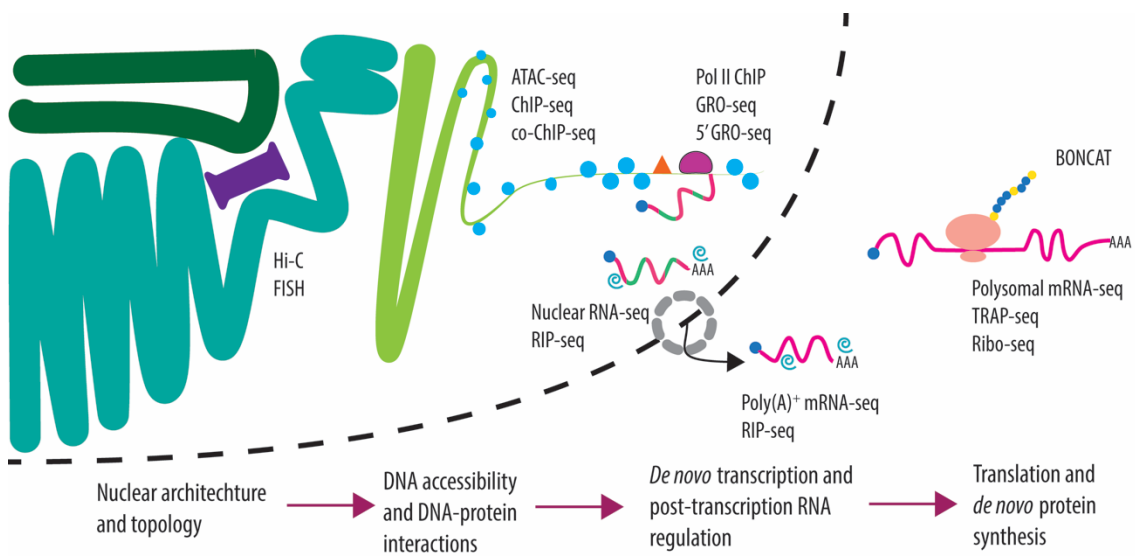


Figure 1.2. Techniques that resolve specific aspects of gene regulation in the nucleus. Regions of chromatin accessible to transcription factors are assayed by DNase-seq, MNase-seq, FAIRE-seq, and ATAC-seq. Chromosomal interactions are surveyed by Hi-C. Regions of DNA that interact with specific proteins including transcription factors, chromatin remodeling proteins, specifically modified histones, and specifically phosphorylated isoforms of Pol II are captured by ChIP and its variations including co-ChIP and RE-ChIP. RNAs within the nucleus, including nascent pre-mRNA are surveyed by 50 GRO-seq and GRO-seq, which monitor active transcription. Nuclear RNA-seq can profile all RNA within the nucleus or molecules with a specific feature, such as poly(A)+ tail.

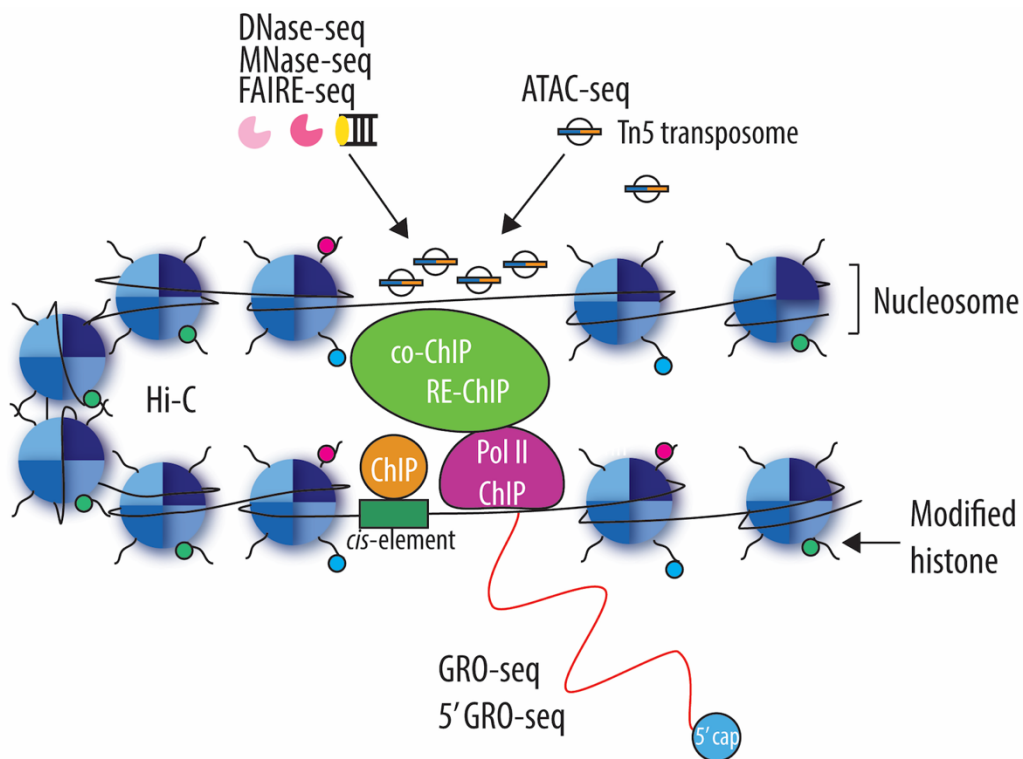


Figure 1.3. Techniques to investigate multiple scales of RNA regulation, including translation, association with specific RNA-binding proteins and de novo protein synthesis. Nascent RNA synthesis is surveyed by GRO-seq. Total cellular mRNA is assayed by poly(A)⁺ RNA-seq. RNAs that co-immunopurify with specific RNA binding proteins are quantified by RIP-seq. Ribosome-associated RNAs are assayed by TRAP-seq and polysomal mRNA-seq. Ribosome footprinting is achieved by Ribo-seq. De novo synthesized proteins are assayed by BONCAT.

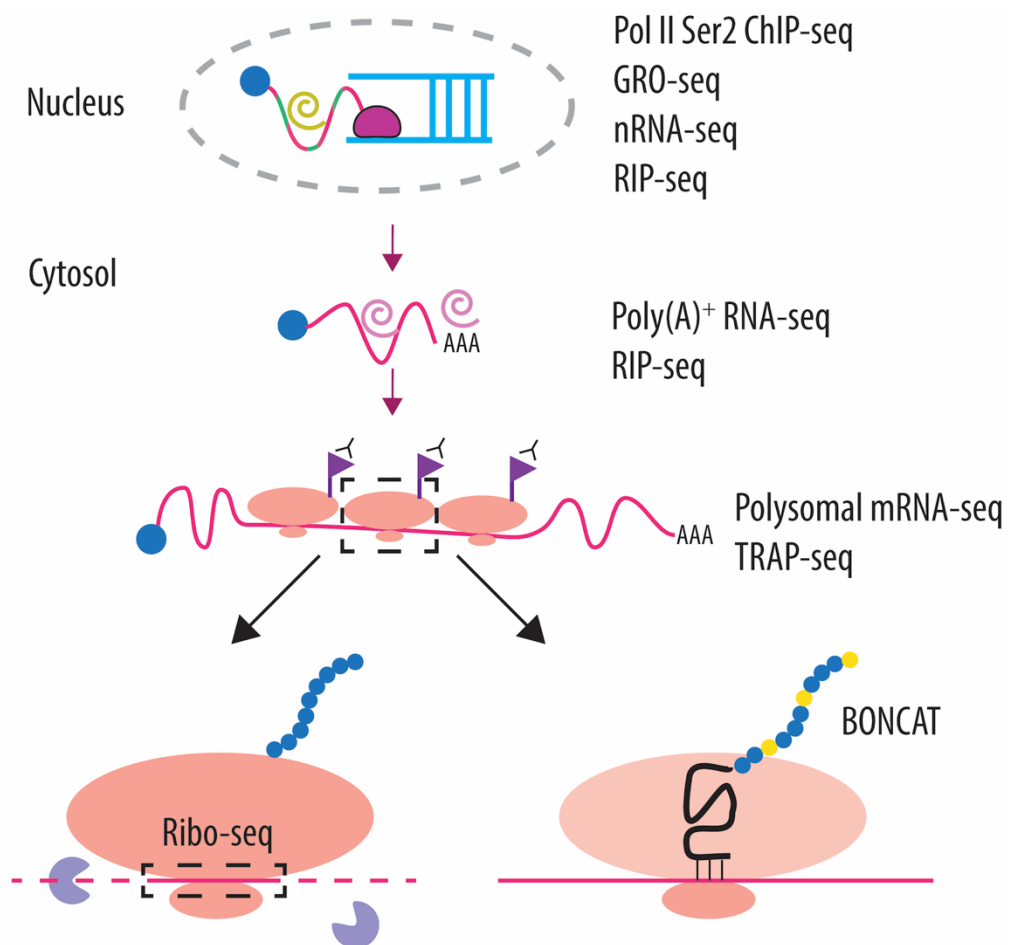


Table 1.1. Multi-scale gene regulation assay multiplexing with nucleus- and protein-targeted capture

Technology	Interaction or RNA population monitored	Performed on plants?	Specific cell-type targeted analysis	Representative citations
DNA based				
Hi-C seq	Intra- and inter-chromosomal interactions	Yes	Yes ¹ : C, N, I	[2,5]
Padlock FISH	Subnuclear DNA localization	Yes	Yes ¹ : C, N, I	[4]
ChIP-seq	DNA-Protein	Yes	Yes ¹ : C, N, I	
RE-ChIP-seq	DNA-Protein complex	Yes	Yes: C, N, I	[6,41]
co-ChIP-seq	DNA-Protein-Protein	No	Yes: C, N, I	[7]
ATAC-seq-seq	Transposase hypersensitive sites (THS)	Yes	Yes ¹ : C, N, I	[9]
scATAC-seq	Single cell ATAC-seq	No	Yes ¹ : C, N, I	[11]
Phospho Pol II ChIP-seq	Transcript elongation	Yes	Yes: C, N, I	[14]
RNA based				
GRO-seq	Nascent RNA	Yes	Yes ¹ : C, N, I	[16]
5' GRO-seq	5' transcriptions start site (TSS) region of nascent RNA	Yes	Yes: C, N, I	[16]
nRNA-seq	Nuclear-localized RNA	Yes	Yes ¹ : C, N, I	[22]
PIP-seq	Mapping of nRNA-protein interactions		Yes ¹ : C, N, I	[21]
RIP-seq	RNA binding protein associated RNA	Yes	Yes: C, N, I	[24,25]
Polysomal mRNA-seq	Polysome-associated mRNA obtained by conventional sedimentation	Yes	Yes: C	[28]
TRAP-seq	Ribosome-associated mRNA obtained by affinity purification of ribosomes	Yes	Yes ¹ : C, T	[28,30-34]
Ribo-seq	Ribosome footprint mapping on RNAs	Yes	Yes: C, T	[28,29]
Protein based				
BONCAT	De novo protein synthesis	Yes	Yes	[40]

¹ Method accomplished in plants with one or more methods targeting components of specific cells including nuclei, proteins, or ribosomes.

C, FACS, Fluorescence-activated cell sorting; I, INTACT, isolation of nuclei tagged in specific cell types; N, FANS, Fluorescence-activated nuclei sorting; T, TRAP, translating ribosome affinity purification.

1.8 References and recommended reading

Papers of particular interest, published within the period of review, have been highlighted as:

* of special interest

** of outstanding interest

1. ** Walley JW, Sartor RC, Shen Z, Schmitz RJ, Wu KJ, Urich MA, Nery JR, Smith LG, Schnable JC, Ecker JR, et al.: **Integration of omic networks in a developmental atlas of maize**. *Science* 2016, **353**:814–818.

This report demonstrates disconnections between transcript and protein accumulation genome wide

2. Dekker J, Rippe K, Dekker M, Kleckner N: **Capturing chromosome conformation**. *Science* 2002, **295**:1306–1311.
3. Feng S, Cokus SJ, Schubert V, Zhai J, Pellegrini M, Jacobsen SE: **Genome-wide Hi-C analyses in wild-type and mutants reveal high-resolution chromatin interactions in Arabidopsis**. *Mol. Cell* 2014, **55**:694–707.
4. Feng C-M, Qiu Y, Van Buskirk EK, Yang EJ, Chen M: **Light-regulated gene repositioning in Arabidopsis**. *Nat. Commun.* 2014, **5**:3027.
5. Moissiard G, Cokus SJ, Cary J, Feng S, Billi AC, Stroud H, Husmann D, Zhan Y, Lajoie BR, McCord RP, et al.: **MORC family ATPases required for heterochromatin condensation and gene silencing**. *Science* 2012, **336**:1448–1451.
6. * Bi X, Cheng Y, Hu B, Ma X, Wu R, Wang J, Liu C: **Non-random domain organization of the Arabidopsis genome at the nuclear periphery [Internet]**. *Genome Res.* 2017, doi:10.1101/gr.215186.116.

The coupling of ChIP-seq of the nuclear pore complex with Hi-C resolves spatiotemporal dynamics within the nucleus

7. * Weiner A, Lara-Astiaso D, Krupalnik V, Gafni O, David E, Winter DR, Hanna JH, Amit I: **Co-ChIP enables genome-wide mapping of histone mark co-occurrence at single-molecule resolution**. *Nat. Biotechnol.* 2016, **34**:953–961.

This report introduces co-ChIP to identify simultaneous protein-protein interactions in respect to DNA binding

8. Buenrostro JD, Giresi PG, Zaba LC, Chang HY, Greenleaf WJ: **Transposition of native chromatin for fast and sensitive epigenomic profiling of open chromatin, DNA-binding proteins and nucleosome position.** *Nat. Methods* 2013, **10**:1213–1218.
9. * Wilkins O, Hafemeister C, Plessis A, Holloway-Phillips MM, Pham GM, Nicotra AB, Gregorio GB, Jagadish SV, Septiningsih EM, Bonneau R, et al.: **EGRINs (Environmental Gene Regulatory Influence Networks) in rice that function in the response to water deficit, high temperature, and agricultural environments.** *Plant Cell* 2016, **28**:2365–2384.

This report first demonstrates ATAC-seq in a plant, evaluating chromatin dynamics in field-grown rice

- 10.**Lu Z, Hofmeister BT, Vollmers C, DuBois RM, Schmitz RJ: **Combining ATAC-seq with nuclei sorting for discovery of cis-regulatory regions in plant genomes [Internet].** *Nucleic Acids Res.* 2016, doi:10.1093/nar/gkw1179.

This study multiplexes ATAC-seq with FANS to refine nuclei isolation and demonstrate transcription factor footprinting

11. Buenrostro JD, Wu B, Litzenburger UM, Ruff D, Gonzales ML, Snyder MP, Chang HY, Greenleaf WJ: **Single-cell chromatin accessibility reveals principles of regulatory variation.** *Nature* 2015, **523**:486–490.
12. Bailey-Serres J: **Microgenomics: genome-scale, cell-specific monitoring of multiple gene regulation tiers.** *Annu. Rev. Plant Biol.* 2013, **64**:293–325.
13. Meier I, Richards EJ, Evans DE: **Cell biology of the plant nucleus.** *Annu. Rev. Plant Biol.* 2017, **68**:139–172.
- 14.* Antosz W, Pfab A, Ehrnsberger HF, Holzinger P, Köllen K, Mortensen SA, Bruckmann A, Schubert T, Längst G, Griesenbeck J, et al.: **The composition of the Arabidopsis RNA Polymerase II transcript elongation complex reveals the interplay between elongation and mRNA processing factors.** *Plant Cell* 2017, **29**:854–870.

This report investigates the functional significance of Ser2 phosphorylation of the carboxy terminal domain of RNA polymerase II in Arabidopsis

15. Erhard KF, Talbot J-ERB, Deans NC, McClish AE, Hollick JB: **Nascent transcription affected by RNA Polymerase IV in Zea mays.** *Genetics* 2015, **199**:1107–1125.

- 16** Hetzel J, Duttke SH, Benner C, Chory J: **Nascent RNA sequencing reveals distinct features in plant transcription.** *Proc. Natl. Acad. Sci. U. S. A.* 2016, **113**:12316–12321.

This report introduces 5' GRO-seq and improves the GRO-seq protocol in Arabidopsis

17. Jacob Y, Mongkolsiriwatana C, Veley KM, Kim SY, Michaels SD: **The nuclear pore protein AtTPR is required for RNA homeostasis, flowering time, and auxin signaling.** *Plant Physiol.* 2007, **144**:1383–1390.
18. Park MY, Wu G, Gonzalez-Sulser A, Vaucheret H, Poethig RS: **Nuclear processing and export of microRNAs in Arabidopsis.** *Proc. Natl. Acad. Sci. U. S. A.* 2005, **102**:3691–3696.
19. Goldberg RB, Hoschek G, Kamalay JC, Timberlake WE: **Sequence complexity of nuclear and polysomal RNA in leaves of the tobacco plant.** *Cell* 1978, **14**:123–131.
20. Bazin J., Bailey-Serres, J: **Emerging roles of long non-coding RNA in root developmental plasticity and regulation of phosphate homeostasis.** 2016, *Front. Plant Sci.* doi: 10.3389/fpls.2015.00400
- 21.** Foley SW, Gosai SJ, Wang D, Selamoglu N, Sollitti, AC, Köster T, Steffen A, Lyons E, Daldal F, Garcia BA, Staiger D, Deal RB, Gregory BD: **A global view of RNA-protein interactions identifies post-transcriptional regulators of root hair cell fate** 2017, *Developmental Cell* **41**: 204–220.

Multiplexing INTACT and RNA binding protein footprinting exposes regulation of RNA binding protein associated with epidermal cell and root function

- 22.** You Y, Sawikowska A, Neumann M, Posé D, Capovilla G, Langenecker T, Neher RA, Krajewski P, Schmid M: **Temporal dynamics of gene expression and histone marks at the Arabidopsis shoot meristem during flowering.** *Nat. Commun.* 2017, **8**:15120.

This report couples INTACT with RNA-seq to investigate the nuclear transcriptome

- 23.** Moreno-Romero J, Santos-Gonzalez J, Hennig L, Kohler C: **Applying the INTACT method to purify endosperm nuclei and to generate parental-specific epigenome profiles.** *Nat. Protoc.* 2017, **12**:238–254.

This report utilizes INTACT to identify parental lineages of endosperm nuclei

24. Bobik K, McCray TN, Ernest B, Fernandez JC, Howell KA, Lane T, Staton M, Burch-Smith TM: **The chloroplast RNA helicase ISE2 is required for multiple chloroplast RNA processing steps in *Arabidopsis thaliana* [Internet].** *Plant J.* 2017, doi:10.1111/tpj.13550.
25. Sorenson R, Bailey-Serres J: **Selective mRNA sequestration by OLIGOURIDYLATE-BINDING PROTEIN 1 contributes to translational control during hypoxia in *Arabidopsis*.** *Proc. Natl. Acad. Sci. U. S. A.* 2014, **111**:2373–2378.
26. Roy B, von Arnim AG: **Translational regulation of cytoplasmic mRNAs.** *Arabidopsis Book* 2013, **11**:e0165.
27. Browning KS, Bailey-Serres J: **Mechanism of cytoplasmic mRNA translation.** *Arabidopsis Book* 2015, **13**:e0176.
28. Hsu PY, Calviello L, Wu H-YL, Li F-W, Rothfels CJ, Ohler U, Benfey PN: **Super-resolution ribosome profiling reveals unannotated translation events in *Arabidopsis* [Internet].** *Proc. Natl. Acad. Sci. U. S. A.* 2016, doi:10.1073/pnas.1614788113.
29. Juntawong P, Girke T, Bazin J, Bailey-Serres J: **Translational dynamics revealed by genome-wide profiling of ribosome footprints in *Arabidopsis*.** *Proc. Natl. Acad. Sci. U. S. A.* 2014, **111**:E203–212.
30. Zanetti ME, Chang I-F, Gong F, Galbraith DW, Bailey-Serres J: **Immunopurification of polyribosomal complexes of *Arabidopsis* for global analysis of gene expression.** *Plant Physiol.* 2005, **138**:624–635.
31. Mustroph A, Zanetti ME, Jang CJH, Holtan HE, Repetti PP, Galbraith DW, Girke T, Bailey-Serres J: **Profiling translatomes of discrete cell populations resolves altered cellular priorities during hypoxia in *Arabidopsis*.** *Proc. Natl. Acad. Sci. U. S. A.* 2009, **106**:18843–18848.
32. Jiao Y, Meyerowitz EM: **Cell-type specific analysis of translating RNAs in developing flowers reveals new levels of control.** *Mol. Syst. Biol.* 2010, **6**:419.
33. Reynoso MA, Blanco FA, Bailey-Serres J, Crespi M, Zanetti ME: **Selective recruitment of mRNAs and miRNAs to polyribosomes in response to rhizobia infection in *Medicago truncatula*.** *Plant J.* 2013, **73**:289–301.
34. Ron M, Kajala K, Pauluzzi G, Wang D, Reynoso MA, Zumstein K, Garcha J, Winte S, Masson H, Inagaki S, et al.: **Hairy root transformation using *Agrobacterium rhizogenes* as a tool for exploring cell type-specific gene expression and function using tomato as a model.** *Plant Physiol.* 2014, **166**:455–469.

- 35.* Zhao D, Hamilton JP, Hardigan M, Yin D, He T, Vaillancourt B, Reynoso M, Pauluzzi G, Funkhouser S, Cui Y, et al.: **Analysis of ribosome-associated mRNAs in rice reveals the importance of transcript size and GC content in translation.** *G3: Genes|Genomes|Genetics* 2017, **7**:203–219.

This report introduces the TRAP technology in rice

36. Dieterich DC, Link AJ, Graumann J, Tirrell DA, Schuman EM: **Selective identification of newly synthesized proteins in mammalian cells using bioorthogonal noncanonical amino acid tagging (BONCAT).** *Proc. Natl. Acad. Sci. U. S. A.* 2006, **103**:9482–9487.
37. Bagert JD, Xie YJ, Sweredoski MJ, Qi Y, Hess S, Schuman EM, Tirrell DA: **Quantitative, time-resolved proteomic analysis by combining bioorthogonal noncanonical amino acid tagging and pulsed stable isotope labeling by amino acids in cell culture.** *Mol. Cell. Proteomics* 2014, **13**:1352–1358.
38. Genheden M, Kenney JW, Johnston HE, Manousopoulou A, Garbis SD, Proud CG: **BDNF stimulation of protein synthesis in cortical neurons requires the MAP kinase-interacting kinase MNK1.** *J. Neurosci.* 2015, **35**:972–984.
39. Zhang G, Bowling H, Hom N, Kirshenbaum K, Klann E, Chao MV, Neubert TA: **In-depth quantitative proteomic analysis of de novo protein synthesis induced by brain-derived neurotrophic factor.** *J. Proteome Res.* 2014, **13**:5707–5714.
- 40.** Glenn WS, Stone SE, Ho SH, Sweredoski MJ, Moradian A, Hess S, Bailey-Serres J, Tirrell DA: **Bioorthogonal noncanonical amino acid tagging (BONCAT) enables time-resolved analysis of protein synthesis in native plant tissue.** *Plant Physiol.* 2017, **173**:1543–1553.

This report introduces the use of bioorthogonal labeling of *de novo* synthesized proteins in actively growing plants in control and heat stress conditions

41. Sequeira-Mendes J, Aragüez I, Peiró R, Mendez-Giraldez R, Zhang X, Jacobsen SE, Bastolla U, Gutierrez C: **The functional topography of the Arabidopsis genome is organized in a reduced number of linear motifs of chromatin states.** *The Plant Cell* 2014, **26**:2351-2366.

Chapter 2

Integrated nuclear and cytoplasmic gene regulation defines dynamic responses to oxygen availability

2.1. Abstract

2.1.1. Background

Plants are resilient to transient limitations in molecular oxygen, which is mandatory for the efficient production of energy needed for diverse cellular processes and growth. A highly reversible response to oxygen deprivation (hypoxia) is the coordinate upregulation of ~50 hypoxia-responsive genes (*HRG*) transcripts and their preferential translation in *Arabidopsis thaliana*. Little is known of the effect of hypoxia on nuclear gene regulatory processes, including histone modifications, chromatin accessibility, RNA polymerase II (RNAPII) elongation and the connection to cytoplasmic translation, sequestration or turnover.

2.1.2. Results

Here, we assayed nine readouts of chromatin and transcription and contrasted them with polyadenylated and ribosome-associated mRNA populations of seedlings exposed to control (normoxic), hypoxic, or

reoxygenation conditions. This identified nuclear-regulated processes contributing to dynamics in gene activity. The *HRGs* were characterized by increased chromatin accessibility, pronounced elevation of Histone 3-lysine 9 acetylation (H3K9Ac), maintained Histone 3-lysine 4 trimethylation (H3K4me3), and eviction of the Histone 2A.Z variant along the gene body. Chromatin immunopurification-DNA sequencing and motif searching determined over half of the *HRGs* promoters were bound by members of the Ethylene Responsive Factor group VII transcription factors including HYPOXIA RESPONSIVE ETHYLENE RESPONSIVE FACTOR 2 (HRE2). The HRE2 binding site unexpectedly differed from the *cis*-element defined for constitutively expressed ERFVII family members in protoplast transactivation assays, but resembled the binding motif characteristic of other ERFs. A systematic analysis of hypoxic stress and reoxygenation uncovered gene regulation that was anticipatory of prolonged stress or reoxygenation. Genes associated with heat and other extreme stresses were engaged by RNAPII without a rise in nuclear or polyadenylated RNAs unless hypoxia was prolonged or reoxygenation occurred. These poised genes lost H3K4me3 and accumulated H3K9Ac during the stress. Motif search analyses determined that many are likely targets of HEAT SHOCK FACTOR transcriptional activators. By contrast, genes associated with ribosome biogenesis continued to be transcribed but their transcripts were retained in the nucleus until reaeration, at which time they increased in the polyadenylated and ribosome-associated mRNA pool. These transcribed but nuclear-retained

transcripts were characterized by a modest decline in H3K4me3 and increase in Histone 3-lysine 14 acetylation (H3K14Ac) during the stress.

2.1.3. Conclusions

We resolved multiple modes of differential transcriptional regulation in response to hypoxic stress. *HRGs* displayed H2A.Z eviction, H3K9Ac accumulation and RNAPII elongation accompanied with elevation of polyadenylated mRNAs that were effectively recruited to ribosomes. Genes associated with extreme stress were progressively induced: first RNAPII was poised and elongation stalled with export after prolonged stress or reaeration. Housekeeping genes, such as those encoding ribosomal subunits, continued to be transcribed during the stress but were preferentially retained in the nucleus until reaeration. Many genes associated with developmental processes were progressively transcriptionally and translationally repressed until reaeration. Thus, hypoxia launches complex nuclear to cytoplasmic regulatory mechanisms to fine tune metabolic and developmental adaptations that include preparation for recovery.

2.1.4. Keywords: *Arabidopsis thaliana*, Hypoxia, Histone modification, Histone variant, ATAC-seq, Chromatin accessibility, Nuclear Transcriptome, PolyA Transcriptome, Translatome

2.2. Background

The expression of nucleus-encoded protein coding genes in eukaryotes is regulated at multiple levels with major control imparted through chromatin structure, recruitment of RNA polymerase II (RNAPII) to the transcription start site, co-transcriptional pre-mRNA processing and export to the cytoplasm, and mRNA translation by ribosomes. Many factors finely regulate these diverse processes in specific cell types or in response to chemical or environmental stimuli. In plants, which must readily adjust to changes in the environment, gene regulation is highly responsive to enable cellular adjustments that enhance survival. A condition that plant cells regularly encounter is transient low oxygen stress (hypoxia), due to poor oxygen diffusion into internal tissues or a decline in external oxygen availability as a result of flooding or encasement within compact soil or ice [1,2]. The regulation of transcription and translation in response to hypoxia is well-documented, but whether there is integration of these nuclear and cytoplasmic processes has yet to be explored.

Gene regulation begins at the DNA level with the accessibility of transcription factors to their binding sites which is influenced by the topological organization of chromatin and epigenetic factors including cytosine methylation of DNA and specific variants or post-translationally modified histones that form the octamer core of nucleosomes. These include high levels of the tri-methylated Histone 3 lysine 27 (H3K27me3) in the gene body near the 5' transcriptional start site (TSS) of transcriptionally repressed genes and the prevalence of H3K4me3

near the TSS of actively transcribed genes [3,4]. Moreover, enrichment in acetylated Histone H3 lysine tails (H3K9Ac, H3K14Ac) that reduce interactions between DNA and histones is correlated with upregulation of genes in response to environmental stress. Often the Histone 2A variant H2A.Z is located at the first (+1) nucleosome within the gene body, a configuration proposed to reduce the energy required for commencement of transcriptional elongation, as observed under osmotic stress [5–7]. A cadre of chromatin remodelers are responsible for dynamically regulating the presence of a nucleosome-depleted region just 5' of the TSS. These enzymes are ATP dependent and therefore could be influenced by limitations in cellular ATP content under hypoxia. Use of DNase I hypersensitivity site mapping has exposed dynamics in chromatin near TSSs and other regions in response to changes in light and other environmental factors [8,9], but chromatin dynamics have not been explored in response to transient hypoxia.

As transcription commences, the phosphorylation of specific residues within the heptad repeats of the carboxyl terminal domain (CTD) of RNAPII orchestrate interactions with factors that facilitate transcription-coupled histone modifications as well as the co-transcriptional processes including 5' capping, splicing, polyadenylation, and nuclear export [10,11]. Phosphorylation of Serine 2 and 5 (Ser2P, Ser5P) are the major CTD modifications, with Ser5P characteristic of RNAPII at initiation and Ser2P associated with active elongation and 3' end formation. The transcription elongator complex P-TEFb (positive

transcription elongation factor b) includes two kinases CDKC2 and CYCT1 that are responsible for Ser2P of the CTD repeats in *Arabidopsis* [12].

Histone H3 modifications and Histone H2 replacement with H2A.Z occurs during transcriptional elongation, facilitated by interaction of the histone modifying machinery such as RNAPII-associated factor 1 complex (PAF1-C) with the specifically phosphorylated CTD. The question of whether histone modifications and variants contribute to transcription or merely report transcriptional activity is debated in plants [3] but there is increased acceptance that histone marks promote factors critical for progression in the steps of the transcription cycle [4]. For example, the positioning of H3K4me3 near the 5' terminus is a prerequisite for modification of Histone H3 lysine 9 acetylation (H3K9Ac). More recently, the genomic distribution of Histone H3 modifications along a transcription unit was shown to report the duration of time RNAPII-Ser2P-CTD resides in a specific location along a transcription unit [13]. In animals, promoter proximal pausing of RNAPII 30-60 nt downstream of the TSS acts as a checkpoint for transcription that is common among genes activated by stimuli such as heat stress [14]. However, global nuclear run-on sequencing (GRO-seq) in *Arabidopsis* seedlings found limited evidence of promoter proximal pausing but confirmed 3' pausing particularly on long genes with high CpG methylation near the polyadenylation site [15]. The correlation found between nascent transcripts and steady-state mRNA levels supports the conclusion that transcription is mostly regulated at the level of initiation rather than during

elongation, at least under the optimal growth conditions that were evaluated. Here, we considered that hypoxia might present a situation where chromatin accessibility, RNAPII elongation and histone modifications may be co-regulated to conserve cellular ATP either during transcription or at downstream steps including the highly energy consuming process of translation.

Our previous work demonstrated that hypoxia stress elicits rapid transcriptional and translational control in seedlings and specific cell types of *Arabidopsis* [16–19]. Transcriptional activation involves the evolutionarily conserved group VII ethylene response factor (ERFVII) transcription factors, whose conditional accumulation is required for regulation of metabolism and development to promote survival of hypoxia [20–28]. Critical to ERFVII function is their selective stabilization mediated by the N-end rule pathway of targeted proteolysis [22,23,27,29]. The constitutively synthesized ERFs RELATED TO APETALA 2.12, 2.13, and 2.13 (RAP2.12, RAP2.2, and RAP2.3) transactivate hypoxia-responsive genes in protoplasts [28,30,31] through an evolutionarily conserved *cis*-acting motif called the hypoxia responsive promoter element (HRPE) [22,30] and other stress-responsive genes via a multimeric GCC motif [32,33]. The abundance and activity of the ERFVIIs is highly controlled, as genes they transactivate include PLANT CYSTEINE OXIDASEs [29,34] that promotes their turnover and the transcription factor HYPOXIA RESPONSE ATTENUATOR 1 (HRA1) that in turn negatively regulates ERFVII function [31,35]. However, of the ~50 genes that are highly upregulated in response to

hypoxia, only about 50% have a recognizable HRPE within their promoter [30] and no genome-scale analyses of ERFVII binding has been reported.

There is evidence of post-transcriptional regulation at multiple levels in response to hypoxia in seedlings of *Arabidopsis*. This includes alternative splicing ([16–18] and increased retention of transcripts within the nucleus [36]. Translation is dramatically downregulated and more selective under hypoxia, presumably as a mechanism to conserve energy [16–18]. Moreover, mRNAs that hypoxia-upregulated and successfully recruited to ribosomes for translation do so by avoiding sequestration in translationally inactive complexes resembling stress granules via the RNA-binding protein OLIGOURIDYLATE BINDING PROTEIN 1C (UBP1C) [19] and CALMODULIN BINDING PROTEIN 38 (CML38) [37]. No recognizable RNA sequence elements are correlated with maintenance of translation under hypoxia besides low GC content and thermostability of the 5' untranslated region [19,38,39]. mRNAs that maintain translational competency are those that show strong upregulation in response to the hypoxia [17]. The finding that promoter sequences confer translational competency to mRNAs during starvation in yeast [40] raises the interesting question whether ERFVII upregulated transcription provides an advantage under hypoxia.

Here we hypothesized that the hypoxia response genes (*HRGs*), that display pronounced increases in abundance and effective translation, may benefit from coordination of their transcriptional, co- and post-transcriptional regulation. To gain deep insight, we monitored histone modifications and

variants, chromatin accessibility, and the distribution of RNAPII-Ser2P along gene bodies of seedlings deprived of oxygen. We also identified genes bound by an ERFVII. These assays focused on chromatin and transcription were contrasted to RNA-seq data obtained for three populations of RNA: nuclear RNA, total polyadenylated RNA and ribosome-associated polyadenylated RNA. These data expose multiple modes of adjustments in the nuclear regulation of genes in response to hypoxia and connections with translational activity.

2.3. Materials and methods

2.3.1. Genetic Material

The following genotypes were used for genome wide experiments: Col-0, Histone modification ChIP-seq, RNAP II ChIP-seq; *pHTA11:HTA11-3xFLAG* [7], H2A.Z ChIP-seq; *pUBQ:NTF/pACT2:BirA* [8,41], ATAC-seq, nRNA-seq, polyA mRNA-seq; *p35S:HF-RPL18* [43], TRAP-seq, mRNA-seq; *p35S:C2A-HRE2-HA* [22], HRE2 ChIP-seq; *p35S:FLAG-RAP2.12* [30], RAP2.12 ChIP-seq.

2.3.2. Growth and Treatment Conditions

Arabidopsis seeds were surface sterilized by incubation in 70% EtOH for 5 min, followed by incubation in 20% (v/v) bleach, 0.01% (v/v) TWEEN-20, followed by three washes in ddH₂O for 5 min, in triplicate. Sterilized seeds were placed onto 1x MS media (1.0x Murishige Skoog (MS) salts, 0.4% (w/v) Phytigel

(Sigma-Aldrich), and 1% (w/v) Suc, pH 5.7) in 9 cm² Petri dishes and stratified by incubation at 4°C for 3 d in complete darkness. Following stratification, plates were placed vertically into a growth chamber (Percival) with 16h light / 8h dark cycle at ~120 μmol photons·s⁻¹·m⁻², at 23 °C for 7 d.

2.3.3. Seedling Treatments

For hypoxic stress, seedlings were removed from the growth chamber at Zeitgeber time (ZT) 16 and were subjected to hypoxic stress by bubbling argon gas into sealed chambers in complete darkness for 2 or 9 h at 24 °C. The chamber set-up was as described by [16]. Oxygen partial pressure in the chamber was measured with the NeoFox Sport O₂ sensor and probe (Ocean Optics). Control samples were placed in an identical chamber that was open to ambient air under the same light and temperature conditions. Post hypoxia aeration was achieved by removing plates from the chamber and placing them into identical chambers in ambient air. Tissue was rapidly harvested into liquid N₂ and stored at -80 °C.

2.3.4. Chromatin Immunopurification (ChIP)

ChIP was performed according to [41] with minor modifications. Seedlings were grown on Petri dishes and treated as described above. For the HRE2 ChIP experiments, seedlings were pre-treated by flooding with 10 mL of 100 μM Calpain inhibitor IV (American Peptide) and 1% (v/v) DMSO for 2 h prior to the

hypoxia treatment. For all genotypes, following hypoxia treatment, seedlings were immediately cross-linked in 1% (v/v) formaldehyde nuclei purification buffer (NPB: 20 mM MOPS, pH 7.0, 40 mM NaCl, 90 mM KCl, 2 mM EDTA, and 0.5 mM EGTA) in a vacuum chamber under house vacuum for 10 min. The reaction was quenched by addition of 1.875 mL 5M glycine to reach a concentration of 125 mM followed by vacuum infiltration for 5 min. This was followed by three washes in 30 mL ddH₂O. Seedlings were blotted dry and then pulverized under liquid N₂. To isolate nuclei, 0.5 g tissue was thawed to 4°C in 10 mL NPB that additionally contained 0.5 mM spermidine, 0.2 mM spermine, and 1 X Plant Protease Inhibitor Cocktail (Sigma-Aldrich P9599). Nuclei were pelleted by centrifugation in 4°C at 1200g for 10 min. The nuclei were washed in 10 mL NPbt (NPB, 0.1% Triton X-100) and pelleted by centrifugation in 4°C at 1200g for 10 min in triplicate. Following the final NPbt wash, the supernatant was aspirated and the nuclei pellet was resuspended in 120 µL NPB, and lysed with the addition of 120 µL 2X nuclei lysis buffer (NLB: 100 mM Tris, pH 8.0, 20 mM EDTA, 2% [w/v] SDS, and 2 X Plant Protease Inhibitor Cocktail) by vortexing for 2 min at 23-25 °C. The chromatin was sheared into 200 to 600 bp fragments by sonication (Diagenode, Denville, NJ) with 40 cycles of 30 s ON and 30 s OFF at 4°C. The sample was cleared by centrifugation at 16,000g at 4°C for 2 min and the supernatant was diluted ten-fold with dilution buffer (DB: 16.7 mM Tris, pH8.0, 167 mM NaCl, 1.1% (v/v) Triton X-100, 1.2 mM EDTA). The entire chromatin fraction was precleared by incubation with uncoupled Protein G

Dynabeads (ThermoFisher) for 30 min followed by collection of the supernatant. Three hundred microliters of the input chromatin (1 mL for HRE2) was incubated with 3 μ L of anti-H3K4me3 (ab8580, Abcam), anti-H3K27me3 (07-449, EMD Millipore), anti-H3K9Ac (ab4441, Abcam), anti-H3K14Ac (ab52946, Abcam), anti-p-CTD RNA Polymerase II (ab5095, Abcam), anti-FLAG (F1804, Sigma), or anti-HA (h3663, Sigma) for 4 h (overnight for HRE2) while rocking at 4°C. Protein G Dynabeads (30 μ L) were washed in DB, added to the chromatin fraction and allowed to incubate for 2 h while rocking at 4°C. Beads were magnetically captured and washed sequentially in 1 mL for 5 min with four buffers: low NaCl₂ wash buffer (20 mM Tris, pH 8.0, 150 mM NaCl, 0.1% [w/v] SDS, 1% [v/v] Triton X-100, 2mM EDTA), high NaCl₂ wash buffer (20 mM Tris, pH 8.0, 500 mM NaCl₂, 0.1% [w/v] SDS, 1% [v/v] Triton X-100, 2mM EDTA), LiCl wash buffer (10 mM Tris, pH 8.0, 250 mM LiCl, 1% [w/v] sodium deoxycholate, 1% [v/v] Nonidet P-40, 1 mM EDTA), and standard TE buffer (10 mM Tris, pH 8.0, 1 mM EDTA). The beads were then washed twice with 10 mM Tris, pH 8.0 and resuspended in 25 μ L of tagmentation reaction mix (10 mM Tris, pH 8.0, 5 mM MgCl₂, 10% [w/v] dimethylformamide) containing 1 μ L of Tagment DNA Enzyme (NExtera DNA Sample Prep Kit, Illumina) and incubated at 37°C for 1 minute. Beads were washed twice with low NaCl₂ wash buffer and then once in standard TE buffer. The chromatin was eluted from the beads by heating for 15 min at 65°C in elution buffer (EB: 100 mM NaHCO₃ and 1% [w/v] SDS) and reverse cross-linked by the addition of 20 μ L 5 M NaCl₂ with heating at 65°C overnight. Following reverse

cross-linking, Proteinase K (0.8 units; New England Biolabs) was added and the sample was incubated at 55°C for 15 min. The final tagged ChIP-DNA sample was purified using Qiagen MinElute columns according to the manufacturer's instructions and eluted with 14 μ L of EB.

2.3.5. ChIPmentation Library Preparation

ChIPmentation library preparation for short-read sequencing (ChIP-seq) was performed according to [70], with minor modifications. Final library enrichment was performed in a 50 μ L reaction containing 12 μ L ChIP DNA, 0.75 μ M primers, and 25 μ L 2X NEBNext PCR Master Mix. To determine the appropriate amplification cycle number, a qPCR reaction was performed on 1 μ L of tagmented ChIP DNA in a 10 μ L reaction volume containing 0.15 μ M primers, 1X SybrGreen (ThermoFisher), and 5 μ L 2X NEBNext PCR Master Mix (New England Biolabs) with the following program: 72°C for 5 min, 98°C for 30 s, 24 cycles of 98°C for 10 s, 63°C for 30 s, 72°C for 30 s, and a final elongation at 72°C for 1 min. Libraries were amplified for n cycles, where n is equal to the rounded up Cq value determined in the qPCR reaction. Amplified libraries were purified and size selected using SPRI AMPure XP beads (Beckman). AMPure XP beads were added at a 0.7:1.0 bead to sample ratio, and the remaining DNA was recovered by the addition of AMPure XP beads at a 2.0:1.0 bead to sample ratio and eluted in 13 μ L of EB. Quantification of the final libraries was performed with Quant-iT PicoGreen (ThermoFisher), and library fragment distribution was

evaluated by use of the the Agilent 2100 Bioanalyzer using the high sensitivity DNA chip. Final libraries were multiplexed to >5 nM final concentration and sequenced on the HiSeq 3000/4000 at the UC Davis DNA Technologies Core.

2.3.6. Isolation of Nuclei Tagged in Specific Cell Types (INTACT)

INTACT was performed according to [41] with modifications. Frozen pulverized tissue (0.5 g) of *pUBQ:NTF/pACT2:BirA* seedlings was thawed in 10 mL of cold NPB buffer and was filtered through 70 μ M nylon mesh. Nuclei were pelleted by centrifugation at 1200g for 7 min at 4°C, and the nuclear pellet was resuspended and washed twice in NPB containing 0.1% (v/v) Tween-20 (NPBt), and the washed pellet was resuspended in 1 mL of NPB. M280 Streptavidin Dynabeads (10 μ L; Invitrogen) washed with 1 mL NPB and resuspended in the original volume were added to the nuclei and the sample was allowed to rock for 30 min at 4°C. The bead-nuclei mixture was diluted to 14 mL with NPBt and incubated with rocking for 30 s at 4°C. The beads were magnetically collected, the supernatant removed, the beads washed twice with NPBt, and resuspended in 1 mL of NPBt. A 25 μ L fraction was removed to quantify nuclei following addition of 1 μ L of 1.0 μ g/ μ L Propidium Iodide following incubation on ice for 5 min before visualization and quantification with a C-Chip hemocytometer (Incyto) using a fluorescence microscopy.

2.3.7. Assay for Transposase Accessible Chromatin (ATAC)

Fifty-thousand INTACT-purified nuclei from root tissue were magnetically captured and any remaining supernatant was removed. Nuclei were resuspended in 50 μ L of transposition mix (1X TD buffer, 2.5 μ L TDE1 transposase) and were incubated for 30 min at 37°C with occasional mixing. The transposed DNA was purified with Qiagen MinElute PCR purification columns, and the purified DNA was eluted in 11 μ L of EB. For library construction, a reaction was prepared to amplify the sample in a two step process. The reaction was assembled containing transposed DNA (10 μ L), 5 μ M Ad1.1 and an indexing primer [71], 1X NEBNext High Fidelity PCR mix and cycled in the following program: 72°C 5 min; 98°C 30 s; 3 cycles of 98°C 10 s, 63°C 30s, 72°C 1 min; 4°C and the samples were placed on ice. Then a qPCR was performed using an aliquot of the amplified library with the following program: 98°C for 30 s; 20 cycles of 98°C for 10 s, 63°C for 30 s, 72°C for 1 min. The original PCR reaction was resumed for n additional cycles, where n is the cycle at which the qPCR reaction was at 1/3 of its maximum fluorescence intensity. Amplified DNA was then purified with Qiagen MinElute PCR purification columns and eluted in 20 μ L of EB. Amplified libraries were purified and size selected for fragments between 200 to 600 bp using SPRI AMPure XP beads (Beckman). AMPure XP beads were added at a 0.55:1.0 bead to sample ratio, and the remaining DNA was recovered by the addition of AMPure XP beads at a 1.55:1.0 bead to sample ratio and eluted in 13 μ L of EB. Library concentration was determined using the NEBNext

(New England Biolabs) library quantification kit. Final libraries were multiplexed to >5 nM final concentration and sequenced on the HiSeq 3000/4000 at the UC Davis DNA Technologies Core.

2.3.8. INTACT followed by Nuclear RNA Extraction

Fifty-thousand INTACT-purified nuclei were collected magnetically and the supernatant was removed, and resuspended in 20 μ L of NPB. Nuclear RNA was extracted and purified using the Qiagen RNeasy Micro kit, and eluted in 20 μ L of H₂O. The RNA was then DNaseI digested with with 1 μ L (2U/ μ L) of Turbo DNaseI (Ambion) and incubated for 30 min at 37°C. DNaseI was inactivated by adding EDTA to 15 mM, and heated at 75°C for 10 min, centrifuged at 2000g for 5 min and transferred to a new tube. The RNA was then purified using AMPure XP beads and eluted in 15 μ L H₂O. Ribosomal RNA was depleted from the sample using the plant Ribo-Zero rRNA removal kit (Illumina) according to the manufacturer's instructions.

2.3.9. Total RNA Isolation and PolyA RNA Affinity Purification

Total RNA was extracted from 50 mg frozen pulverized tissue by addition of 800 μ L Trizol (Life Sciences) and incubation for 5 min at room temperature. Chloroform (200 μ L) was added and the sample briefly vortexed and incubated at room temperature for 3 min. Following incubation, the samples were centrifuged at 12,000g for 15 min at 4°C, and the clear phase was transferred to a new tube.

RNA was precipitated by addition of 500 μ L isopropanol, vortexing briefly, and incubation at room temperature for 10 min, and pelleted by centrifugation at 12,000g for 10 min at 4°C. Purified RNA was resuspended in 50 μ L EB and DNaseI digested with 2.5 μ L of TURBO DNaseI (Ambion) for 30 min at 37°C. DNaseI was inactivated by addition of EDTA to 15 mM and heat treatment at 75°C for 10 min. The RNA was pelleted by centrifugation at 2000g for 5 min and transferred to a new tube. The RNA was then purified using AMPure XP beads and eluted in 50 μ L H₂O. For polyA RNA selection, the total RNA sample was heated for 2 min at 65°C and placed on ice, after which 50 μ L of Dynabeads Oligo (dT)₂₅ pre-washed with wash buffer (WB: 10 mM Tris, pH 7.5, 150 mM LiCl, 1 mM EDTA) were added and the sample incubated at room temperature for 15 min with agitation. The beads were magnetically separated and washed twice with WB. For RNA elution, 50 μ L EB was added and the sample heated for 2 min at 80°C and the eluted RNA was transferred to a new tube. The polyA RNA selection was repeated a second time and eluted in a volume of 16 μ L.

2.3.10. Translating Ribosome Affinity Purification (TRAP)-seq

TRAP of mRNA-ribosome complexes was performed following the procedure of [18]. Briefly, pulverized tissue (1 mL) from the *35S:HF-RPL18* genotype was added to 5 mL of polysome extraction buffer (PEB: 200 mM Tris, pH 9.0, 200 mM KCl, 25 mM EGTA, 35 mM MgCl₂, 1% PTE, 1 mM DTT, 1 mM PMSF, 100 μ g/mL cycloheximide, 50 μ g/mL chloramphenicol) containing 1%

detergent mix (20% (w/v) polyoxyethylene(23)lauryl ether, 20% (v/v) Triton X-100, 20% (v/v) Octylphenyl-polyethylene glycol, 20% (v/v) Polyoxyethylene sorbitan monolaurate 20) and homogenized with a glass homogenizer on ice. The homogenized mixture was allowed to stand for 10 min on ice and then centrifuged at 16,000g at 4°C for 15 min. Following centrifugation, the supernatant was transferred to a new tube and filtered through one layer of Miracloth (Millipore) to produce the clarified extract.

Protein G Dynabeads (50uL; ThermoFisher) were prewashed twice with 1.5 mL of wash buffer (WB-T: 200 mM Tris, pH 9.0, 200 mM KCl, 25 mM EGTA, 35 mM MgCl₂, 5 mM PMSF, 50 µg/mL cycloheximide, 50 µg/mL chloramphenicol) by suspension and magnetic collection, with final re-suspension in the original volume. These were added to the clarified tissue extract and incubated at 4°C for 2 h with gentle rocking. The beads were collected magnetically, the supernatant was removed, and the beads were gently resuspended in 6 mL WB-T for 5 min at 4°C with rocking. This wash step was repeated two additional times, after which the beads were resuspended in 1 mL WB-T and transferred to a new tube and the supernatant was removed.

RNA was purified from the sample and the reserved clarified extract by addition of 105 µl of LBB (LBB: 100 mM Tris, pH 8.0, 500 mM LiCl, 10 mM EDTA, 1% (w/v) SDS, 5 mM DTT, 1.5% (v/v) Antifoam A, 5 µl/mL 2-mercaptoethanol) followed by vortexing for 5 min. Samples were incubated at room temperature for 10 min, centrifuged at 13,000g for 10 min and transferred to

a new tube. Poly(A)⁺ RNA selection was performed by addition of 1 μ l of 12.5 μ M biotin-20nt-dT oligos (Integrated DNA Technologies) to 200 μ l of the TRAP or RNA lysate sample, followed by incubation at room temperature for 10 min. In a separate tube 20 μ l magnetic streptavidin beads (New England Biolabs) were washed with 200 μ l LBB. The lysate was added to the washed beads and incubated at room temperature for 10 min with gentle agitation. The beads were magnetically separated and washed sequentially with wash buffer A (WBA: 10 mM Tris, pH 8.0, 150 mM LiCl, 1 mM EDTA, 0.1% (w/v) SDS), wash buffer B (WBB: 10 mM Tris, pH 8.0, 150 mM LiCl, 1 mM EDTA), and low salt buffer (LSB: 20 mM Tris, pH 8.0, 150 mM NaCl, 1 mM EDTA). Following washes, the pellet was resuspended in 16 μ l 10 mM Tris, pH 8.0 containing 1 mM 2-Mercaptoethanol and heated at 80°C for 2 min. The beads were magnetically collected, the supernatant was transferred to a new tube, and the poly(A)⁺ RNA selection process was repeated, and the samples combined in a new tube before storage at -80°C.

2.3.11. Bioinformatic Analyses

For all high throughput outputs, short reads were trimmed using FASTX-toolkit to remove barcodes and filter short and low quality reads prior to alignment to the TAIR10 genome with Tophat2. Read quality reports were generated using fastqc. For all datasets, counting of aligned reads was performed on entire transcripts (GenomicFeatures, citation) using the latest

Araport 11 annotation (201606) and reads per kilobase of transcript per million mapped reads (RPKM) values were calculated. Differentially expressed genes were determined by edgeR, $|FC| > 1$, $FDR < 0.01$.

Data visualization and file generation: Bigwig files for Integrated Genome Viewer (IGV) visualization were generated from aligned bam files and normalized by RPKM values using the deepTools command bamCoverage with the -normalizeUsingRPKM specification. Within IGV, all chromatin based outputs were normalized to the same scale and all RNA outputs were normalized to a separate scale.

Peak calling: For ChIP-seq and ATAC-seq datasets, peak calling was performed using independent replicates as input for HOMER using the findPeaks command [72]. Peaks identified from comparable sampling times (2 h, 9 h) were combined, and counting was performed on individual replicates. Peaks were annotated using the HOMER command annotatePeaks.pl. Differential regulation of peaks was performed using edgeR.

Motif discovery: HRE2 peaks identified by HOMER command findPeaks were used as an input for the HOMER command findMotifsGenome.pl. The matrix for the top HRE2 motif ($P:1e-69$) was used as input the MEME command ceqlogo to generate the motif logo.

DAP-seq motif analysis: Sequences of promoter regions spanning 1 kb upstream to 500 bp downstream of the TSS were extracted for genes within each cluster. The promoter sequences were compared against each TF, per TF

family, using motif matrices identified by [52]. The number of significant motifs identified within the promoters of each cluster were quantitated and normalized to the number of genes within each cluster.

t-distributed stochastic neighbor embedding (t-SNE): t-SNE analysis was performed according to [73]. Briefly, a principal component analysis was performed using RPKM values for each replicated dataset and timepoint. t-SNE was then performed on PCs 1-10 and the results were plotted using ggplot2.

2.3.12. Bioinformatic tools

Analyses were performed with Bioconductor R packages particularly the Next Generation Sequencing analysis software of systemPipeR [74]. Programs used within that platform included:

BiocParallel [75]

BatchJobs [76]

Tophat [77]

GenomicFeatures [78]

GenomicRanges [78]

edgeR [79]

gplots [80]

ggplot2 [81]

RColorBrewer [82]

Dplyr [83]

biomaRt [84]

ChIPseeker [85]

rtracklayer [86]

Rtsne [87]

Python/Perl packages

fastx_toolkit [88]

Fastqc [89]

MEME [90]

Homer [72]

deepTools [91]

circos [92]

Bedtools [93]

samtools [94]

2.4. Results

2.4.1. Establishment of a multiscale dataset for evaluation of dynamics in gene regulatory control in response to hypoxic and reoxygenation stress

To gain a more comprehensive understanding of dynamics in protein-coding gene transcript abundance from the stage of transcriptional elongation through mRNA translation in response to short term hypoxic stress, we

performed a series of chromatin and RNA-based assays on 7-day-old seedlings. Growth conditions as well as the control (normoxic, 2NS) and non-lethal hypoxic stress (2 h hypoxia, 2HS) were identical to those we used previously to evaluate the transcriptome, translome and ribosome footprints [16–18]. At the DNA level, we adopted chromatin immunopurification sequencing (ChIP-seq) of the Ser2P phospho-isoform of the RNAPII CTD to monitor genes undergoing transcriptional elongation. To obtain the nuclear pool of gene transcripts (nRNA) we utilized Nuclei Tagged in Specific Cell Types (INTACT) [41][42]. RNA-seq libraries were prepared for rRNA-depleted nRNA [42], total cellular polyadenylated RNA (polyA; transcriptome) and polyadenylated ribosome-associated RNAs obtained by Translating Ribosome Affinity Purification (TRAP; translome) [17,43].

All RNA-seq libraries were prepared in the same manner, with the exception that nRNA was rRNA subtracted rather than oligo(d)T selected, so that transcripts at any stage of synthesis or maturation would be included in the population. Each duplicated ChIP-seq and triplicated RNA-seq sample yielded over 5 million reads that mapped to gene bodies (exons and introns). Reproducibility between biological replicates was generally high, with polyA RNA displaying the least and nRNA the greatest variation (Supplemental Data S1a). The four gene expression readouts were distinguishable at the global scale when the individual samples were compared by t-Distributed Stochastic Neighbor Embedding (Fig. 1b), with polyA RNA plotting between the nuclear and

ribosome-associated RNA samples. Our analysis additionally included nRNA and polyA RNA samples obtained for seedlings that were hypoxic-stressed for 2 h and then reoxygenated for 1 h (1R) or hypoxic-stressed for 9 h (9HS), both sub-lethal stresses. This combined RNAPII and transcript-based deep-sequence dataset provides a foundation to address the integration of chromatin and transcription with nuclear and cytoplasmic post-transcriptional processes that culminate in mRNA translation.

Dynamics in post-translational modifications of histones and regions of chromatin accessibility may also contribute to transcriptional regulation in response to oxygen availability. Therefore, we used ChIP-seq to survey Histone H3 modifications generally associated with gene activation (H3K4me3, H3K9Ac, and H3K14Ac) and repression (H3K27me3), as well to evaluate the distribution of the Histone H2 variant (H2A.Z) associated with regulation of chromatin accessibility in connection with external stimuli in plants [5–7,44,45] (Fig. 1a). To evaluate dynamics in regions of accessible chromatin we performed Assay for Transposase-Accessible Chromatin sequencing (ATAC-seq) on INTACT-purified nuclei. Finally, to monitor binding of a ERFVII, ChIP-seq was performed with lines expressing a version of RAP2.12 or HRE2 that is not a target of N-end rule turnover, yielding an informative dataset for HRE2 in hypoxic seedlings (2HS). Together, these genome-scale DNA- and RNA-based datasets can be used to evaluate individual or groups of genes.

To begin the multiscale analysis, we surveyed the distribution of read abundance (reads per kilobase per million reads, RPKM) under the two conditions (2NS and 2HS) across annotated gene bodies for the four modified histones, H2A.Z, Ser2P and specific RNA subpopulations. As expected for comparison of changes in chromatin versus transcripts, the range in read abundance was lower for the ChIP-seq than the RNA-seq outputs (Fig 1c). At this global scale, the read distributions showed limited change in response to hypoxic stress. To ensure the hypoxic response was as expected, we tracked *ALCOHOL DEHYDROGENASE 1 (ADH1)*, which is required for anaerobic metabolism and survival of hypoxia [1] and one of the previously identified group of 49 ubiquitously up-regulated hypoxia-responsive genes (HRGs) [1][18,46] (Fig. 1c) Comparison of the abundance of the H3 modifications and H2A.Z on *ADH1* under the two conditions exposed a slight decrease in H3K27me3 and H2A.Z levels, with a more pronounced increase in H3K4me3 and H3K9Ac. By contrast, the association of H3K14Ac with the *HRGs*, including *ADH1*, was unchanged. Read distributions for the four transcript readouts were consistent with expectations. First, the range in Ser2P abundance was narrower than that of nRNA, polyA, and ribosome-associated mRNA. Second, an increase in Ser2P corresponded to elevation of *ADH1* transcripts in all three RNA populations. Together, these results confirm that rapid modifications of nucleosome features accompany conditional changes in RNAPII engagement and transcript

accumulation, indicating these datasets may be valuable for study of integrated nuclear and cytoplasmic gene regulation in response to a hypoxic stress.

2.4.2. Histone modifications and chromatin accessibility near transcription start sites are reversibly regulated by hypoxic stress and reoxygenation

To gain a global perspective of dynamics in chromatin features in response to hypoxia, the average distribution of the histone variant H2A.Z and four H3 modifications (H3K27me3, H3K4me3, H3K9Ac, H3K14Ac) were plotted relative to each protein-coding gene body (Fig. 2a). Under control conditions, the H3 modifications associated with gene activity were enriched at the 5' end of the first exon, just downstream of transcription start site (TSS), whereas H3K27me3 was distributed more evenly across the gene body. This and the other histone marks tapered off just 5' of transcription end site (TES), determined from the most frequent site of polyadenylation. As expected, levels of all modified Histone H3 and H2A.Z were generally lower in the 1 kb region upstream of the TSS. Downstream of the TES these nucleosome features were more evenly distributed along gene body region, except for H3K27me3, which was notably lower. Following 2 h of hypoxic stress, a similar distribution profile was observed for each histone modification monitored. The reduction in H3K4me3 was the most dramatic, followed by an increase in H3K14Ac particularly proximal to the TSS. The 5' proximal placement of H3K4me3, H3K9Ac and H3K14Ac and broad

distribution of H3K27me3 across the gene body is consistent with prior reports [47,48].

To determine whether hypoxia or reoxygenation influenced the openness of chromatin regions, defined by accessibility to Tn5 insertion, we surveyed dynamics in genome-wide distribution of ATAC-seq reads (Fig. 2b) and found they were located predominated within 500 bp 5' of the TSSs as reported by others for *Arabidopsis* [49–51]. Hypoxic stress increased the height of the ATAC-seq read peak, within 100 bp 5' of the TSS and > 300 bp 3' of the TES, relative to control samples. Remarkably, the peak was further amplified following 1 h of reoxygenation (1R). This lead us to test whether ATAC-seq reads around the TSS and TES was altered by more prolonged but sublethal hypoxic stress. We observed less accessibility after 9 h of stress (9HS) relative to control seedlings maintained under the same light regime (9NS). In all five treatment samples, the ATAC-seq reads that mapped within genic regions were generally unchanged. Altogether, these data suggest that chromatin that is accessible to Tn5 insertion due to space between nucleosomes is dynamically regulated by sublethal hypoxic stress and reoxygenation, and is generally limited to a region of ~200 bp 5' of the TSS and a broader region of ~400 bp 3' of the TES.

To map chromatin accessible regions near individual genes, the ATAC-seq data was processed to identify transposase hypersensitive sites (THS) by use of the peak-calling program HOMER for each condition and time point. The mean width of THSs was ~160 nt. Consistent with Fig. 2b, a greater number of

THSs were detectable at 2HS and 1R than at 2NS. Similarly, fewer THSs were found at 9HS than 9NS. More than 80% of the THSs identified for each condition mapped within 1 kb from annotated TSSs, the presumed promoter regions (Fig. 2d). The pairwise comparison of the peak volumes of THSs ranging from 130 to 1000 bp that mapped at any location was used to identify differentially accessible chromatin regions ($|\text{Log}_2$ fold change $|\geq 1$; p value < 0.05) (Fig. 2e) (Supplemental Data S1b). A short duration of hypoxia resulted in 687 upregulated THSs, including 32 with greater than a 4-fold change. The number of upregulated THSs increased to 1262 following 9 h of stress. Over 1265 and 1207 THSs were downregulated at 2HS and 9HS, respectively. Regional changes in chromatin conformation upon reoxygenation were more similar to hypoxic than control seedlings. The comparison of the 2 h hypoxic stress and reoxygenation samples exposed >2300 regions that were more open and >3000 that were closed after reaeration. Together, these data demonstrate that chromatin accessibility is highly orchestrated in response to changes in oxygen availability.

2.4.3. Survey of chromatin and RNA data for genes groups known to be opposingly regulated by hypoxia

As the initial global analysis of the chromatin and RNA outputs indicated changes in response to hypoxia, we determined the mean \log_2 fold change for the 20,649 genes (average CPM > 2 in any sample), allowing differentially up- and down-regulated genes (DRGs) to be identified for each of the analyses

(Supplemental Data S1c). The fold-change values were compared at the genome-scale (Fig. 3a) and for two groups of genes that show coordinate but distinct regulation in response to hypoxia, the 49 HRGs and 223 cytosolic ribosomal proteins (RPs) [16–18] (Supplemental Fig. 1).

Consistent with prior reports, *HRG* mRNAs were highly induced and effectively translated, whereas the RP mRNAs were maintained at pre-stress levels in the transcriptome but were less engaged in translation (Supplemental Figs. 1, 2). The significant increase in Ser2P reads on the *HRGs* was accompanied by an even more pronounced rise measured for nRNA. As a group, the *HRGs* increased in both the polyA and TRAP RNA populations. For the *RPs*, Ser2P reads per transcript declined slightly, indicating their overall transcription is only somewhat reduced during this short-term stress. Interestingly, this was accompanied by a slight rise in RP transcripts in the nuclear pool, despite a maintenance at the polyA RNA level. Confirming prior results, *HRG* mRNAs were translated at levels similar to their abundance, whereas *RP* mRNAs were translationally downregulated under the stress (Supplemental Figs. 1, 2).

The FC values for the histone data surveyed indicated dynamics in histone modifications and H2A.Z association in response to hypoxia (Fig. 3b). By comparing the change in Ser2P and H3K4me3, H3K9Ac or H3K14Ac modifications as well as change in H2A.Z incorporation, we identified a positive correlation between Ser2P and H3K9Ac (Fig 3b; $r = 0.43$; $r = 0.17$ for *HRGs*) and a negative correlation between change in Ser2P and H2A.Z (Fig 3c; $r = -0.27$).

H2A.Z levels versus Ser2P were markedly negatively correlated for *HRGs* ($r = -0.79$), due to a pronounced decline in H2A.Z association under the stress (Fig. 3a). In fact, the association of this H2 variant declined significantly for 7 *HRGs* but showed no change for any of the *RPs*. For H3K9Ac, levels significantly increase for 16 *HRGs*, but not for any of the *RPs*. Thus, an increase in H3K9Ac and decline in H2A.Z is a characteristic of *HRGs* and is absent from the opposingly regulated *RPs*.

A genome browser was used to view the data for representative genes for the 2 h hypoxic stress and control samples (Fig 3f). Both *ADH1* and *PLANT CYSTEINE OXIDASE2 [PCO2]* showed evidence of upregulation in H3K9Ac, Ser2P, nRNA, polyA and TRAP data characteristic of *HRGs*. For both, the decrease in H2A.Z is evident (*ADH1*, $-0.33 \log_2$ FC; *PCO2*, $-1.15 \log_2$ FC). *PCO2* provides an example of an *HRG* with hypoxia-elevated H3K4me3 and H3K14Ac. Both of these genes show an increase in ATAC-seq reads near their TSS and are bound by HRE2. *RPL37B* is a typical *RP*, with relatively minor changes in all readouts. An example of a housekeeping gene, *ACT2* had maintained H3K4me3, H3K9Ac, and H3K14Ac, along with a region of accessible chromatin flanking the TSS. Lastly, the heat stress-induced gene (*HEAT SHOCK PROTEIN 70-4 [HSP70-4]*) provides an example of a gene with a marked increase in Ser2P association along the genic region, concomitant with an increase in nRNA but no elevation of polyA RNA. The intriguing patterns observed for the *HRGs*, *RPs*, *HSP70-4* and other genes we surveyed led us to perform a more systematic

analysis to identify similarly modulated genes across the continuum from transcriptional elongation to translation.

2.4.4. Distinct levels of gene regulation are observed for subsets of genes

To further explore possible coordination of nuclear and cytoplasmic processes in response to hypoxia, the dynamics in transcript elongation (Ser2P), nuclear RNA, polyA mRNA, and ribosome-associated mRNA levels (TRAP) were analyzed in combination (Fig 3b). A four-way comparison of elevated DRGs in these data determined that there are underappreciated levels of regulation in operation during hypoxia. First, the varied numbers of DRGs were called for each readout: Ser2P-ChIP (974), nRNA-Seq (1,722), polyA (602) and TRAP-Seq (1,349). Of these, only 216 genes were consistently elevated in all four assays of RNA and some were not observed in other readouts (Ser2P-ChIP [475]; nRNA-Seq [890]; polyA [47], TRAP-Seq [592]). By contrast, a similar four-way analysis performed for the down DRGs (Fig. 3c) found the majority (72%) of the down DRGs in the polyA population were significantly reduced in at least one other dataset. Only 10 genes were significantly downregulated in all four readouts. These data are striking because Ser2P-ChIP (206) and polyA (291) identified the fewest and nRNA (2,608) and TRAP RNA (578) the most down DRGs. Consistent with the analysis of the *HRGs* and *RPs*, these data demonstrate that differential regulation in response to hypoxic stress includes processes

associated with nascent transcript elongation and transcript retention within or export from the nucleus.

To resolve cohorts of genes with similar patterns of regulation, DRGs identified in at least one of the four (Ser2P, nRNA, polyA, TRAP) datasets were separated by partition around medoids (PAM) clustering and viewed in a heatmap of \log_2 fold-change values (2HS/2NS) (Fig 4a; Supplemental Data S1c). Gene Ontology (GO) term enrichment was evaluated for each cluster to identify co-regulated genes with similar roles (Supplemental Dataset 1b,c). This exposed a strong and coordinate regulation across readouts for three up-regulated (1, 2, 3) and one down-regulated (16) cluster (Fig. 4a), pointing to coordinate homodirectional transcriptional and post-transcriptional control of expression of these genes. The other clusters showed differences in dynamics for one or more of the readouts, indicating differential control occurs at a specific step, such as nuclear retention, cytoplasmic turnover or translation. To assist in identifying associations between the chromatin and RNA readouts evaluated, the average signal value for each data type across the genic region was determined for each cluster and plotted for the genic region, from -1 kb upstream to +1 kb downstream (Fig 4b; Supplemental Fig. 4). For these same gene groups, the signal values for H3K9Ac and H3K14Ac were monitored across genes of each cluster for the 9HS and its control timepoint (Supplemental Fig. 5). These were collectively used to explore if dynamics in gene activity was coordinated or differentially regulated at a specific step in the nucleus or cytoplasm.

2.4.5. Identification of chromatin features associated with distinctions in abundance and translation of individual mRNAs

The concerted upregulation of cluster 1-3 genes, which together included 46 of the 49 *HRGs*, was accompanied by changes in chromatin including enhanced accessibility, increased H3K9Ac and decreased H2A.Z (Fig. 4b; Supplemental Fig. 4), as illustrated for the *HRGs ADH1* and *PCO2* (Fig. 3e). Genes in cluster 1 were the most significantly upregulated from transcriptional elongation through translation and were highly enriched for terms related to responses to decreased oxygen levels and hypoxia ($p \text{ adj.} < 6.73e^{-22}$). The decrease in H2A.Z on these genes was pronounced. Cluster 4 was predominantly upregulated at the level of nuclear RNA whereas cluster 5 transcripts displayed increased translational status.

A notable feature of clusters 1-5 was the increase in H3K9Ac that extended 5' of the TSS and well into the 3' portion of the gene body. This rise in H3K9Ac was the most dramatic for cluster 1 and the least dramatic for cluster 5, indicating this mark was correlated with with active transcription under hypoxic stress. H3K9Ac drifted down for all of the down DRGs as H2A.Z levels rose (clusters 10, 12-16). In animals, the H3K9Ac modification is promoted by the presence of H3K4me3 and stimulates the recruitment of the super elongation complex (SEC) for release of poised RNAPII complexes (reviewed by [4]). The elevation in Ser2P levels and increase in chromatin accessibility near the TSS of

these genes also supports the conclusion that the elevation of nRNA and polyA RNA for clusters 1-3 corresponds with hypoxia-responsive activation of transcription. Consistent with the more modest upregulation of nRNA and polyA RNA levels of genes in clusters 4 and 5, these displayed a slight decline in H3K4me3 and a limited increase in H3K9Ac. Moreover, all of the upregulated clusters except 5 had lower H2A.Z association on the gene body under hypoxia, with the reduction inversely proportional to the increase in transcript upregulation. In general, H3K14Ac levels rose as the stress was prolonged (Supplemental Fig. 5), particularly for the upregulated clusters. Altogether, these data distinguish the histone marks of genes that are the most highly upregulated by hypoxic-stress.

Upregulation at predominantly one level of evaluation was evident for genes in clusters 6, 7, and 9. The first two were unusual in the pronounced upregulation of nRNA. But data for these genes was difficult to interpret because of high levels of Ser2P and similar low levels of most chromatin marks throughout these regions. On the other hand, cluster 9 was striking for the strong upregulation of Ser2P reads across the genic regions. Similar to cluster 1, these genes displayed increased chromatin accessibility near their TSS, but their histone features were unusual as the increase in H3K9Ac was accompanied with a drop in H3K4me3 not evident in the coordinately upregulated clusters 1-4. By 9 h of stress cluster 9 was more similar to clusters 1-4 in its further elevation in H3K9Ac and H3K14Ac, chromatin accessibility, and elevation in polyA and TRAP RNA (Supplemental Fig. 5). Remarkably, both clusters 2 and 9 are significantly

enriched in GO terms associated with heat stress, oxidative stress, hydrogen peroxide, and reactive oxygen species (ROS). *HSP70-4*, a member of cluster 2 (Fig. 3e), displayed high levels of Ser2P at 2HS with limited increases in mRNA abundance. The transient delay in the elevation of many extreme stress genes in the nRNA and polyA suggests they may be poised in an unusual manner or may be limited in termination until the stress exceeds a threshold or reoxygenation occurs.

Survey of the down DRGs revealed complex regulation at the level of histone modification and H2A.Z association, Ser2P levels, and within the nuclear and cytoplasmic RNA populations. By contrast to clusters 1-5 and 9, clusters 10-16 were oppositely defined by a general downregulation in at least one RNA based assay, with Cluster 16 demonstrating the strongest downregulation with decreases observed in nRNA, polyA, and TRAP. Concomitant with reduced levels of nRNA and polyA mRNA, these genes displayed increased H2A.Z and decreased H3K9Ac association at both 2HS and 9HS. These results support the role of this H3 modification and H2 variant in the regulation of transcription in response to hypoxic stress (Fig 3c, d). Interestingly, of the downregulated clusters only 15 and 16 were strongly enriched for GO categories (cluster 15: root development and regulation of growth ($p \text{ adj.} < 3.7e^{-8}$); cluster 16: regulation of transcription and RNA biosynthesis ($p \text{ adj.} < 7.78e^{-7}$)). Unsurprisingly, these clusters with strong downregulation at the translational level were associated with energy intensive processes, possibly aiding energy conservation when ATP

production is less efficient. Interestingly, despite an unchanging average of H2A.Z association, genes within clusters 11 and 13 exhibited variance with H2A.Z association, with both increased and decreased H2A.Z levels under hypoxic stress. Additionally, cluster 11 and 13 genes displayed strong dynamic regulation within the nucleus. In response to 2HS, a strong reduction in nRNA is observed, but responses to both prolonged stress and reoxygenation were distinct. Under prolonged stress, downregulation of many genes within these clusters was still observed, but the nuclear levels of these transcripts rose by 9HS, providing strong evidence that they continued to be transcribed during the stress. Upon reoxygenation, cluster 11 and 13 transcripts were once again highly enriched within the nucleus. Together these data uncover remarkable and underappreciated variation in nuclear transcript regulation, particularly of the down DRGs.

2.4.6. ERFVII and Heat Shock Factor *cis*-elements are enriched in the coordinately upregulated and RNAPII paused gene promoters, respectively

To further elucidate the regulation of individual clusters, the role of transcription factors and *cis*-regulatory elements was investigated within the promoters of genes within each cluster. First, to identify the binding motif of the ERFVII *HRE2*, peaks identified from *HRE2* ChIP-seq were used as input for motif discovery. A multimeric 5'-GCC-3' binding motif that was significantly overrepresented (p-value < $1e^{-351}$) was identified and used for downstream

analysis (Fig. 4c). The putative *HRE2* binding site (*HRE2* motif) was then compared against the promoter region encompassing 1500 bp 3' and 500 bp downstream of the TSS for each gene within each cluster of Fig. 4a to identify the frequency of the motif presence. Cluster 1, defined by the strongest coordinate upregulation, showed a 2-fold enrichment in presence of the GCC multimer, suggesting that *HRE2* may bind within the promoter region of cluster 1 genes (Fig. 4d). Of these genes 34, showed significant *HRE2* binding *in vivo* based on the *HRE2* ChIP-seq (Supplemental Dataset 1d), as illustrated by *ADH1* and *PCO2* (Fig. 3e). Interestingly, the *HRE2* motif differed from the Hypoxia Responsive *cis*-Element (HRPE) shown to be necessary and sufficient to mediate transactivation by RAP2.12 or the other two constitutively expressed ERFVIs (RAP2.2 and RAP2.3) in *Arabidopsis* protoplasts [30,31].

ChIP-seq was also attempted for RAP2.12 but failed because of low yields of immuno-purified chromatin due to intrinsic low factor abundance, even when an N-terminally epitope tagged version of these proteins that is not an N-end rule target was used and seedlings were pretreated with the proteasome inhibitor MG132. A directed search for the HRPE motif in the promoter regions of the cluster genes confirmed that this sequence is also enriched within cluster 1 genes (Fig. 4d). Taken together, these data suggest that genes within cluster 1 may be under the regulation of *HRE2* via a GCC-type motif similar to a typical ERF *cis*-element as well as the HRPE of the RAP-type ERFVIs. Transactivation of the *LATERAL ORGAN BOUNDARY 41* (*LBD41*) promoter and a minimal

promoter with three copies of the HRPE was more than 40-fold higher with RAP2.12 than HRE2 [30,31], supporting the conclusion that these ERFVIs are not identical in function.

The unusual pattern of Ser2P association in cluster 9 genes was correlated with the strong upregulation of GO terms associated with heat stress in several clusters (2, 3 and 9). We also noted strong upregulation of members of the heat shock factor (HSF) transcription factor family in clusters 2 and 3 (*HSFA2*, *HSFA4A*, *HSFA7A*, *HSFB2A*). To explore the involvement of HSFs in hypoxic responses, the binding motifs identified by DNA affinity purification and sequencing (DAP-seq) for each family member [52] was utilized in an identical enrichment analysis. This determined that HSF *cis*-elements (HSEs) were slightly enriched in promoters of cluster 1-4 genes and highly enriched within the promoters of cluster 9 genes. As cluster 9 is defined by a strong RNAPII engagement with limited polyA induction at 2HS, these HSF-regulated genes may be transcriptionally primed, possibly with termination of elongation occurring only if the stress is sufficiently prolonged or upon reoxygenation.

2.4.7. Prolonged hypoxia reinforces H3 acetylation and perturbs circadian-regulated genes and prolonged stress

To better understand the chromatin and RNA dynamics that occur as hypoxic stress is prolonged, we compared the progressive changes in H3K9Ac and H3K14Ac along with nRNA and polyA RNA. These readouts were selected

due to the opposing trend in H3K9Ac and H3K14Ac in the upregulated HRGs and downregulated genes (Fig. 3a; Supplemental Figs. 3 and 4), and consistent with prior reports that these acetylated histones become more robust during longer exposure to various abiotic stresses [3,47,53,54]. As anticipated, most *HRGs* were upregulated at both 2HS and 9HS in nuclear and polyA RNA (Fig. 5a). Similar H3K9Ac enrichment was observed at 2HS and 9HS for the *HRGs*, whereas H3K14Ac enrichment was observed only at 9HS and was limited (Supplemental Fig. 1, 3). Regulation of *RPs* was more nuanced at 9HS based on several criteria. First, at 9HS, *RP* mRNAs increased in nRNA despite a general reduction in polyA at 9HS. This suggests that these transcripts are actively synthesized but retained within the nucleus as the stress was prolonged. In fact, most transcripts showed retention in the nucleus at 9HS (Supplemental Fig. 2). Remarkably, the rise in *RP* accompanied an increase in H3K14Ac (Supplemental Fig. 1, 3). This indicates that *RPs* transcripts are actively synthesized but are impaired in nuclear export, potentially replenishing transcript levels prior to reoxygenation when *RP* translation is restored [16,17,19].

Looking more globally, Fig. 5b was generated to compare trends in up- and down-regulated DRGs at 2HS and 9HS in the nRNA and polyA populations. As seen at 2HS, greater numbers of up and down DRGs were identified in nRNA at 9HS. The large overlap between DRGs at the two time points demonstrated homodirectional regulation of many genes. Notably, some that were upregulated in nRNA at 2HS became upregulated in polyA at 9HS. The detection of many up

and down DRGs unique to the nRNA and polyA at 9HS indicates ongoing changes in regulation as the stress progressed.

Similar results were found when investigating genes with differential levels of H3K9Ac and H3K14Ac (Fig. 5c). As observed for the *HRG PCO2*, levels of H3K9Ac and H3K14Ac tended to be higher at 9HS (Fig. 5a; Supplemental Figs. 1 and 3). This was quantified as an over three-fold increase in H3K9Ac up-DRGs at 9HS as compared to 2HS (1,243/352). The upregulation in H3K14Ac was more pronounced after more prolonged stress, with two up-DRGs at 2HS and 546 at 9HS. The up-DRGs (295) with increases in both H3K9Ac and H3K14Ac suggests that some genes are targeted for H3 acetylation at multiple amino acid residues. Down-DRGs showed varied combination of change in both H3 modifications. The *RPs*, for example, increased in H3K14Ac but had varied change in H3K9Ac (Fig. 5a; Supplemental Fig. 3; clusters 5 and 8). The down-DRGs of clusters 2 and 14 showed a drop in H3K9Ac and rise in H3K14Ac that resulted in a similar peak of both marks proximal to the TSS (Supplemental Fig. S4). This could indicate a pause in elongation is sustained on many down-DRGs.

Because prolonged hypoxic stress resulted in additional DRGs, PAM clustering was performed on the unified group of 4,124 DRGs from 2HS and 9HS (Fig. 5e; Supplemental Data S1c). The pattern of 16 clusters confirmed differential regulation in both nRNA and polyA RNA populations, identifying many with enriched or depleted nRNA at 9HS (clusters 4-5, 7-12, 15). We also confirmed a trend of increased for H3K9Ac and H3K14Ac for up the up-DRGs

clusters (1-7) and a decline in H3K9Ac for all but one strongly down-DRG cluster (clusters 10-12, 14-16). Evaluation of GO terms indicated that nuclear enrichment was enhanced for genes associated with translation and glucose metabolism (clusters 5 and 8), by contrast to ADP binding (cluster 7). Cluster 6 was notable for the enrichment in genes with circadian up regulation in the evening (i.e. *REVEILLE2/CIRCADIAN1 (CIR1)* [At5g37260 and *PSEUDORESPONSE REGULATOR 5* [AT5G24470]). Intriguingly, the greater abundance of these transcripts at 9HS was a consequence of disruption of their cycling. The high levels of H3K9Ac and H3K14Ac at 9HS corresponded with higher levels of their transcript in the polyA population (Fig. 5f). This suggests that for these circadian-associated genes their transcription continues or their turnover is inhibited in response to HS initiated at the end of the day and prolonged beyond the anticipated dawn. Amongst the down DRGs, levels of transcripts associated with photosynthesis (cluster 12) and root development (clusters 12, 14, and 15) displayed a coordinate decline in the RNA and polyA RNA populations. Altogether, these results demonstrate that responses to hypoxic stress are dynamically regulated at various levels of chromatin and polyA transcript production in response to short- and long-term stress.

2.4.8. Hypoxia stress recovery includes mobilization of nuclear-retained transcripts to the polyA and translating ribosome pool

We decided to explore the relationship between nRNA and polyA RNA in response to reoxygenation to test the hypothesis that transcripts retained in the nucleus may be exported and translated upon reoxygenation. This could be independent of or overlap with sequestration of a subset of mRNAs in UBP1C complexes until their translation is restored upon reoxygenation [16,19]

Seedlings were aerated for 1 h (1R) following 2HS to investigate nuclear dynamics or 2 h (2R) to investigate translational dynamics. Evaluation of log₂ fold change levels for nRNA, polyA and TRAP RNA revealed that *RP* mRNA levels declined within the nucleus concomitant with their increase in the polyA and TRAP RNA (Fig. 6a; Supplemental Fig. 2)). By contrast, *HRG* transcripts fell precipitously in the nRNA, polyA and TRAP populations upon reoxygenation. Interestingly, *ADH1* abundance in the polyA pool at 2HS and 1R were similar, but lower in nRNA and TRAP (Fig. 6a and c), suggesting that this transcript remains stable and translated upon reoxygenation. This contrasts to *PCO2*, which was dramatically downregulated in all RNA populations upon reoxygenation (Fig. 6c).

The three-way comparison of recovery-regulated DRGs in nRNA, polyA, and TRAP also showed that changes in nRNA and TRAP RNA was distinct from polyA for a large number of genes (Fig. 6b). PAM clustering of the DRGs resolved a strong trend toward return to non-stress conditions for nRNA, polyA, and TRAP upon reoxygenation (Supplemental Data S1b, c). Of the patterns

resolved by clustering, the shift from nuclear retention to polyA and translation observed for the 154 genes in cluster 8 genes was the most notable. Of these genes, over 50% were member of a cluster with bias in nRNA accumulation at 2HS (i.e., Fig. 4a, clusters 4, 6-9). GO term enrichment of these included heat stress response ($p \text{ adj.} < 2.16e^{-22}$; i.e., *HSP70-4* and *HSP20 like, AT1G53540*) (Fig. 6c), response to reactive oxygen species ($< 4.95e^{-16}$), response to water deprivation ($< 1.35e^{-08}$), response to unfolded protein ($< 1.82e^{-07}$), cellular response to starvation ($< 1.35e^{-07}$), ER nucleus signaling pathway ($< 1.48e^{-07}$) and other stresses. This pattern of regulation suggests that retention of transcripts within the nucleus during hypoxic stress may allow for these genes to be rapidly exported and translated upon reaeration. The reoxygenation analysis also considered dynamics in chromatin accessibility (Fig. 2b and e). We found that accessible regions near TSSs increased at the global level upon reoxygenation, with increases and decreases in over 2000 individual THSs relative to 2HS (Fig. 2c and e). In summary, upregulation of transcripts in the polyA and TRAP RNA populations under reoxygenation included mobilization of transcripts apparently synthesized and retained the nucleus during the stress to the translationally active pool.

2.5. Discussion

This primary accomplishment of this genome-scale study is the demonstration that gene expression in response to hypoxia and reoxygenation is

regulated within the nucleus at pre- and co-transcriptional levels that influence the polyA transcriptome and ribosome-engaged translome. By use of eight genome-scale assays of chromatin and three RNA subpopulations evaluated by use of RNA-sequencing, evidence was obtained of poised gene regulation that influenced the transcriptome in a time dependent manner including: rapidly in response to hypoxia, as the duration of stress was prolonged, or once re-aeration occurred. This study resolved hypoxia-responsive dynamics in the (1) position and degree of open chromatin near the TSS of genes, (2) post-translational methylation and acetylation of residues of Histone H3, (3) eviction of the histone variant H2A.Z, (4) engagement of RNAP II with the Ser2P modification of the CTD associated with elongation and gene transcript synthesis, and (5) abundance of transcripts within the nucleus, whether nascent or polyadenylated. These analyses of gene regulation expanded the number of coordinately-regulated *HRGs* from 49 to over 200. They also resolved modes of regulation that involve non-continuous regulation of responses to hypoxia and reoxygenation. These included (1) ephemeral or anticipatory up-regulation associated with increased engagement of RNAPII-Ser2P without significant increases in polyA RNA until the stress was prolonged or re-aeration occurred, and (2) a homeostasis response whereby genes associated with growth continued to be transcribed during the stress, but their transcripts were nuclear retained until the return to well-aerated conditions. In seeking common features co-regulated genes, we recognized enrichment of motifs associated with specific

transcription factor families and characteristic patterns of Histone H3 modification or H2A.Z eviction. Although regions of accessible chromatin were modulated by the stress, variation in accessibility was not necessarily a clear predictor of dynamics in RNAPII engagement, mRNA or polyA transcript accumulation, suggesting that many promoter regions are actively remodeled in response to altered oxygen availability. Altogether, the data demonstrate gene regulatory control occurs at multiple levels that can function in concert to finely regulate both short- and long-term hypoxic stress and reoxygenation responses.

Global analyses revealed that hypoxic stress affects nucleosome dynamics at the levels of chromatin accessibility, histone methylation and acetylation, and through the histone variant H2A.Z. Despite global dynamics observed for each factor (Fig. 2a), changes in H3K9Ac and H2A.Z were strongly correlated with RNAPII engagement (Figs. 3c and d) in response to short-term hypoxic stress. These results suggest that regulation of H3K9Ac and H2A.Z occurs rapidly and have the greatest impact on gene regulatory control in response to short-term hypoxic stress. In response to prolonged hypoxic stress, an intensification of H3K9Ac was observed, demonstrating that regulation of this modification occurs throughout the duration of the stress (Fig. 5c). Conversely, H3K14Ac, which demonstrated limited dynamics in short-term hypoxic stress, displayed more pronounced regulation under prolonged stress, demonstrating H3 modifications are temporally regulated throughout the stress. Both H3K9Ac and H3K14Ac have a demonstrated role in the regulation of gene activity in abiotic

stresses [47,48,54], but may function to regulate unique subsets of genes. These results demonstrate that histone modifications are highly dynamic in hypoxic stress in a manner correlated with transcriptional activity

This study determined that *HRGs* are characterized by pronounced upregulation in transcription and polyA transcript accumulation that is accompanied by proportional translation. Prior studies have shown that these gene transcripts are well-translated during the stress because they avoid sequestration in UBP1C-containing cytoplasmic complexes associated with exclusion from translation and further stabilization or decay [17,19]. A characteristic of the genes that were highly upregulated from transcription to translation was a pronounced decline in H2A.Z that was broadly distributed along the gene body within 2 h of hypoxia (Fig. 4b; Supplemental Figs. 3 and 4). The role of H2A.Z in regulation of transcription is complicated. Its presence within the +1 nucleosome is associated with promotion or repression of transcription, whereas its distribution across the gene body is generally associated with nonproductive transcription [5,6]. The decline in this Histone 2A variant along the most upregulated genes was similar to that observed in response to heat stress for heat-induced mRNAs [5–7,44,45], suggesting that eviction of H2A.Z is important in upregulation in response to extreme stress responses. H2A.Z has been found to be associated with heat responsive genes under control conditions, whereby H2A.Z is evicted in response to heat stress [7]. It is hypothesized that this additional level of regulation allows for the rapid induction

of key TFs that trigger transcriptome-wide changes. In response to hypoxia, three *HRGs*, one heat-stress and one oxidative-stress response gene encoding transcription factors showed significant reductions in H2A.Z (*HRE2*, *LBD41*, *HSFB2B*, *ZAT10*). For these and the majority of cluster 1-3 genes, the reduction in H2A.Z distributed broadly along the body of genes was accompanied by an increase in chromatin accessibility in the promoter proximal region and strong elevation of Ser2P and H3K9Ac along the gene body (Fig. 4b; Supplemental Fig. 4), the later two indicative of an increase in active transcription. In *Arabidopsis*, H2A.Z deposition is dependent on ACTIN-RELATED PROTEIN 6 (ARP6), a component of the PHOTOPERIOD-INDEPENDENT EARLY FLOWERING 1 (PIE1) complex. Despite disruption of H2A.Z deposition in an *arp6* background, few hypoxia induced genes are mis-regulated, highlighting the necessity of hypoxia regulated transcription factor activity [45]. Many of the 200+ hypoxia-upregulated genes had one or more *cis*-element within 500 bp of the TSS associated with regulation by hypoxia-stabilized ERFVII transcription factors and a number were bound by the ERFVII HRE2 (Fig. 4c). We propose that the combination of eviction of H2A.Z and ERFVII-regulated transcriptional activation increases the likelihood that newly synthesized transcripts are efficiently exported and translated under hypoxia.

A second finding was that many genes associated with heat stress are transiently activated by hypoxic stress and reoxygenation. The association of RNAPII-Ser2P on these transcripts was not necessarily accompanied by an

increase in nRNA or polyA RNA until the stress was prolonged or reaeration occurred. Previously, genes associated with heat stress were recognized as highly induced when *Arabidopsis* seedlings were rapidly transferred from aerated conditions to strict anoxia [55,56]. Pre-treatment of seedlings with heat stress conferred increased resiliency to anoxia, whereas loss-of-function mutants for *HEAT SHOCK FACTOR A2* (*hsfa2*) or *hsf1a hsf1b* had reduced heat-dependent acclimation to anoxia [57]. This was interpreted as evidence of overlap between anoxic and heat stress mechanisms, since environments where heat stress precedes a severe limitation in oxygen are not known. Remarkably, many genes related to heat stress showed a progressive or primed activation, as evidence by increased association of RNAPII-Ser2P without a concomitant elevation in polyA after short-term hypoxia (Fig. 3d, clusters 2 and 9). These included *HSFB2A*, *HSFA7A*, and *HSF4/TBF1*. Of these, *HSFB2A* was primarily upregulated at the nuclear level at 2HS and at the polyA level at 9HS (progressive), whereas *HSF4* showed RNAP-Ser2P engagement at 2HS with limited polyA RNA accumulation until seedlings were reoxygenated (primed) (Fig. 5c, Fig. 6, c and d; Supplemental Fig. 5). Heat stress *cis*-elements (HSEs) were enriched within the promoter regions of genes that displayed increased transcription without concordant increases in polyA (progressive or primed), suggesting that HSFs may poise their target genes during short-term hypoxic stress (Fig 4d).

The progressive upregulation of heat-stress genes was pronounced for *HSP70-4*. This gene displayed a reduction in H2A.Z along the gene body

concomitant with highly increased RNAP II-Ser2P association and nRNA accumulation, despite limited upregulation of polyA RNA at 2HS. This suggests that the ARP6-dependent decrease in H2A.Z can take place in the absence of thermal regulation but may not be followed by fully productive expression. Based on the distribution of reads for Ser2P and nRNA along this gene, by 2HS there may be a lack of cleavage and polyadenylation of these nascent transcripts. Notably, the *HSF70-4* mRNA which was exported was engaged in translation at 2HS (Fig. 3e). Yet, *HSF70-4* transcripts in the nRNA and ribosome-associated fraction increased significantly by 9HS (Fig. 5c) and after reoxygenation (Fig. 6c), suggesting cells prepare in advance to produce this chaperone as cellular damage increases during the stress and upon recovery. Curtailment of production of this cytoplasmic chaperone as hypoxia begins could limit accumulation of an ATPase that would put demands on limited energy reserves. However, upon reoxygenation, the synthesis of HSP70 along with many other proteins associated with the unfolded protein response and protection from ROS could aid the return to homeostasis. In animals, HSP70 prevents the formation of and promotes the disassembly of stress granules formed by nucleation of translationally repressed mRNAs bound by the assembly prone RNA binding proteins including T-Cell-Restricted Intracellular Antigen-1 and related proteins (TIA1/R) [58,59]. In response to heat stress, the formation of stress granules leads to increased production of HSP70, which function to disassemble these complexes as a potential feedback mechanism. *Arabidopsis* UBP1 and RNA

BINDING PROTEIN 45/47 are the functional orthologs of TIA1/R [19]. Increased HSP70 synthesis could function analogously in the disassembly of mRNA-protein complexes that form to sequester transcripts during hypoxia, including mRNA protein complexes containing the UBP1C or CALMODULIN-LIKE 38 [19,37,60].

The investigation of the nucleosome dynamics of cluster 2 and 9 genes revealed that they undergo similar histone changes with one notable exception. All undergo a general loss of H2A.Z within the gene body in conjunction with increased H3K9Ac levels near their TSS. Intriguingly, cluster 9 showed a loss of H3K4me3 proximal to the TSS, that was not evident for cluster 2 or other highly upregulated genes. It can be hypothesized that the distinction in H3K4me3 regulation observed for cluster 2 and 9 may distinguish genes with RNAPII-Ser2P that is conditionally productive versus non-productive, respectively. The enrichment for HSF binding motifs in cluster 2 and 9 genes suggests that members of this family regulate these genes. Previously, upregulation under heat stress of transcriptional activator *HSFA2* (Cluster 2) but not *HSFB1* (Cluster 9) was shown to be dependent on recruitment of ANTI-SILENCING FUNCTION 1 (ASF1A/B), which promotes with H3K56 acetylation and was associated with RNAPII binding along the gene body [61]. The combination of histone modifications could reflect distinctions in HSFs or histone chaperone activities that influences RNAPII on these genes. An important question is whether different HSFs may recruit different chromatin remodelers or histone modification enzymes. We predict that recruitment of specific transcription factors influences

chromatin modifications or accessibility that has ramifications on RNAPII CTD modifications or rates of elongation that tune timing and activity of cohorts of stress responsive genes. Such a scenario may be responsible for the progressive upregulation of cluster 2 genes or the more primed upregulation of the cluster 9 genes. A key question for future studies is whether or not the nRNAs, such as that of *HSP70-4*, that accumulates in the nRNA is fully spliced and polyadenylated.

This study included analysis of the cis-element target of ERFs. Enigmatically, ChIP-seq of the hypoxia-induced ERFVII HRE2 led to the identity of a multimeric GCC cis-element that did correspond to the HRPE element found to evolutionarily conserved in HRGs and sufficient for transactivation in protoplasts [30]. The HRE2 binding motif strongly resembled the double GCC motif of the Ethylene Binding Protein (EBP) box cis-element first defined for EREBP2 of *Nicotiana tabacum* [62]. Strikingly, RAP2.3 was shown to bind the *ACID INSENSITIVE 5 (ABI5)* promoter in the region of its two EBP boxes and transactivation of the *ABI5* promoter was demonstrated in protoplasts by all three constitutively expressed ERFVIIIs (RAP2.2/2.3/2.12), in an EBP box-dependent manner [32]. On one hand, HRE2 may only bind to a multimeric GCC motif, as it was not effective at activation via the HRPE in protoplasts [30]. Yet the cumulative evidence indicates the ERFVIIIs may activate HRPE and GCC motifs *in planta*. The predicted HRPE contains includes 5'-GCC-3' followed a potential

5'-GCC-3'; perhaps more significantly, the 33bp sequence used to define the HRPE contained a tandem 5'-GCC-3'.

In mammalian systems, it is understood that in response to hypoxia regulation of histone modifications and transcriptional activity occurs. The similarity to plants is remarkably analogous. Hypoxic-responsive genes are activated by the two-subunit Hypoxia Inducible Factor (HIF) transcription factor complex, that includes the oxygen-destabilized HIF1A subunit [63]. Although like the three RAP/ERFVIs, this is a constitutively synthesized protein; it is the oxygen-dependent activity of prolylhydroxylases that govern the modification of HIF1a that triggers its oxygen-dependent turnover. In animals, the chromatin landscape is additionally regulated through chromatin accessibility [64] and the post-translational modification of histones [65] in an oxygen sensitive manner. It has been shown that HIF signaling itself directly mediates histone modification of target genes through the interaction with chromatin modifying enzymes [66]. Additionally, several histone modifying enzymes are directly targeted by HIF transcriptional activation, and HIF1A expression itself is regulated by histone acetylation [67], confirming the integration of epigenetic regulation. The analogy of low-oxygen stabilized transcriptional regulators and their coordination with chromatin modifications hints that mammals and plants have evolved convergent mechanisms of hypoxia signaling. Indeed, this extends beyond transcriptional regulation as cytoplasmic sequestration and selective translation of mRNAs is also observed in these two kingdoms [16,17,68,69].

This study reveals additional levels of gene regulation that occur in response to hypoxia stress in *Arabidopsis*. Despite prior understanding of genome-wide hypoxic responses at the level of polyA transcriptome and translome, additional factors affecting gene regulation were elucidated to yield a more comprehensive understanding of hypoxic stress responses. Most notably, this study demonstrates that aspects of RNA regulation become evident when technologies such as INTACT and TRAP are applied that enable contrasting total nuclear, polyadenylated and translated mRNAs. The illumination of poised RNAPII and nuclear retention of mRNAs raises the question whether these phenomena might be more widespread. It is possible that the pronounced integration of nuclear and cytoplasmic gene regulation or the anticipatory regulation involving poised or stalled RNAPII or nucleus-retained polyadenylated mRNA may occur in other abiotic and/or biotic stress responses. Importantly, a previous unidentified heat response was observed strictly within the nucleus, suggesting that conserved stress responses may be additionally regulated in other stresses.

2.6. Conclusions

This study provides a deep investigation into nuclear gene regulatory processes in hypoxic stress and reveals distinct regulation within the nucleus that fine tunes cellular and physiological acclimation to transient deficiencies in oxygen availability. We determined that rapid regulation of chromatin occurs in

response to short-term hypoxic stress but continues to be regulated as the stress is prolonged. Concordant regulation from chromatin organization, to transcriptional activity, polyadenylated mRNA accumulation, and translation is observed for subsets of hypoxia up-regulated genes, while more discontinuous upregulation in mRNA production, export to the cytoplasm and recruitment to ribosomes is observed for other subsets of genes. These findings identify new mechanisms relevant to low oxygen stress survival and other environmental challenges. The datasets generated in this study provide a resource for genome-scale chromatin accessibility, histone modifications, RNAP II engagement, nuclear transcript accumulation data for *Arabidopsis* seedlings grown under controlled conditions.

2.7. Acknowledgements

We thank Mauricio Reynoso, Roger Deal, Marko Bajic, Maureen Hummel, Lauren Dedow, Sonja Winte, Jérémie Bazin, Thomas Girke, and Thomas Eulgem for helpful discussions. This work was supported by U.S. National Science Foundation (Grant Nos. IOS-1121626, IOS-1238243 and MCB-1716913) and the U.S. Department of Agriculture, National Institute of Food and Agriculture - Agriculture and Food Research Initiative (Grant No. 2011-04015) to J.B.-S.

2.8. References

1. Bailey-Serres J, Voeselek LACJ. Flooding stress: acclimations and genetic diversity. *Annu Rev Plant Biol.* 2008;59:313–39.
2. Voeselek LACJ, Bailey-Serres J. Flood adaptive traits and processes: an overview. *New Phytol.* 2015;206:57–73.
3. Asensi-Fabado M-A, Amtmann A, Perrella G. Plant responses to abiotic stress: The chromatin context of transcriptional regulation. *Biochim Biophys Acta.* 2017;1860:106–22.
4. Gates LA, Foulds CE, O'Malley BW. Histone Marks in the “Driver”s Seat’: Functional Roles in Steering the Transcription Cycle. *Trends Biochem Sci.* 2017;42:977–89.
5. Kumar SV, Wigge PA. H2A.Z-containing nucleosomes mediate the thermosensory response in *Arabidopsis*. *Cell.* 2010;140:136–47.
6. Sura W, Kabza M, Karlowski WM, Bieluszewski T, Kus-Slowinska M, Pawelozek Ł, et al. Dual Role of the Histone Variant H2A.Z in Transcriptional Regulation of Stress-Response Genes. *Plant Cell.* 2017;29:791–807.
7. Cortijo S, Charoensawan V, Brestovitsky A, Buning R, Ravarani C, Rhodes D, et al. Transcriptional Regulation of the Ambient Temperature Response by H2A.Z Nucleosomes and HSF1 Transcription Factors in *Arabidopsis*. *Mol Plant.* 2017;10:1258–73.
8. Sullivan AM, Arsovski AA, Lempe J, Bubb KL, Weirauch MT, Sabo PJ, et al. Mapping and dynamics of regulatory DNA and transcription factor networks in *A. thaliana*. *Cell Rep.* 2014;8:2015–30.
9. Sullivan AM, Bubb KL, Sandstrom R, Stamatoyannopoulos JA, Queitsch C. DNase I hypersensitivity mapping, genomic footprinting, and transcription factor networks in plants. *Current Plant Biology.* 2015;3-4:40–7.
10. Hajheidari M, Koncz C, Eick D. Emerging roles for RNA polymerase II CTD in *Arabidopsis*. *Trends Plant Sci.* 2013;18:633–43.
11. Milligan L, Huynh-Thu VA, Delan-Forino C, Tuck A, Petfalski E, Lombraña R, et al. Strand-specific, high-resolution mapping of modified RNA polymerase II. *Mol Syst Biol.* 2016;12:874.
12. Wang Z-W, Wu Z, Raitskin O, Sun Q, Dean C. Antisense-mediated FLC transcriptional repression requires the P-TEFb transcription elongation factor. *Proc Natl Acad Sci U S A.* 2014;111:7468–73.

13. Fong N, Saldi T, Sheridan RM, Cortazar MA, Bentley DL. RNA Pol II Dynamics Modulate Co-transcriptional Chromatin Modification, CTD Phosphorylation, and Transcriptional Direction. *Mol Cell*. 2017;66:546–57.e3.
14. Jonkers I, Lis JT. Getting up to speed with transcription elongation by RNA polymerase II. *Nat Rev Mol Cell Biol*. 2015;16:167–77.
15. Hetzel J, Duttke SH, Benner C, Chory J. Nascent RNA sequencing reveals distinct features in plant transcription. *Proc Natl Acad Sci U S A*. 2016;113:12316–21.
16. Branco-Price C, Kaiser KA, Jang CJH, Larive CK, Bailey-Serres J. Selective mRNA translation coordinates energetic and metabolic adjustments to cellular oxygen deprivation and reoxygenation in *Arabidopsis thaliana*. *Plant J*. 2008;56:743–55.
17. Juntawong P, Girke T, Bazin J, Bailey-Serres J. Translational dynamics revealed by genome-wide profiling of ribosome footprints in *Arabidopsis*. *Proc Natl Acad Sci U S A*. 2014;111:E203–12.
18. Mustruph A, Zanetti ME, Jang CJH, Holtan HE, Repetti PP, Galbraith DW, et al. Profiling translomes of discrete cell populations resolves altered cellular priorities during hypoxia in *Arabidopsis*. *Proc Natl Acad Sci U S A*. 2009;106:18843–8.
19. Sorenson R, Bailey-Serres J. Selective mRNA sequestration by OLIGOURIDYLATE-BINDING PROTEIN 1 contributes to translational control during hypoxia in *Arabidopsis*. *Proc Natl Acad Sci U S A*. 2014;111:2373–8.
20. Xu K, Xu X, Fukao T, Canlas P, Maghirang-Rodriguez R, Heuer S, et al. Sub1A is an ethylene-response-factor-like gene that confers submergence tolerance to rice. *Nature*. 2006;442:705–8.
21. Hattori Y, Nagai K, Furukawa S, Song X-J, Kawano R, Sakakibara H, et al. The ethylene response factors SNORKEL1 and SNORKEL2 allow rice to adapt to deep water. *Nature*. 2009;460:1026–30.
22. Gibbs DJ, Lee SC, Isa NM, Gramuglia S, Fukao T, Bassel GW, et al. Homeostatic response to hypoxia is regulated by the N-end rule pathway in plants. *Nature*. 2011;479:415–8.
23. Licausi F, Kosmacz M, Weits DA, Giuntoli B, Giorgi FM, Voisenek LACJ, et al. Oxygen sensing in plants is mediated by an N-end rule pathway for protein destabilization. *Nature*. 2011;479:419–22.

24. Yang C-Y, Hsu F-C, Li J-P, Wang N-N, Shih M-C. The AP2/ERF transcription factor AtERF73/HRE1 modulates ethylene responses during hypoxia in Arabidopsis. *Plant Physiol.* 2011;156:202–12.
25. Abbas M, Berckhan S, Rooney DJ, Gibbs DJ, Vicente Conde J, Sousa Correia C, et al. Oxygen sensing coordinates photomorphogenesis to facilitate seedling survival. *Curr Biol.* 2015;25:1483–8.
26. Eysholdt-Derzso E, Sauter M. Root Bending Is Antagonistically Affected by Hypoxia and ERF-Mediated Transcription via Auxin Signaling. *Plant Physiol.* 2017;175:412–23.
27. Paul MV, Iyer S, Amerhauser C, Lehmann M, van Dongen JT, Geigenberger P. Oxygen Sensing via the Ethylene Response Transcription Factor RAP2.12 Affects Plant Metabolism and Performance under Both Normoxia and Hypoxia. *Plant Physiol.* 2016;172:141–53.
28. Giuntoli B, Perata P. Group VII Ethylene Response Factors in Arabidopsis: regulation and physiological roles. *Plant Physiol* [Internet]. 2017; Available from: <http://dx.doi.org/10.1104/pp.17.01225>
29. White MD, Klecker M, Hopkinson RJ, Weits DA, Mueller C, Naumann C, et al. Plant cysteine oxidases are dioxygenases that directly enable arginyl transferase-catalysed arginylation of N-end rule targets. *Nat Commun.* 2017;8:14690.
30. Gasch P, Fundinger M, Müller JT, Lee T, Bailey-Serres J, Mustroph A. Redundant ERF-VII transcription factors bind an evolutionarily-conserved cis-motif to regulate hypoxia-responsive gene expression in Arabidopsis. *Plant Cell* [Internet]. American Society of Plant Biologists; 2015; Available from: <http://www.plantcell.org/content/early/2015/12/14/tpc.15.00866>
31. Giuntoli B, Lee SC, Licausi F, Kosmacz M, Oosumi T, van Dongen JT, et al. A trihelix DNA binding protein counterbalances hypoxia-responsive transcriptional activation in Arabidopsis. *PLoS Biol.* 2014;12:e1001950.
32. Gibbs DJ, Md Isa N, Movahedi M, Lozano-Juste J, Mendiondo GM, Berckhan S, et al. Nitric oxide sensing in plants is mediated by proteolytic control of group VII ERF transcription factors. *Mol Cell.* 2014;53:369–79.
33. Marín-de la Rosa N, Sotillo B, Miskolczi P, Gibbs DJ, Vicente J, Carbonero P, et al. Large-scale identification of gibberellin-related transcription factors defines group VII ETHYLENE RESPONSE FACTORS as functional DELLA partners. *Plant Physiol.* 2014;166:1022–32.

34. Weits DA, Giuntoli B, Kosmacz M, Parlanti S, Hubberten H-M, Riegler H, et al. Plant cysteine oxidases control the oxygen-dependent branch of the N-end-rule pathway. *Nat Commun.* 2014;5:3425.
35. Giuntoli B, Licausi F, van Veen H, Perata P. Functional Balancing of the Hypoxia Regulators RAP2.12 and HRA1 Takes Place in vivo in *Arabidopsis thaliana* Plants. *Front Plant Sci.* 2017;8:591.
36. Niedojadło J, Dedeńko K, Niedojadło K. Regulation of poly(A) RNA retention in the nucleus as a survival strategy of plants during hypoxia. *RNA Biol.* 2016;13:531–43.
37. Lokdarshi A, Conner WC, McClintock C, Li T, Roberts DM. *Arabidopsis* CML38, a Calcium Sensor That Localizes to Ribonucleoprotein Complexes under Hypoxia Stress. *Plant Physiol.* 2016;170:1046–59.
38. Branco-Price C, Kawaguchi R, Ferreira RB, Bailey-Serres J. Genome-wide analysis of transcript abundance and translation in *Arabidopsis* seedlings subjected to oxygen deprivation. *Ann Bot. Oxford University Press;* 2005;96:647–60.
39. Sorenson R, Bailey-Serres J. Selective mRNA Translation Tailors Low Oxygen Energetics. In: van Dongen JT, Licausi F, editors. *Low-Oxygen Stress in Plants: Oxygen Sensing and Adaptive Responses to Hypoxia.* Vienna: Springer Vienna; 2014. p. 95–115.
40. Zid BM, O’Shea EK. Promoter sequences direct cytoplasmic localization and translation of mRNAs during starvation in yeast. *Nature.* 2014;514:117–21.
41. Deal RB, Henikoff S. A simple method for gene expression and chromatin profiling of individual cell types within a tissue. *Dev Cell.* 2010;18:1030–40.
42. Reynoso M, Pauluzzi G, Kajala K, Cabanlit S, Velasco J, Bazin J, et al. Nuclear transcriptomes at high resolution using retooled INTACT. *Plant Physiol* [Internet]. 2017; Available from: <http://dx.doi.org/10.1104/pp.17.00688>
43. Zanetti ME, Chang I-F, Gong F, Galbraith DW, Bailey-Serres J. Immunopurification of polyribosomal complexes of *Arabidopsis* for global analysis of gene expression. *Plant Physiol.* 2005;138:624–35.
44. Dai X, Bai Y, Zhao L, Dou X, Liu Y, Wang L, et al. H2A.Z Represses Gene Expression by Modulating Promoter Nucleosome Structure and Enhancer Histone Modifications in *Arabidopsis*. *Mol Plant.* 2017;10:1274–92.

45. Torres ES, Deal RB. The histone variant H2A. Z and chromatin remodeler BRAHMA act coordinately and antagonistically to regulate transcription and nucleosome dynamics in Arabidopsis. *bioRxiv*. Cold Spring Harbor Laboratory; 2018;243790.
46. Mustroph A, Lee SC, Oosumi T, Zanetti ME, Yang H, Ma K, et al. Cross-kingdom comparison of transcriptomic adjustments to low-oxygen stress highlights conserved and plant-specific responses. *Plant Physiol*. 2010;152:1484–500.
47. Kim J-M, To TK, Ishida J, Morosawa T, Kawashima M, Matsui A, et al. Alterations of lysine modifications on the histone H3 N-tail under drought stress conditions in Arabidopsis thaliana. *Plant Cell Physiol*. 2008;49:1580–8.
48. Zhou J, Wang X, He K, Charron J-BF, Elling AA, Deng XW. Genome-wide profiling of histone H3 lysine 9 acetylation and dimethylation in Arabidopsis reveals correlation between multiple histone marks and gene expression. *Plant Mol Biol*. 2010;72:585–95.
49. Lu Z, Hofmeister BT, Vollmers C, DuBois RM, Schmitz RJ. Combining ATAC-seq with nuclei sorting for discovery of cis-regulatory regions in plant genomes. *Nucleic Acids Res* [Internet]. 2016; Available from: <http://dx.doi.org/10.1093/nar/gkw1179>
50. Sijacic P, Bajic M, McKinney EC, Meagher RB, Deal RB. Chromatin accessibility changes between Arabidopsis stem cells and mesophyll cells illuminate cell type-specific transcription factor networks [Internet]. *bioRxiv*. 2017 [cited 2018 Apr 5]. p. 213900. Available from: <https://www.biorxiv.org/content/early/2017/11/03/213900.abstract>
51. Maher KA, Bajic M, Kajala K, Reynoso M, Pauluzzi G, West DA, et al. Profiling of Accessible Chromatin Regions across Multiple Plant Species and Cell Types Reveals Common Gene Regulatory Principles and New Control Modules. *Plant Cell*. 2018;30:15–36.
52. O'Malley RC, Huang S-SC, Song L, Lewsey MG, Bartlett A, Nery JR, et al. Cistrome and Epicistrome Features Shape the Regulatory DNA Landscape. *Cell*. 2016;166:1598.
53. Kwon CS, Lee D, Choi G, Chung W-I. Histone occupancy-dependent and -independent removal of H3K27 trimethylation at cold-responsive genes in Arabidopsis. *Plant J*. 2009;60:112–21.
54. Kim J-M, To TK, Ishida J, Matsui A, Kimura H, Seki M. Transition of chromatin status during the process of recovery from drought stress in Arabidopsis thaliana. *Plant Cell Physiol*. 2012;53:847–56.

55. Loreti E, Poggi A, Novi G, Alpi A, Perata P. A genome-wide analysis of the effects of sucrose on gene expression in *Arabidopsis* seedlings under anoxia. *Plant Physiol.* 2005;137:1130–8.
56. Banti V, Mafessoni F, Loreti E, Alpi A, Perata P. The heat-inducible transcription factor HsfA2 enhances anoxia tolerance in *Arabidopsis*. *Plant Physiol.* 2010;152:1471–83.
57. Banti V, Loreti E, Novi G, Santaniello A, Alpi A, Perata P. Heat acclimation and cross-tolerance against anoxia in *Arabidopsis*. *Plant Cell Environ.* Wiley Online Library; 2008;31:1029–37.
58. Gilks N, Kedersha N, Ayodele M, Shen L, Stoecklin G, Dember LM, et al. Stress granule assembly is mediated by prion-like aggregation of TIA-1. *Mol Biol Cell.* 2004;15:5383–98.
59. Protter DSW, Parker R. Principles and Properties of Stress Granules. *Trends Cell Biol.* 2016;26:668–79.
60. Weber C, Nover L, Fauth M. Plant stress granules and mRNA processing bodies are distinct from heat stress granules. *Plant J.* 2008;56:517–30.
61. Weng M, Yang Y, Feng H, Pan Z, Shen W-H, Zhu Y, et al. Histone chaperone ASF1 is involved in gene transcription activation in response to heat stress in *Arabidopsis thaliana*. *Plant Cell Environ.* 2014;37:2128–38.
62. Sato F, Kitajima S, Koyama T. Ethylene-induced gene expression of osmotin-like protein, a neutral isoform of tobacco PR-5, is mediated by the AGCCGCC eff-sequence. *Plant Cell Physiol.* Oxford University Press; 1996;37:249–55.
63. LaGory EL, Giaccia AJ. The ever-expanding role of HIF in tumour and stromal biology. *Nat Cell Biol.* 2016;18:356–65.
64. Buck MJ, Raaijmakers LM, Ramakrishnan S, Wang D, Valiyaparambil S, Liu S, et al. Alterations in chromatin accessibility and DNA methylation in clear cell renal cell carcinoma. *Oncogene.* 2014;33:4961–5.
65. Chervona Y, Costa M. The control of histone methylation and gene expression by oxidative stress, hypoxia, and metals. *Free Radic Biol Med.* 2012;53:1041–7.
66. Watson JA, Watson CJ, McCann A, Baugh J. Epigenetics, the epicenter of the hypoxic response. *Epigenetics.* 2010;5:293–6.

67. Kim S-H, Jeong J-W, Park JA, Lee J-W, Seo JH, Jung B-K, et al. Regulation of the HIF-1 α stability by histone deacetylases. *Oncol Rep. Spandidos Publications*; 2007;17:647–51.
68. Blais JD, Filipenko V, Bi M, Harding HP, Ron D, Koumenis C, et al. Activating transcription factor 4 is translationally regulated by hypoxic stress. *Mol Cell Biol*. 2004;24:7469–82.
69. Young RM, Wang S-J, Gordan JD, Ji X, Liebhaber SA, Simon MC. Hypoxia-mediated selective mRNA translation by an internal ribosome entry site-independent mechanism. *J Biol Chem*. 2008;283:16309–19.
70. Schmidl C, Rendeiro AF, Sheffield NC, Bock C. ChIPmentation: fast, robust, low-input ChIP-seq for histones and transcription factors. *Nat Methods*. 2015;12:963–5.
71. Buenrostro JD, Giresi PG, Zaba LC, Chang HY, Greenleaf WJ. Transposition of native chromatin for fast and sensitive epigenomic profiling of open chromatin, DNA-binding proteins and nucleosome position. *Nat Methods*. 2013;10:1213–8.
72. Heinz S, Benner C, Spann N, Bertolino E, Lin YC, Laslo P, et al. Simple combinations of lineage-determining transcription factors prime cis-regulatory elements required for macrophage and B cell identities. *Mol Cell*. 2010;38:576–89.
73. Cao J, Packer JS, Ramani V, Cusanovich DA, Huynh C, Daza R, et al. Comprehensive single-cell transcriptional profiling of a multicellular organism. *Science*. 2017;357:661–7.
74. Girke T. systemPipeR: NGS workflow and report generation environment. UC Riverside <https://github.com/tgirke/systemPipeR> [Internet]. 2014; Available from: <http://www.bioconductor.org/packages/release/bioc/html/systemPipeR.html>
75. Morgan M, Carey V, Lawrence M. BiocParallel: Bioconductor facilities for parallel evaluation. R package version 0.4. 2014;1.
76. Bernd Bischl, Michel Lang, Olaf Mersmann, Jörg Rahnenführer, Claus Weihs. BatchJobs and BatchExperiments; Abstraction Mechanisms for Using R in Batch Environments. *J Stat Softw*. 2015;64:1–25.
77. Kim D, Pertea G, Trapnell C, Pimentel H, Kelley R, Salzberg SL. TopHat2: accurate alignment of transcriptomes in the presence of insertions, deletions and gene fusions. *Genome Biol*. 2013;14:R36.

78. Lawrence M, Huber W, Pagès H, Aboyoun P, Carlson M, Gentleman R, et al. Software for computing and annotating genomic ranges. *PLoS Comput Biol*. 2013;9:e1003118.
79. McCarthy DJ, Chen Y, Smyth GK. Differential expression analysis of multifactor RNA-Seq experiments with respect to biological variation. *Nucleic Acids Res*. 2012;40:4288–97.
80. Warnes GR, Bolker B, Bonebakker L, Gentleman R, Huber W, Liaw A, et al. *ggplots*: Various R programming tools for plotting data. R package version. 2009;2:1.
81. Wickham H. *ggplot2: Elegant Graphics for Data Analysis*. Springer Science & Business Media; 2009.
82. Neuwirth E. *RColorBrewer: colorbrewer palettes*. R package version. 2011;1.
83. Wickham H, Francois R. *dplyr: A grammar of data manipulation*. R package version 0.4. 2015;3.
84. Durinck S, Huber W. *biomaRt: Interface to BioMart databases (eg Ensembl, COSMIC, Wormbase and Gramene)*. R package version. 2.
85. Yu G, Wang L-G, He Q-Y. *ChIPseeker: an R/Bioconductor package for ChIP peak annotation, comparison and visualization*. *Bioinformatics*. 2015;31:2382–3.
86. Lawrence M, Gentleman R, Carey V. *rtracklayer: an R package for interfacing with genome browsers*. *Bioinformatics*. 2009;25:1841–2.
87. Krijthe JH. *Rtsne: T-distributed stochastic neighbor embedding using Barnes-Hut implementation*. R package version 0.13, URL <https://github.com/jkrijthe/Rtsne>. 2015;
88. Gordon A, Hannon GJ. *Fastx-toolkit. FASTQ/A short-reads preprocessing tools (unpublished)* http://hannonlab.cshl.edu/fastx_toolkit. 2010;5.
89. Andrews S, Others. *FastQC: a quality control tool for high throughput sequence data*. 2010;
90. Bailey TL, Boden M, Buske FA, Frith M, Grant CE, Clementi L, et al. *MEME SUITE: tools for motif discovery and searching*. *Nucleic Acids Res*. 2009;37:W202–8.
91. Ramírez F, Ryan DP, Grüning B, Bhardwaj V, Kilpert F, Richter AS, et al. *deepTools2: a next generation web server for deep-sequencing data analysis*. *Nucleic Acids Res*. 2016;44:W160–5.

92. Krzywinski M, Schein J, Birol I, Connors J, Gascoyne R, Horsman D, et al. Circos: an information aesthetic for comparative genomics. *Genome Res.* 2009;19:1639–45.
93. Quinlan AR, Hall IM. BEDTools: a flexible suite of utilities for comparing genomic features. *Bioinformatics.* 2010;26:841–2.
94. Li H. A statistical framework for SNP calling, mutation discovery, association mapping and population genetical parameter estimation from sequencing data. *Bioinformatics.* 2011;27:2987–93.

Fig. 2.1. Multiscale chromatin and mRNA gene regulatory analyses of control (normoxic), hypoxic and re-oxygenated seedlings of *Arabidopsis*. **a** Schematic diagram of experiments performed. Seven-day-old seedlings were subjected to control (normoxic) conditions (2NS), 2 or 9 h hypoxic stress (2HS, 9HS), or 2h hypoxic stress followed by 1 or 2 h reoxygenation (1R, 2R). Arrows indicate time of harvest. Gene regulation was evaluated by chromatin immunopurification (ChIP) and to monitor specific forms of Histone 2 and Histone 3 (H2A.Z, H3K4me3, H3K27me3, H3K9Ac, H3K14Ac) and binding regions of the group VII Ethylene Response Factor (ERF) transcription factor HYPOXIA RESPONSIVE ERF 2 (HRE2). Accessible chromatin was identified by Tn5 transposase insertion (ATAC). Nuclei extraction was by Isolation of Nuclei in TArgeted Cell Types (INTACT). The Ser2 phosphorylated form of RNA Polymerase II (RNAPII Ser2P) was obtained by ChIPmentation. Ribosome-associated mRNA was obtained by Translating Ribosome Affinity Purification (TRAP). **b** Demonstration of reproducibility of individual replicates of genome-scale data related to nascent transcription (Ser2P) and RNA (nuclear [nRNA], polyadenylated mRNA [polyA], ribosome-associated polyadenylated mRNA [TRAP]) by use of t-Distributed stochastic neighbor embedding (t-SNE). **c** Violin plots displaying genome-wide abundance (reads per kilobase per million reads [RPKM]) of histone and mRNA-related outputs for the control (2NS) and short-term hypoxic (2HS) treatments. Mean \pm SD are depicted within violins in dark gray. RPKM data for the previously defined 49 core hypoxia responsive up-regulated genes (HRGs) [18] are plotted as orange dots. The HRG, *ALCOHOL DEHYDROGENASE 1 (ADH1)*, is plotted in red and tracked between datasets (red dashed line).

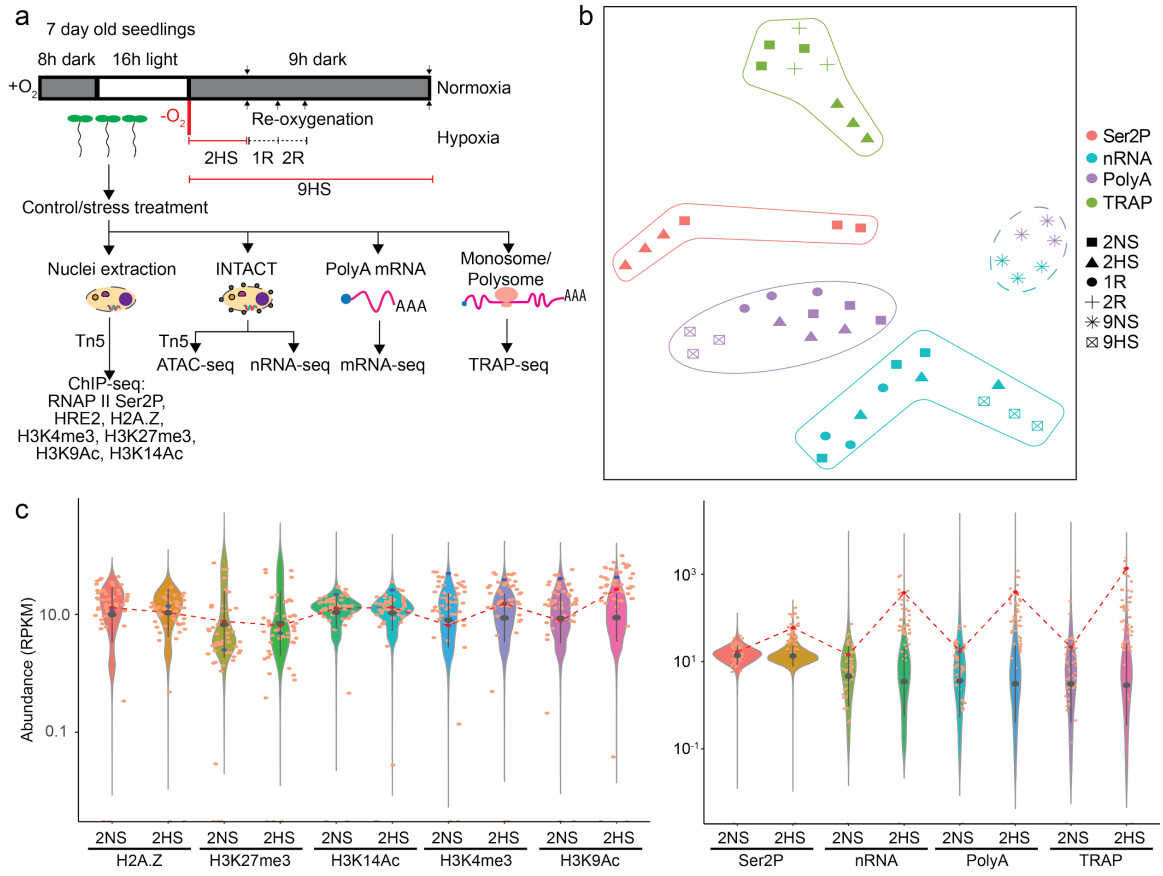


Fig. 2.2. Genome-wide survey of chromatin-level dynamics in response to hypoxic and reoxygenation treatments. **a** Average distribution of four Histone 3 modifications and a Histone 2A variant under control (2NS) and short-term hypoxic (2HS) conditions spanning the region 1 kb upstream of the transcription start site (TSS) to 1 kb downstream of the transcription end site (TES) for protein-coding genes. The y-axis corresponds to signal value. **b** Average distribution of chromatin accessibility spanning 1 kb upstream of the TSS and 1 kb downstream of TES for protein-coding genes as determined by use of ATAC-seq. The mean widths: 2NS 155 bp, 2HS 161 bp, 1R 172, 9NS 160, 9HS 157. **c** Number of transposase (Tn) hypersensitive sites (THS) genome-wide for each condition. **d** Genomic distribution of THS on defined genomic features for each condition. **e** Volcano plots comparing fold change and $-\log_{10}$ p-value of THSs recognized under both conditions in four treatment comparisons. Number of differentially up- and down-regulated shown ($|\text{Log}_2 \text{ fold change}| > 1$; p-value < 0.05.).

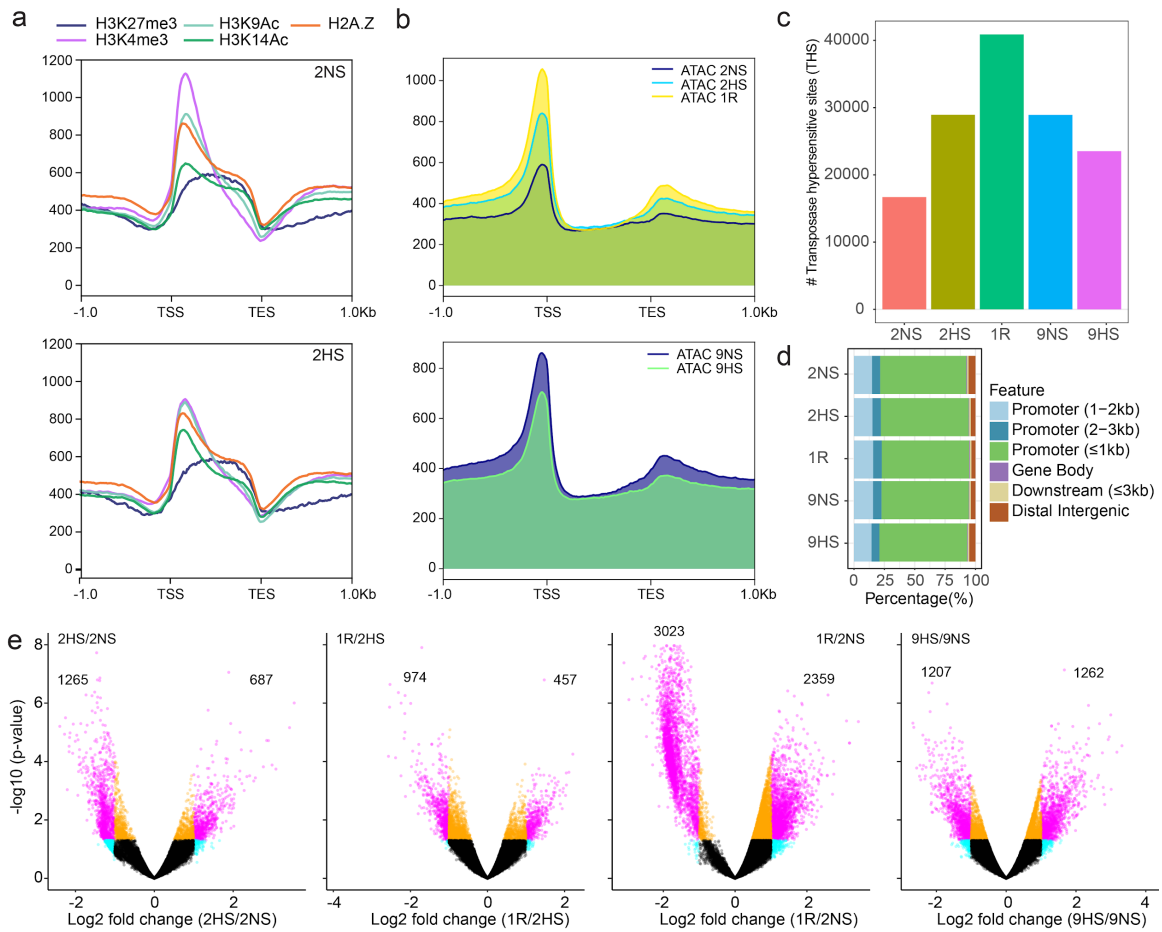


Fig. 2.3. Short term hypoxic stress promotes pronounced changes in chromatin, transcription and nascent transcripts that are not uniformly reflected in transcript steady-state abundance or translation. Comparison of genome-wide data for chromatin and RNA for 2 h hypoxic stress (2HS) relative to the normoxic control (2NS). **a** Violin plots of \log_2 fold change (2HS/2NS) of Histone, Ser2P and mRNA outputs. The 49 core Hypoxia-Responsive Genes [18] are plotted as orange dots with *ADH1* depicted in red and tracked between datasets (red dashed line). Cytosolic ribosomal proteins (RPs) are plotted in blue, with *RIBOSOMAL PROTEIN 37B* tracked between datasets (blue dashed line). Mean \pm SD are depicted within violins in dark gray. **b** Number of differentially regulated genes (DRGs) in response to hypoxic stress ($|\log_2$ fold change| > 1; FDR < 0.05) identified in each of the four readouts related to RNA: Ser2P ChIP, nRNA, polyA RNA, and TRAP RNA. Arc of circle circumference indicated by the thick grey line represents the DRGs in each of the four readouts, with up-regulated (UP) and down-regulated (DOWN) gene data presented in independent circles. Genes consistently differentially regulated in 2 to 4 readouts were tabulated (number in parentheses) and depicted by shading within the circle. Genes differentially regulated in only one readout are represented by the grey line. **c** Comparison of \log_2 fold change (2HS/2NS) between H2A.Z on the gene body and Ser2P on the gene body. **d** Comparison of \log_2 fold change (2HS/2NS) between H3K9Ac and Ser2P on the gene body and polyA mRNA abundance. For c and d, HRGs are plotted in pink and RPs in blue; the Pearson's coefficient of determination is shown. **e** Genome browser view of normalized read coverage on selected genes for the chromatin, RNAPII, HRE2 and RNA outputs for 2NS and 2HS samples. The maximum read scale value used for chromatin and RNA outputs is the same for individual genes. Transcription unit is shown in grey with the TSS marked with an arrow.

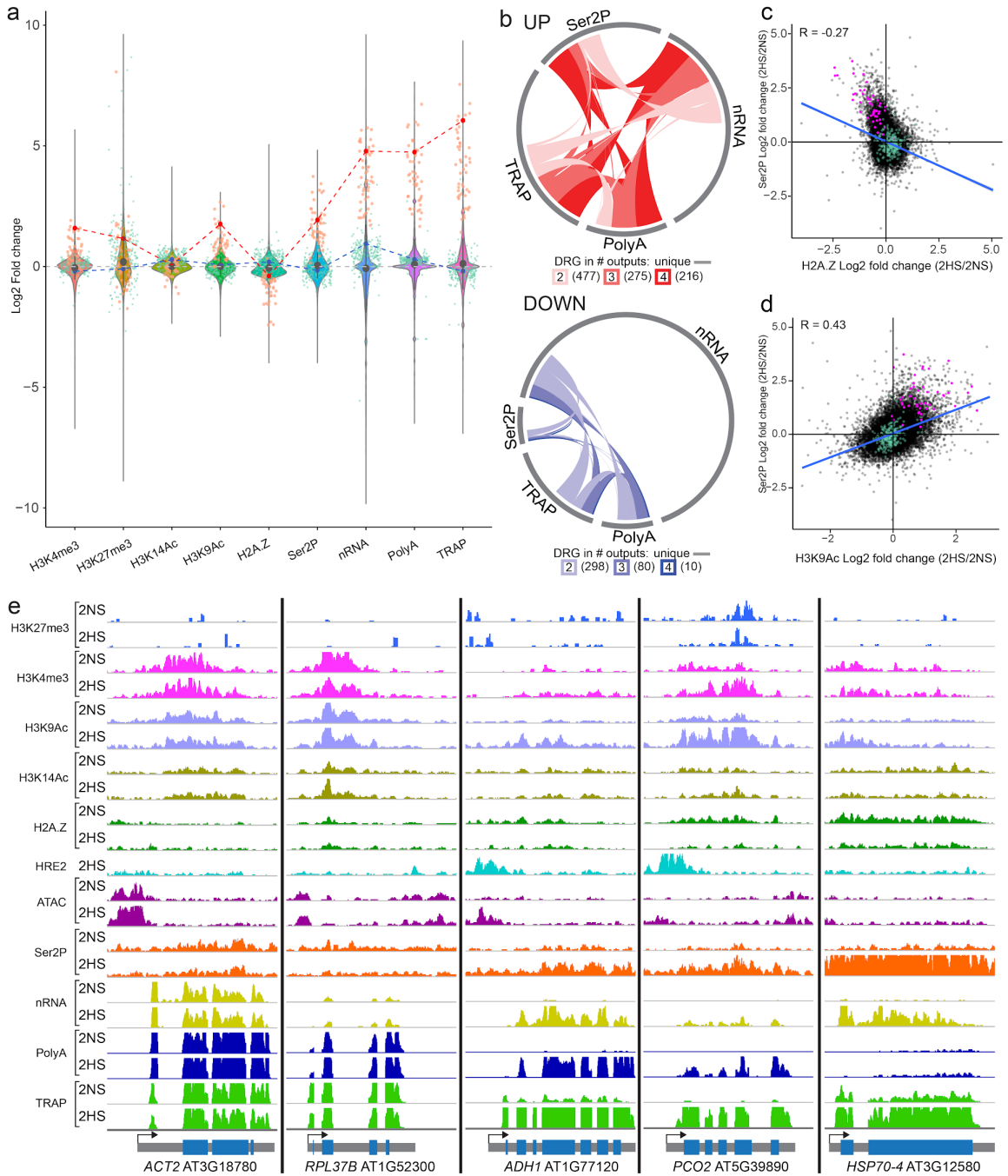


Fig. 2.4. Multi-scale evaluation of differential regulation of subsets of protein-coding genes in response to hypoxic stress identifies coordination of chromatin, transcription and post-transcriptional upregulation in the most strongly upregulated genes. **a** Heatmap showing similarly regulated genes based on four assays of gene activity. Partitioning around medoids (PAM) clustering of 3,042 DRGs; 16 clusters. Selected enriched Gene Ontology terms are shown at right (p adj. $< 1.37E-06$), $|FC| > 1$, p adj. < 0.05 . Clusters displaying increased or decreased translational status (ribosome-associated [TRAP] relative to total abundance [polyA]) are shown. **b** Average signal of various chromatin and RNA outputs for genes of indicated clusters plotted from 1 kb upstream of the TSS to 1 kb downstream of the TES. Signal scale of graph differ. **c** Binding motif prediction based on peak regions of HRE2 binding to chromatin after 2 h hypoxic stress, compared to the HRPE motif that is necessary and sufficient to transactivate gene activation by ERFVIs in protoplasts [30]. **d** Frequency of occurrence in the 16 gene clusters in panel **a** of the HRE2 motif, HRPE motif and ten Heat Shock Response Factor (HSF) transcription factors identified through use of DNA affinity purification and sequencing (DAP-seq) on chromatin by [52].

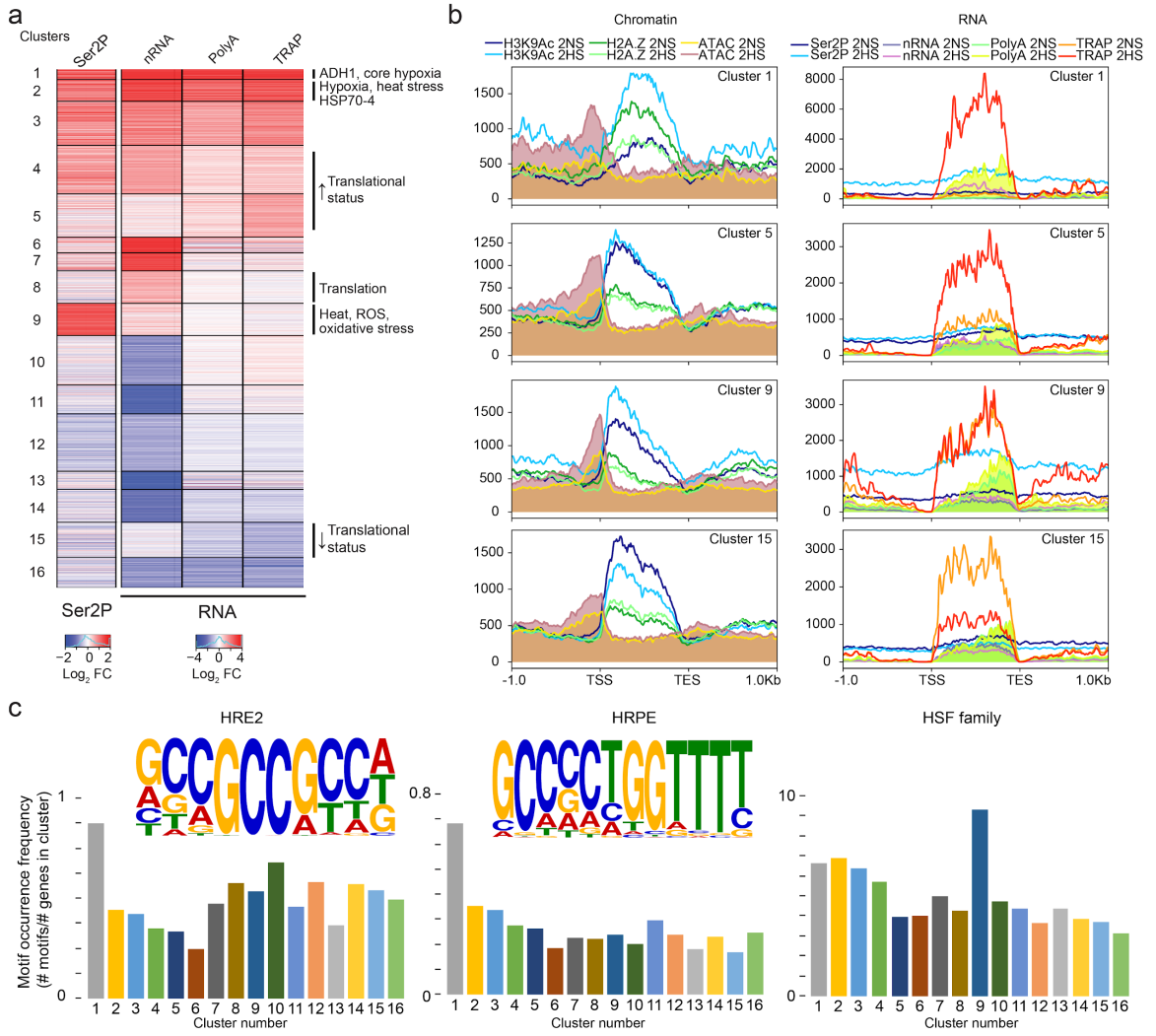


Fig 2.5. Prolonged but sublethal hypoxic stress promotes Histone 3 modifications, impacts nuclear RNA and polyA RNA abundance. Comparison of genome-wide data for chromatin and RNA for 2 h (2HS) and 9 h (9HS) hypoxic stress relative to normoxic control (2NS and 9NS). **a** Violin plot of \log_2 fold change in acetylation of Histone 3 at two sites, nRNA and polyA RNA. Values for individual hypoxia-responsive genes are plotted in orange, with *ADH1* depicted in red and data connected with a dashed red line. Cytosolic ribosomal proteins are plotted in blue, with *RIBOSOMAL PROTEIN 37B* depicted in dark blue and data in replicates connected with a dashed blue line. Mean \pm SD are depicted within violins in dark gray. **b** Number of up- and down- DRGs for the 2HS/2NS and 9HS/9NS comparisons for RNA and chromatin outputs ($|\log_2$ fold change| > 1; FDR < 0.05). The number of distinct readouts with which DRGs overlap and interactions between different comparisons and outputs is depicted: **c** Genome browser view of data for representative genes including *REVEILLE2/CIRCADIAN1 (CIR1)* [At5g37260]. **d** Heatmap showing similarly regulated genes based on change in nRNA and polyA RNA levels after the two durations of hypoxic stress. Partitioning around medoids (PAM) clustering of 4,124 DRGs; 16 clusters. Gene Ontology enrichment examples provided for select clusters (p adj. < 0.05). **f** Average signal of chromatin and RNA readouts for genes of indicated clusters.

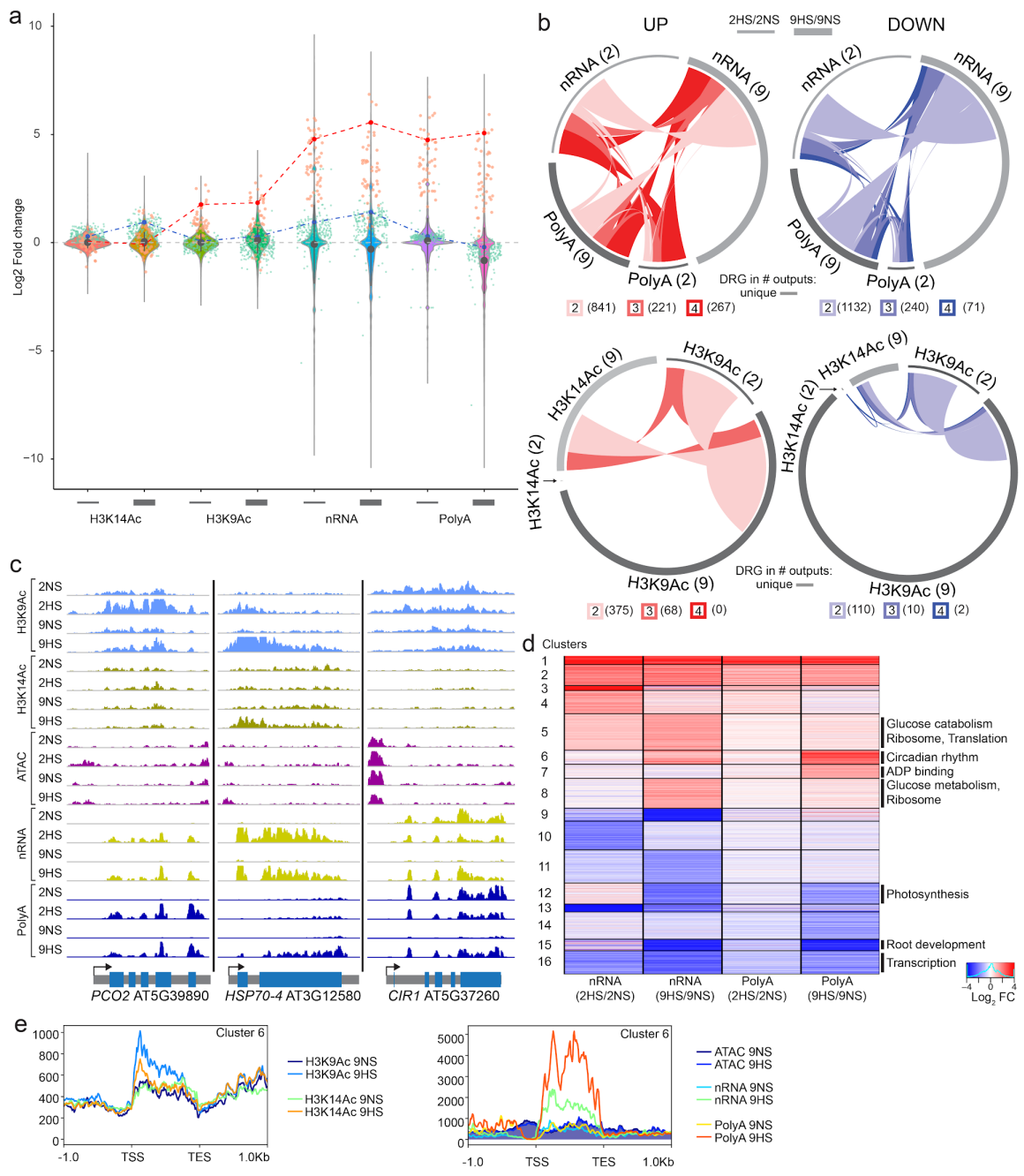
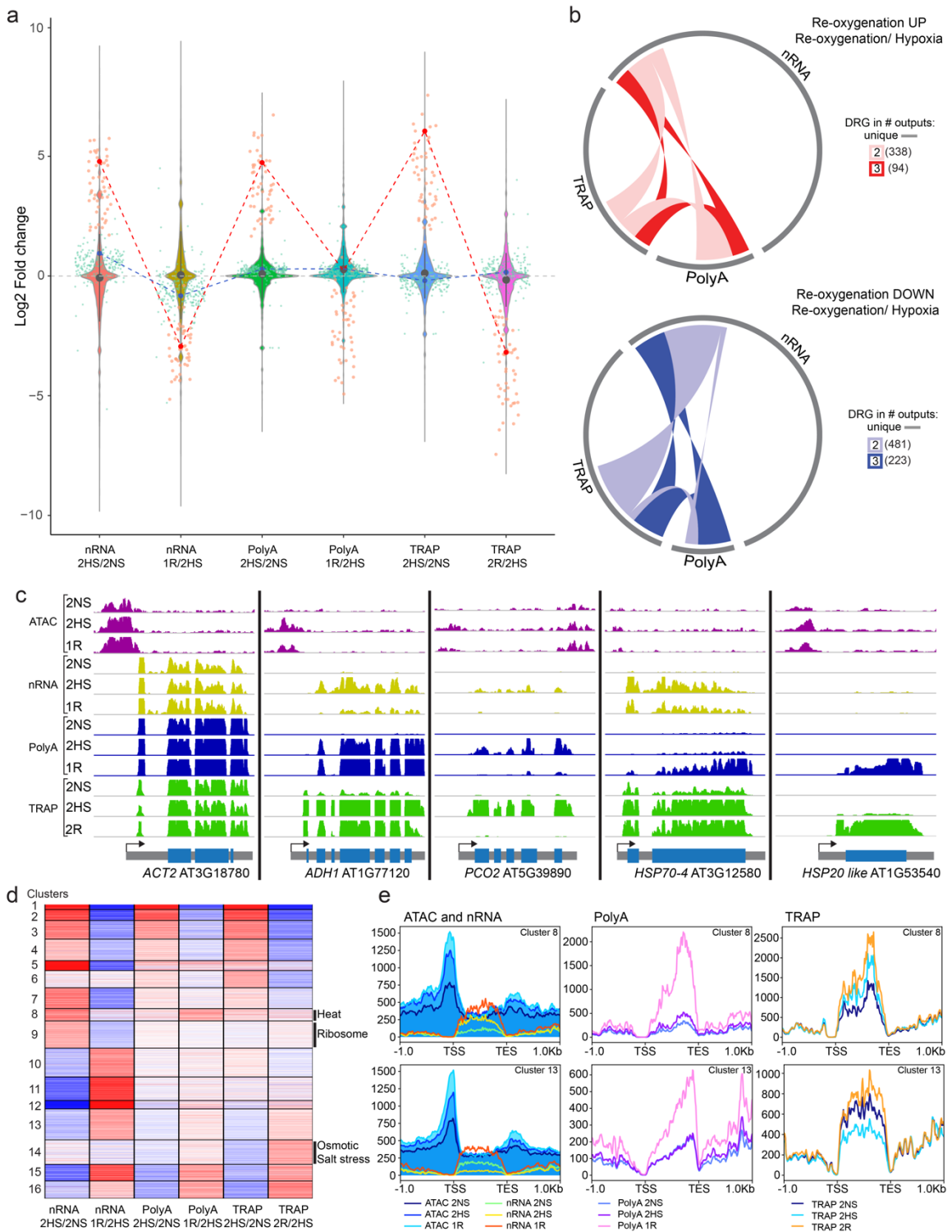
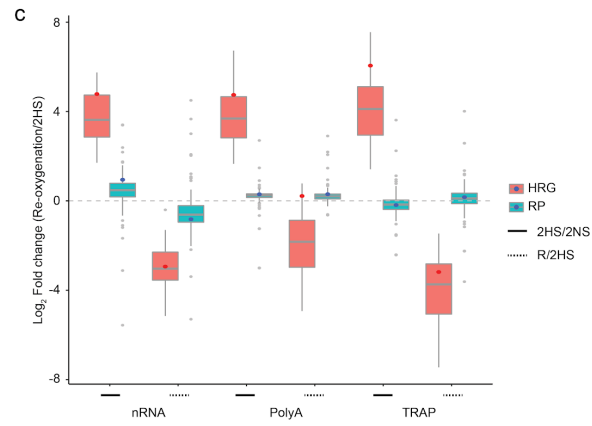
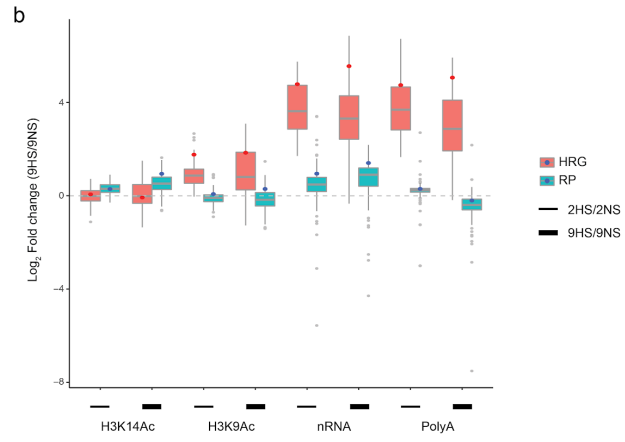
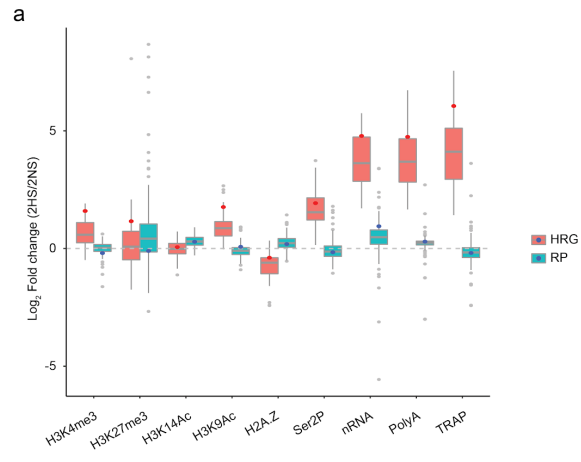


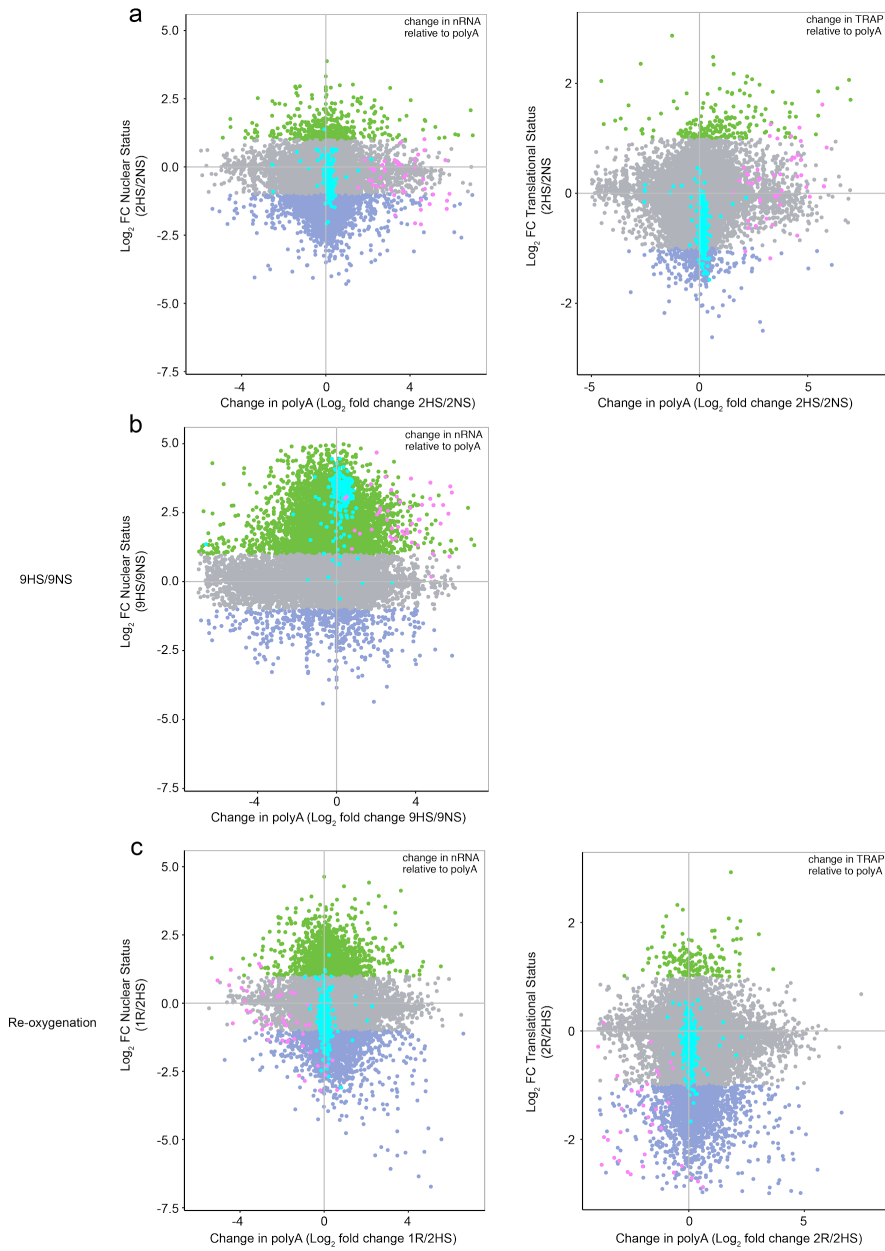
Fig. 2.6. Dynamic responses to reoxygenation include changes in chromatin and RNA populations. Comparison of genome-wide data for chromatin and RNA for 2 h hypoxic stress (2HS) and reoxygenation (1R or 2R) relative to the normoxic control (2NS). **a** Violin plots of \log_2 fold change. Values for individual hypoxia-responsive genes are plotted in orange, with *ADH1* depicted in red and data in replicates connected with a dashed red line. Cytosolic ribosomal proteins (RPs) are plotted in blue, with *RIBOSOMAL PROTEIN 37B* depicted in dark blue and data in replicates connected with a dashed blue line. Mean \pm SD are depicted within violins in dark gray. **b** Overlap in DRGs in the reoxygenation up- and down- DRGs (Reoxygenation / Hypoxia) in comparisons for RNA and chromatin outputs ($|\log_2$ fold change| > 1; FDR < 0.05). **c** Genome browser views of data for representative genes. **d** Heatmap showing similarly regulated genes based on change in nRNA, polyA RNA and TRAP RNA levels contrasting 2HS and reoxygenation. Partitioning around medoids (PAM) clustering of 4,784 DRGs; 16 clusters. Gene Ontology enrichment examples provided ($|\log_2$ fold change| > 1, FDR < 0.01, p adj. < 0.05). **e** Average signal of chromatin and RNA genomic readouts for genes of indicated clusters.



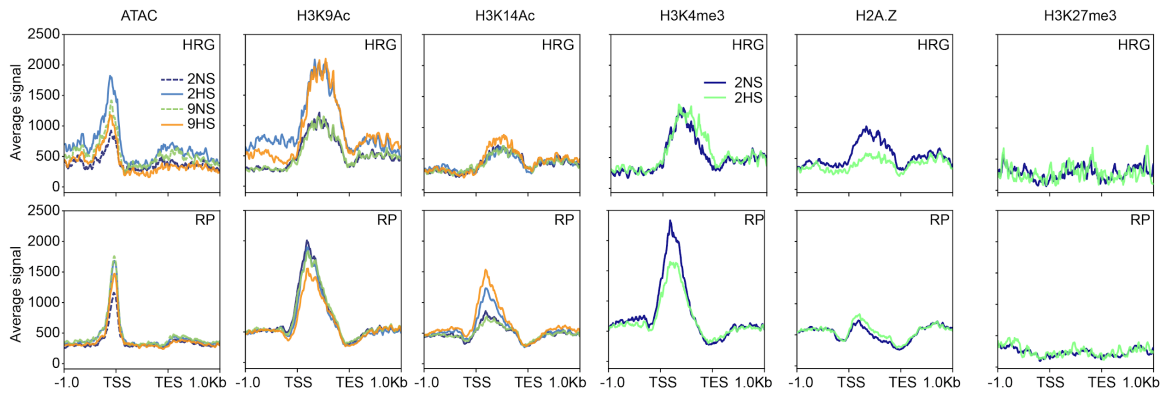
Supplemental Fig. 2.1. Dynamics in histones and RNA populations of the core Hypoxia Responsive Genes (HRGs) and cytosolic ribosomal protein (RP) genes. Box plots of \log_2 fold change assayed for, **a** short term (2 h) hypoxic stress compared to control (2HS/2NS) for data from nine assays; **b** short term (2 h) and long term (9 h) hypoxic stress compared to control (2HS/2NS, 9HS/9NS) for data in four assays and reoxygenation for 1 h or 2 h following 2 h HS (R/2HS) for data in three assays. *ADH1* is depicted as a red dot and *RPL37B* is depicted as a dark blue dot. Range of dataset and upper and lower quantiles are depicted within each boxplot.



Supplemental Fig. 2.2. Comparison of change in nuclear- and ribosome-associated mRNA abundance relative to change in polyA RNA abundance reveals differential regulation of nuclear retention and translation in response to hypoxic stress and reoxygenation. The change in nuclear status (nRNA relative to polyA RNA) and translational status (TRAP RNA relative to polyA RNA) was plotted for, **a** short term (2 h) hypoxic stress compared to control (2HS/2NS); **b** long term (9 h) hypoxic stress compared to control (9HS/9NS); and **c** reoxygenation for 1 h or 2 h following 2 h HS (R/2HS). The 49 Hypoxia Responsive Genes (HRG) are plotted in pink and the 223 cytosolic ribosomal proteins are plotted in cyan. Genes with significant increase (green) or decrease (purple) in nuclear status or translational status are shown; ($|\text{Log}_2 \text{ fold change}| > 1$; $p\text{-value} < 0.05$).



Supplemental Fig. 2.3. Histones and chromatin accessibility of Hypoxia Responsive Genes (HRG) and cytosolic Ribosomal Protein (RP) genes are distinctly regulated by short term (2HS) and prolonged (9HS) hypoxic stress when compared to control samples (2NS and 9NS). Average signal of various chromatin outputs for 49 HRGs and 223 RPs plotted from 1 kb upstream of the TSS to 1 kb downstream of the TES.

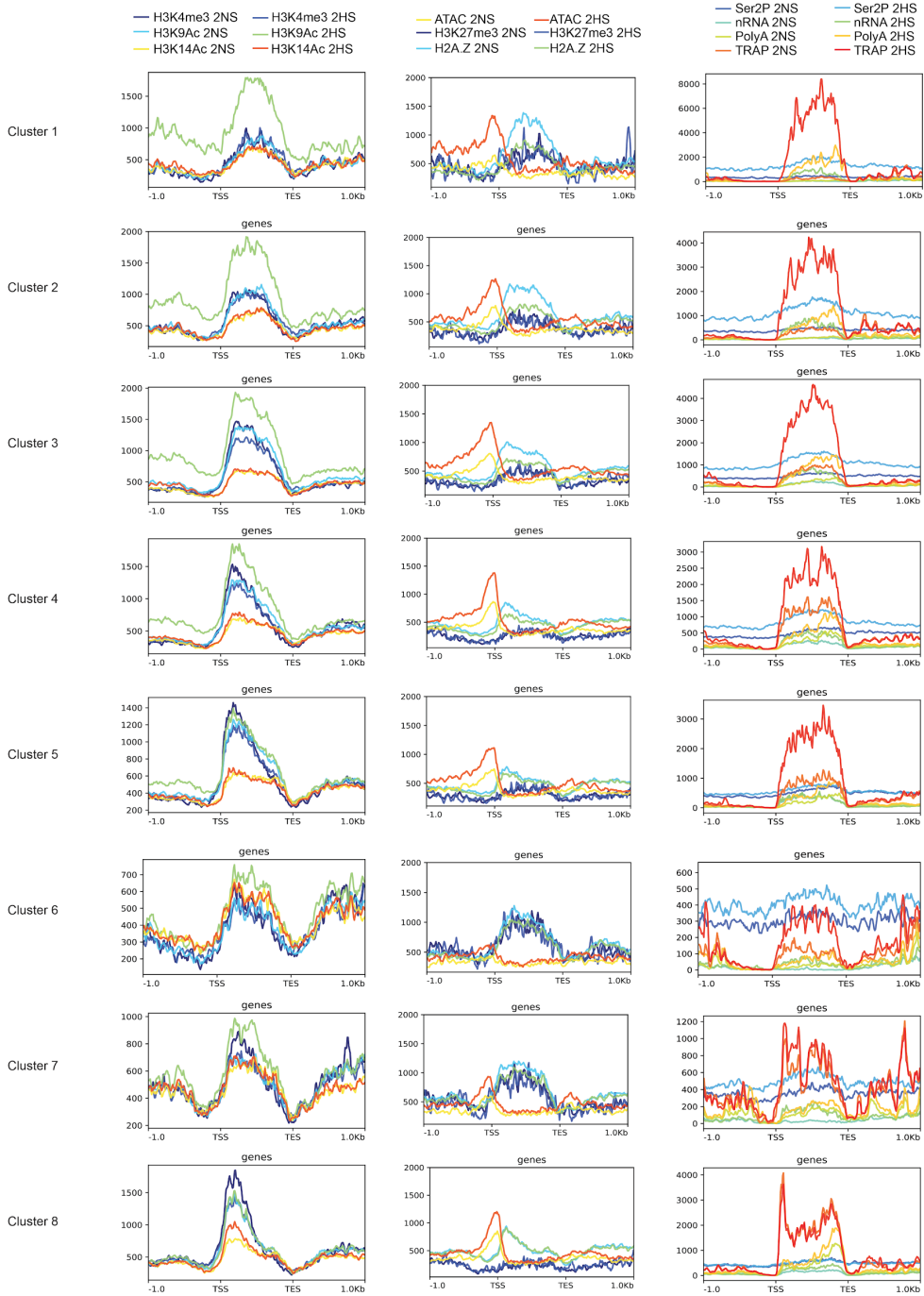


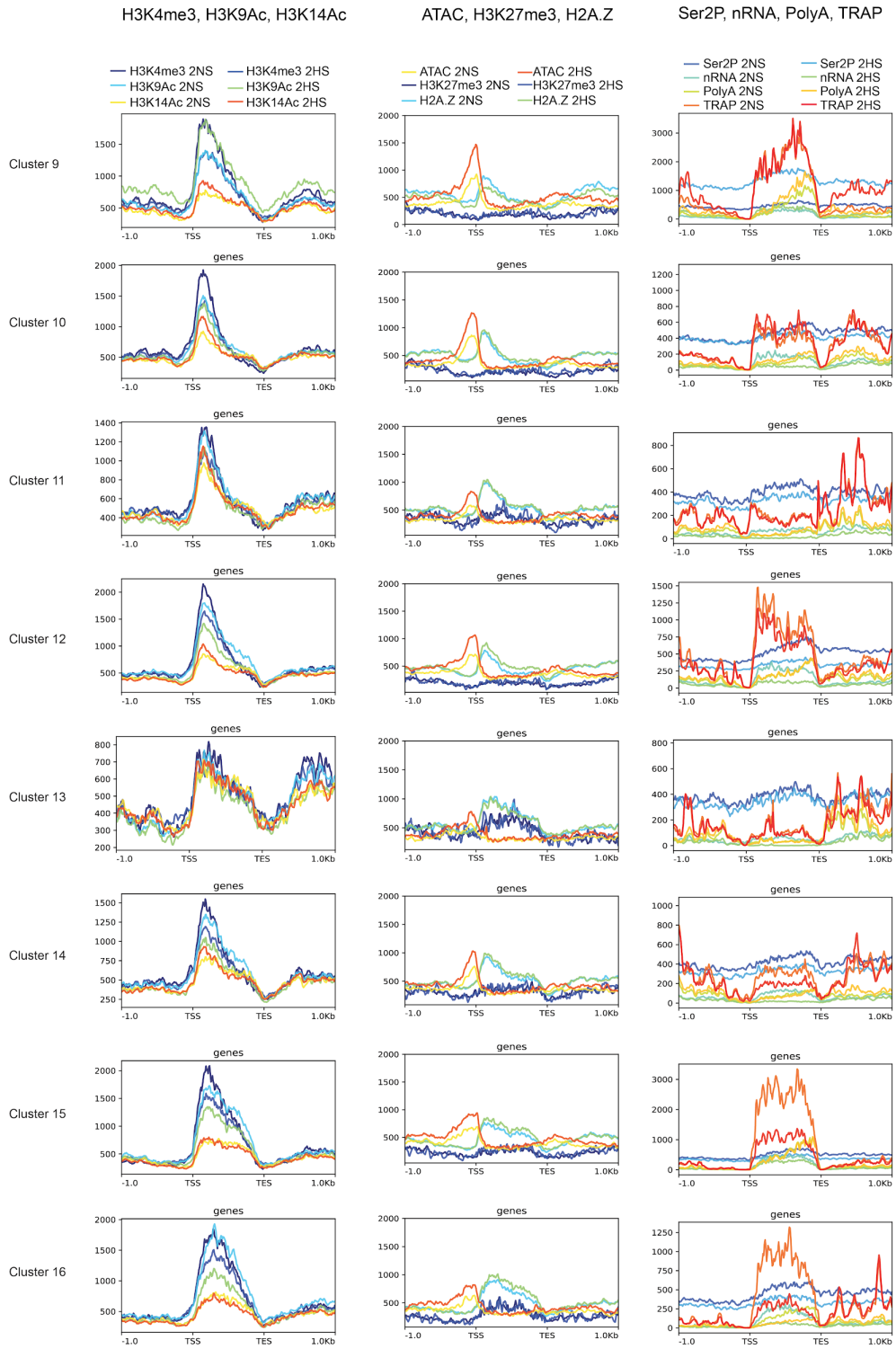
Supplemental Figure 2.4. Distinctions in histones across genes that are co-regulated at the RNA level in response to hypoxic stress. Average signal of all chromatin and RNA outputs for clustered genes identified from the 2 h hypoxic stress comparison (2HS/2NS) in Fig. 4a. Signal values are plotted from 1 kb upstream of the TSS to 1 kb downstream of the TES. Signal scale of graphs differ.

H3K4me3, H3K9Ac, H3K14Ac

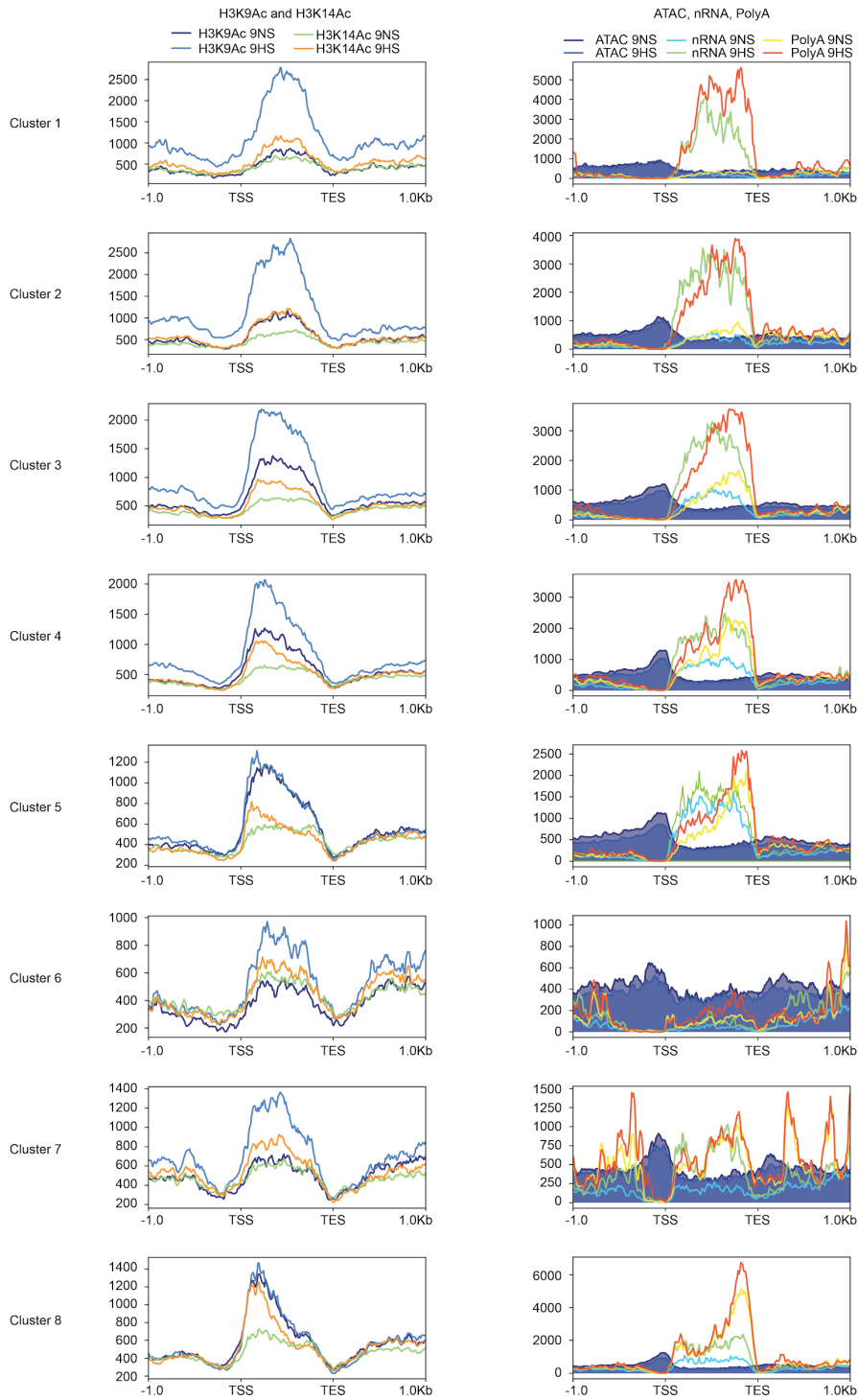
ATAC, H3K27me3, H2A.Z

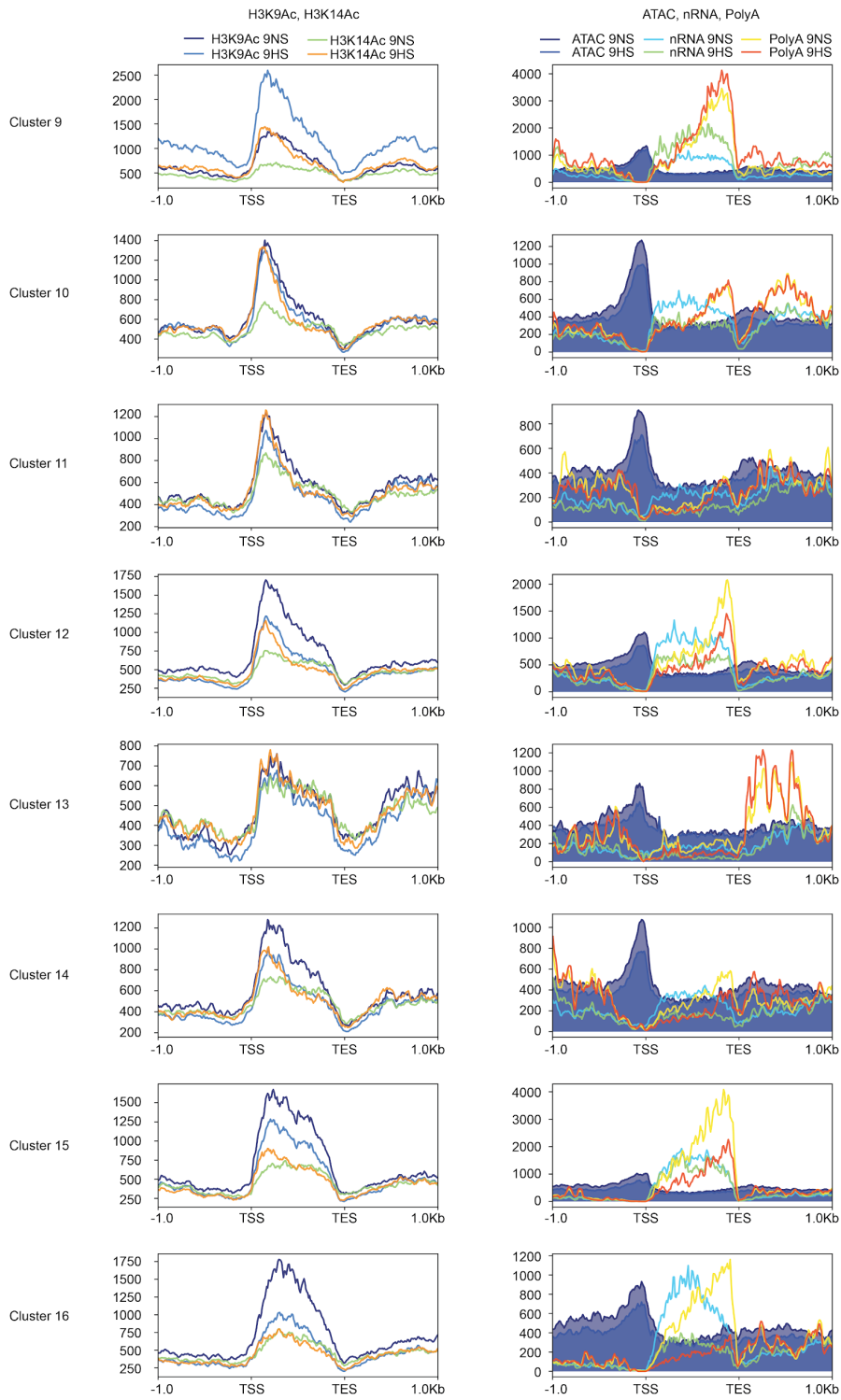
Ser2P, nRNA, PolyA, TRAP



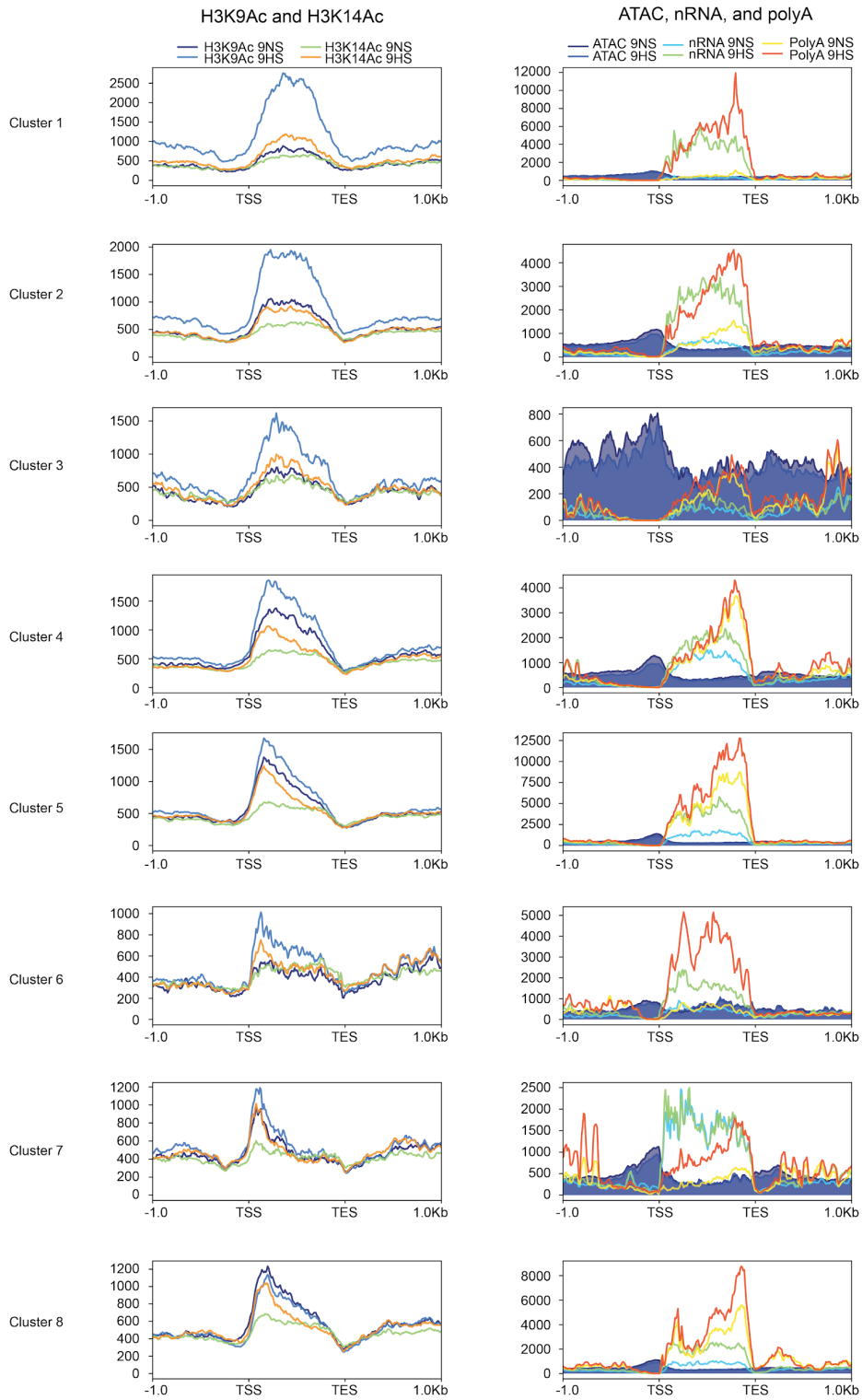


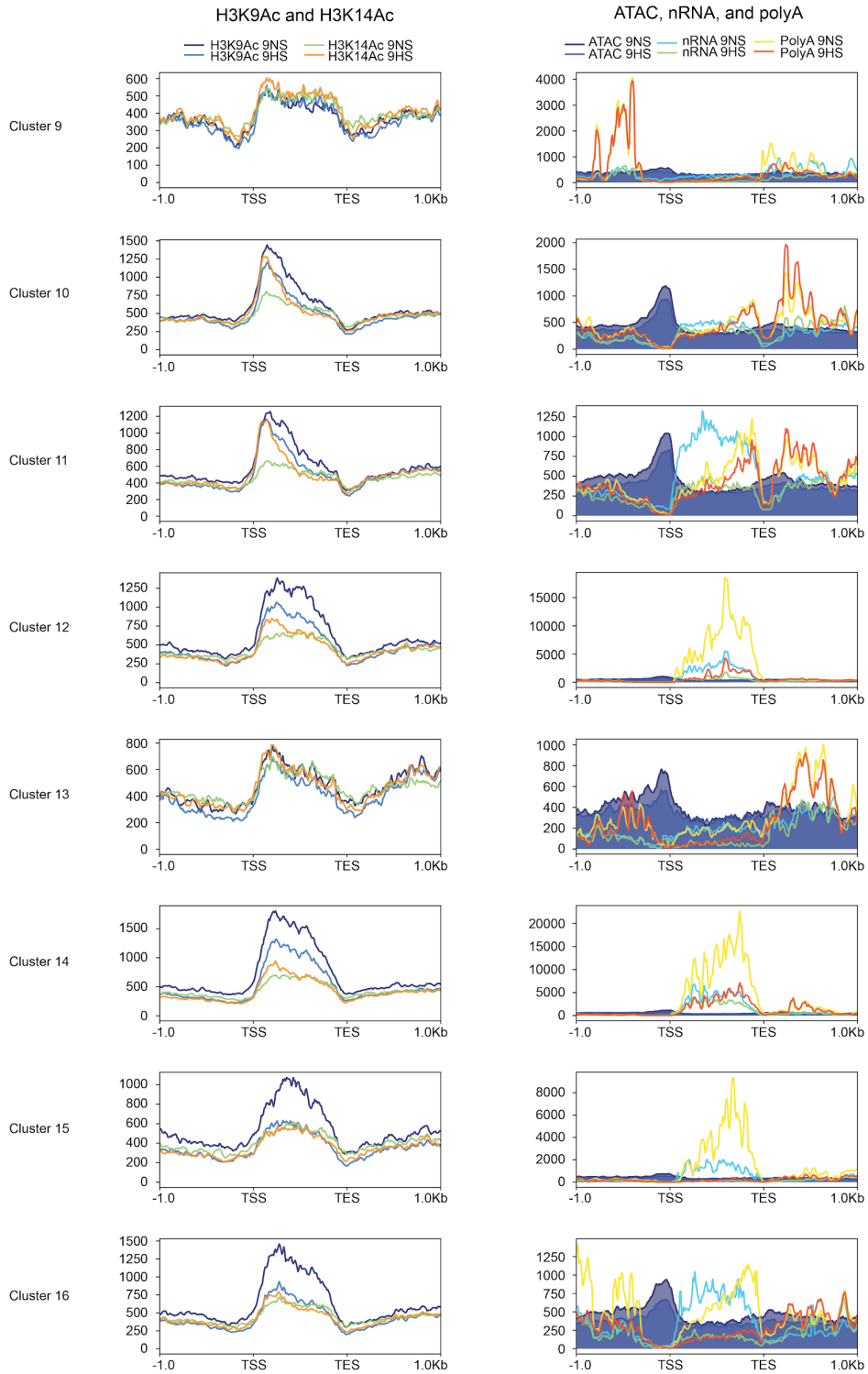
Supplemental Fig. 2.5. Average signal of chromatin and RNA data for co-regulated gene clusters identified from the 2 h hypoxic stress comparison (2HS/2NS) in Fig. 4a in response to prolonged hypoxic stress (9HS/9NS). Signal is plotted from 1 kb upstream of the TSS to 1 kb downstream of the TES. Signal scale of graphs differ.



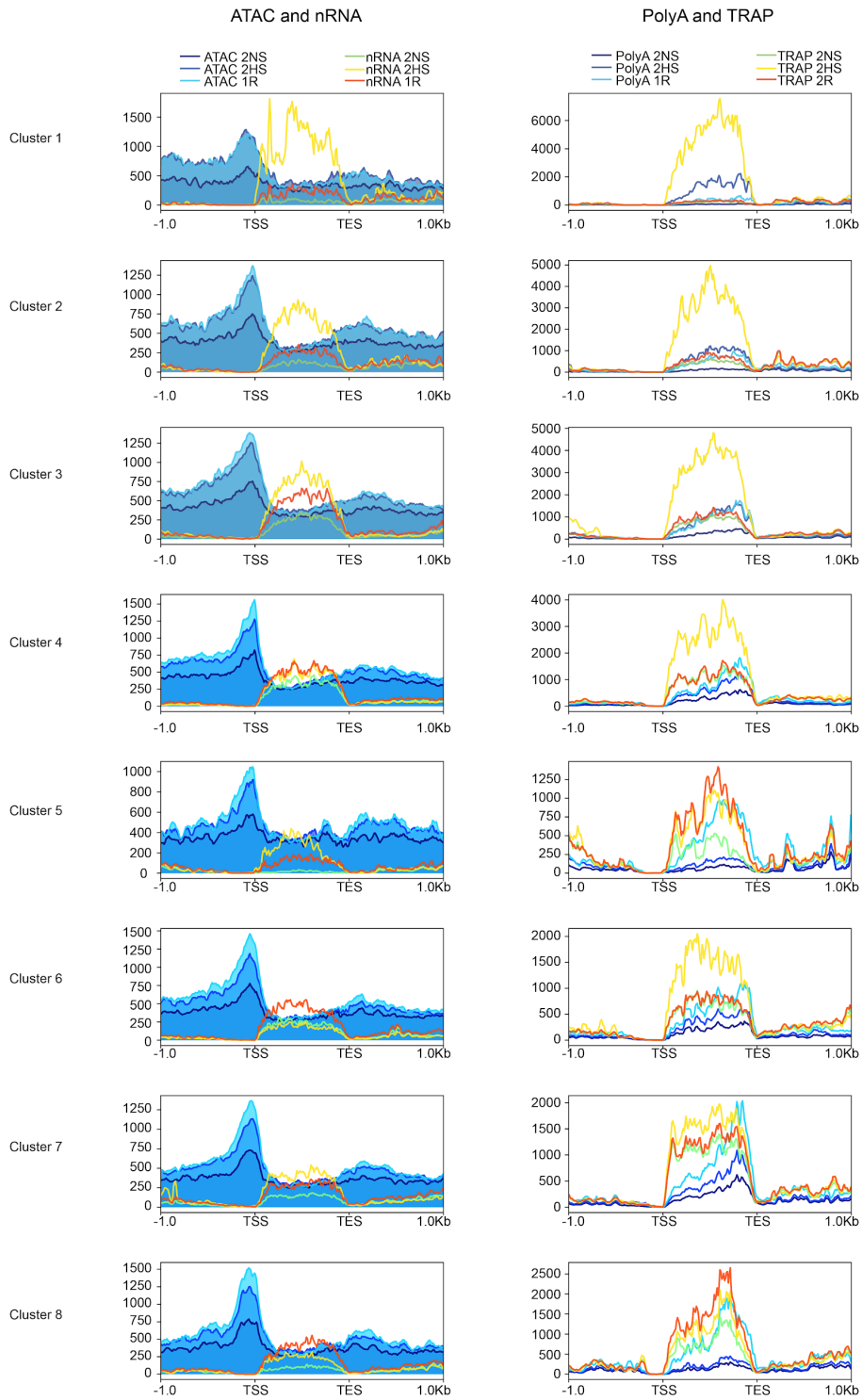


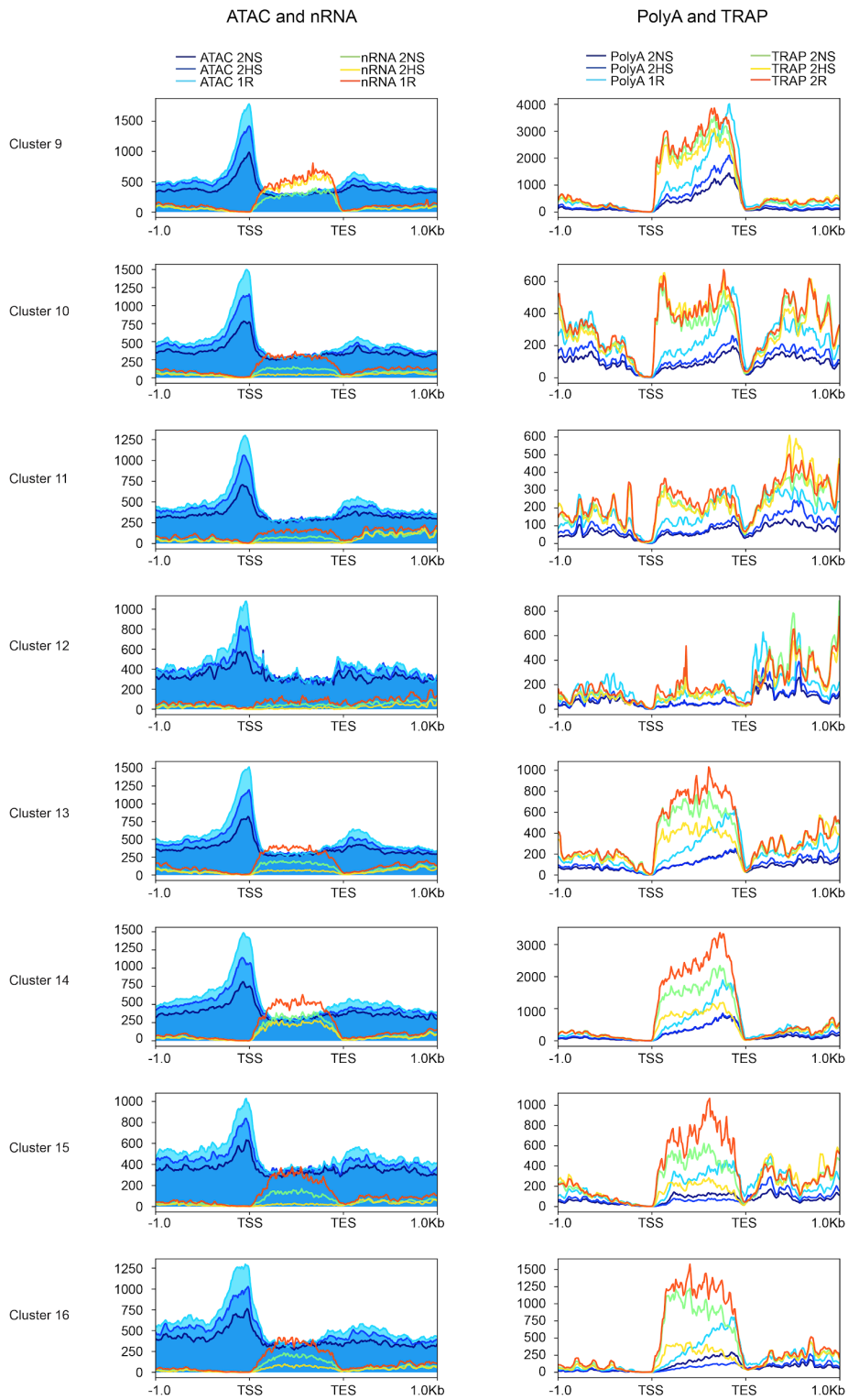
Supplemental Fig. 2.6. Average signal of chromatin and RNA data for co-regulated gene clusters identified from the 9 h hypoxic stress comparison (9HS/9NS) in Fig. 2.5.e. Signal is plotted from 1 kb upstream of the TSS to 1 kb downstream of the TES. Signal scale of graphs differ.



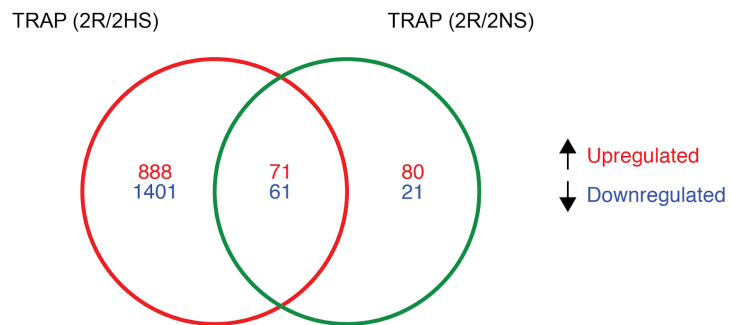
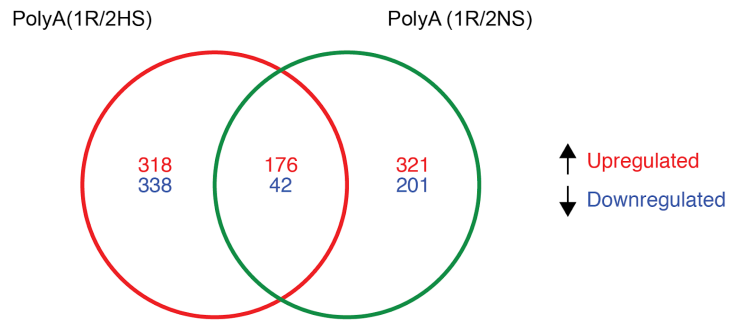
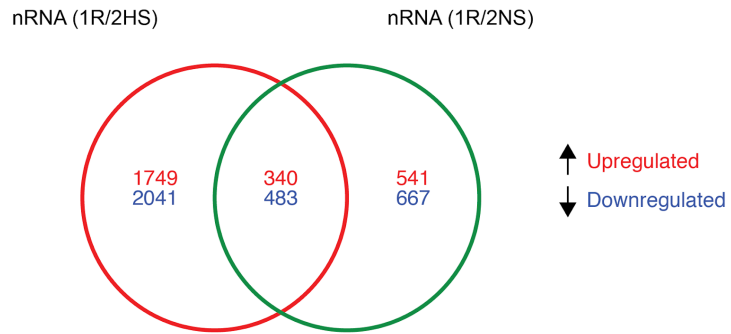


Supplemental Fig. 2.7. Average signal of chromatin and RNA data outputs for co-regulated gene clusters identified from the reoxygenation comparison (1R/2NS) shown in Fig. 2.6.d. Signal is plotted from 1 kb upstream of the TSS to 1 kb downstream of the TES. Signal scale of graphs differ.





Supplemental Fig. 2.8. Identification of genes with up or down-regulated transcripts under reoxygenation. Overlap of differentially regulated genes ($|\text{Log}_2$ fold change $| > 1$, $\text{FDR} < 0.01$) identified in the nRNA, polyA, and TRAP populations under reoxygenation by comparison to short term hypoxic stress (2HS) and nonstress (2NS). reoxygenation regulated genes are specified by the overlap of genes differentially regulated in both comparisons ((R/2NS), (R/2HS)).



Chapter 3

Molecular characterization of SUBMERGENCE 1A and C stability and binding in *Arabidopsis*

3.1. Abstract

Plant responses to hypoxia are mediated through the presence and activity of group VII *ETHYLENE RESPONSE FACTORS* (ERFVIIs). These transcription factors (TFs) include the rice gene, *SUBMERGENCE 1A* (*SUB1A*), that confers tolerance to complete submergence in rice. The *Arabidopsis* ERFVII, *HYPOXIA RESPONSIVE ERF 2* (*HRE2*) is strongly upregulated and associated with plant survival of hypoxic stress. The turnover of *Arabidopsis* ERFVIIs is promoted in an oxygen-dependent manner by the Cys-Arg branch of the N-end Rule Pathway of Targeted Proteolysis (Cys-Arg/NERP), requiring cysteine as the second residue of the protein (NH₂-MC). *HRE2* and *SUB1A* are NH₂-MC ERFVIIs but *SUB1A* is unusual as it is not a NERP substrate based on an *in vitro* assay..The related rice protein *SUB1C* does not have the NH₂-MC feature. Cys-Arg/NERP turnover of *SUB1A* has not been tested *in planta*. In the present study, *in vivo* stability of *SUB1A* was evaluated in *Arabidopsis* in the presence and absence of a required Cys-Arg/NERP component and hypoxic stress. Additionally, genome-wide binding profiles were generated for the ERFVIIs *SUB1A*, *SUB1C*, and *HRE2*. Comparative bioinformatic analyses of

these data was performed and contrasted with chromatin landscape, RNA polymerase II (RNAPII) engagement and gene transcript abundance data. When ectopically expressed in *Arabidopsis*, SUB1A abundance is enhanced in the absence of the Cys-Arg/NERF E3 ligase and proteasome inhibition. SUB1A and SUB1C binding to chromatin is highly similar and regulated in an oxygen-dependent manner. Notably, genes that were up- and down-regulated at the steady-state mRNA level by hypoxic stress displayed distinctions in the position of SUB1A, SUB1C and HRE2 binding to genic regions. HRE2 bound to the promoter regions of many hypoxia-responsive genes, whereas SUB1A and SUB1C were dynamically associated with promoter and transcribed regions, in a manner suggesting that these ERFVIs interact with DNA as well as chromatin-associated proteins or RNAPII. The findings of this study provide a framework for follow-up experiments to further elucidate the roles and regulation of ERFVIs.

3.2. Introduction

As sessile organisms, plants face challenges that can be avoided by mobile organisms. To survive successfully to reproduction, plants require the ability to adapt to and endure daily and seasonal variations in the environment. Plants have evolved a complex and highly tuned capacity to respond to sub-optimal environmental conditions through short- and long-term responses at the epigenetic, transcriptional, post-transcriptional, and post-translational levels. These lead to differential regulation of a wide array of metabolic acclimations as

well as alterations in development that benefit survival and fecundity under chronic stress. Under conditions of acute stress, plants often limit growth to facilitate survival until more favorable conditions arise. Thus, mechanisms for endurance of transient to prolonged acute stress, as well as return to normal growth, are important for the survival and reproduction of plants.

Changes in environmental events and patterns pose a difficulty for plant survival. Increases in weather extremes such as periods of water and temperature extremes lead to significant losses of crops and disturbance of native ecosystems. Flooding, which can include waterlogging of the root system or the partial to complete submergence of above ground organs, is an agronomically important event that leads to significant agricultural losses[1]. Waterlogging and submergence present numerous physiological difficulties, including low oxygen (hypoxia or anoxia), due to a ~10,000 fold decrease in gas diffusion. In the case of submergence, reduced carbon dioxide diffusion and lower light availability limit photosynthesis. Entrapment of the gaseous phytohormone ethylene is also a consequence of decreased gas diffusion. Both scenarios limit the availability of chemical energy for growth.

Crops, with few exceptions, are generally not suited for growth in water inundated environments. Species such as rice (*Oryza sativa*) that survive prolonged waterlogging display a number of developmental adaptations that enhance aeration of submerged organs[2]. Without aeration, roots of many species rapidly become oxygen deprived necessitating consumption of

carbohydrates for ATP production via energy-inefficient anaerobic metabolism. Rice employs two general strategies of to survive submergence: escape and quiescence[2,3]. The escape strategy leads to rapid growth and energy consumption to allow for elongation growth of aboveground organs to above water levels to resume normal aerobic metabolism and foster growth. This strategy is most effective when the plants endure a slowly progressing flood. Conversely, the quiescence strategy is effective when vegetative stage plants are completely submerged by a rapidly established but transient flood. These cultivars dampen overall cellular carbohydrate consumption and anaerobic energy metabolism, allowing plants to survive by limiting growth, until the flooding event subsides. There is also natural genetic variation in survival of complete submergence by *Arabidopsis thaliana*, which limits elongation growth to the leaf petiole under submergence [4,5].

The transition to low oxygen conditions that is associated with submergence and waterlogging stress requires plant cells to shift from aerobic to anaerobic metabolism [6]. Cellular deficiency of oxygen is also characteristic of highly dense organs and zones of active cell division [2,7]. When oxygen availability is insufficient to maintain the activity of cytochrome *c* oxidase as the final electron acceptor in the electron transport chain, plant cells utilize other less efficient metabolic routes to produce ATP [8]. Under submergence, decreased light availability also inhibits photosynthetic rates and the production of carbohydrates that may be consumed within leaf tissue or mobilized to sink

tissues such as the shoot meristem and roots. A switch from anabolism to catabolism also occurs to utilize and recycle nutrients and reserves for necessary but energy intensive processes such as transcription and translation. In many instances, including *Arabidopsis thaliana* rosette leaves, catabolism of carbon reserves is facilitated by an induction of α -amylases to hydrolyze starch. Carbon status additionally affects the hypoxic responses at the transcriptional level, whereby hypoxic responses are dampened in carbon depleted *Arabidopsis* seedlings [9]. The induction of genes related to autophagy also contributes to the degradation and recycling of organellar (*i.e.*, plastid) and cytosolic constituents [10–13].

In mammals, low oxygen responses are mediated through the conditional stabilization of specific transcription factors (TFs). Under normoxia (normal aeration; ~21% O₂), Hypoxia-inducible factor 1-alpha (HIF1 α) is degraded as a result of hydroxylation of specific proline residues by PROLYL-HYDROXYLASE DOMAIN ENZYMES 1/2/3, resulting in HIF1 α targeting for ubiquitination by the E3 ligase von Hippel-Lindau protein (VHL1) and subsequent degradation by the 26S proteasome [14]. In an analogous manner, plant low-oxygen responses are mediated by the stabilization of TFs under oxygen-deficient conditions, specifically by members of the Ethylene Responsive factor (ERF) superfamily group VII (ERFVII) [15–18]. The large family of ERF of plants can be regulated by ethylene and are frequently associated with stress responses [19,20]. These proteins are characterized by the presence of one or more conserved AP2/ERF

DNA binding domain, with the sub-families characterized by the presence of other less conserved regions [19]. Of the 9 reported domains identified for the ERFVIIIs, an N-terminal motif (CVII-1) was identified as present in most but not all sub-clade members of rice and all five ERFVIIIs of *Arabidopsis*. This element was later defined as critical to the regulation of the stability of these protein by the Cys-Arg/N-end rule pathway of targeted proteolysis (NERP) [15–18].

The Cys-Arg/NERP targets proteins that contain specific N-terminal amino acid motifs (degrons) for degradation via the 26S proteasome in *Arabidopsis*, *barley* (*Hordeum vulgare*) and most likely all land plant species [21]. This requires one or multiple enzymatic steps. *Arabidopsis* ERFVIIIs are characterized by the presence of a cysteine following the N-terminal methionine. This NH₂-MC-peptide motif is converted in an oxygen-dependent manner to a degron that leads to ubiquitylation and turnover. First, METHIONINE AMINOPEPTIDASE 1/2 (MAP1/2) cleaves the N-terminal methionine exposing the cysteine residue, which is oxidized by molecular oxygen or nitric oxide (NO). This process is catalyzed by PLANT CYSTEINE OXIDASE 1/2 (PCO1/2) [17,18]. The N-terminal oxidized cysteine (Cys-sulfinic acid) is the substrate of ARGINYL TRANSFERASE 1/2 (ATE1/2), which efficiently transfers an arginine residue from a tRNA^{Arg} to the N-terminus of the protein, making the protein a substrate of the E3 ligase PROTEOLYSIS 6 (PRT6) for ubiquitination and subsequent proteasome-mediated degradation. Based on our understanding from *Arabidopsis*, oxygen-dependent Cys-Arg/NERP regulation limits ERFVII

accumulation when oxygen is available and allows for ERFVII accumulation under low oxygen conditions [22]. When present these TFs activate the conditional activation of genes necessary for anaerobic metabolism, including *ALCOHOL DEHYDROGENASE 1 (ADH1)* and *PYRUVATE DECARBOXYLASE (PDC)* gene family members [23].

In *Arabidopsis*, submergence survival, hypoxia tolerance and anaerobic germination can be modified by manipulation of the expression of the *ERFVII*s [15,16,24,25]. In addition to regulating genes associated with anaerobic metabolism, these TFs also appear to play a role in responses to abscisic acid, salinity as well as developmental processes [26–31][32].

ERFVIIs with the characteristic NH₂-MC terminus are encoded in *Arabidopsis*, rice and other land plant genomes, indicating that the presence and regulation predates the monocot/dicot divergence. ERFVIIs of rice control submergence survival strategies. For example, the submergence quiescence strategy is mediated by the ERFVII *SUBMERGENCE1A (SUB1A)* [33–35]. The ERFVIIs *SNORKEL1* and *SNORKEL2* are necessary for the deepwater rice submergence-escape response [36,37]. Key to the escape response is the localized biosynthesis and response to gibberellins (GA) [38]. The presence of the submergence tolerance conferring allele of *SUB1A* is sufficient to differentially regulate a large number of genes that influence key processes including carbohydrate mobilization, anaerobic metabolism during submergence, and reactive oxygen species generation and photosynthetic recovery upon

re-assembly [34,39–41]. One of the genes that is directly or indirectly regulated by *SUB1A* is its paralog *SUB1C*.

Previous experiments have demonstrated the role of the Cys-Arg/NERP in ERFVII degradation both *in vitro* and *in vivo* [15,16]. In a rabbit reticulocyte *in vitro* transcription/translation system, the five *Arabidopsis* MC-ERFVIIIs were degraded due to the presence of NERP factors in the translation extract. When the N-terminal CVII-1 motif was selectively mutated to change Cys₂ to Ala (C2A mutation), these TFs became stabilized *in vitro*, as demonstrated by increased protein abundance of C2A-ERFVIIIs compared to the native MC-ERFVIIIs. This was confirmed *in vivo* for HYPOXIA RESPONSIVE ERF71/73 (HRE1/HRE2), with greater accumulation of the C2A-mutated version of these proteins when overexpressed in *Arabidopsis* [15,16]. The E3 ligase PRT6, that recognizes specific Cys-Arg/NERP degrons, was shown to be required for turnover of MC-ERFVIIIs. For example, MC-HRE2 was stabilized in the *prt6* mutant background [15,16]. Consistent with the model that MC-ERF turnover by Cys-Arg/NERP becomes limited as oxygen levels decline [1,21], MC-HRE2 levels increased in seedlings under hypoxic-conditions [15,16]. Together, these results demonstrate Cys-Arg/NERP regulates ERFVII protein accumulation.

Gibbs et al. (2011) also found that the rice MC-ERFVII *SUB1A* was not degraded *in vitro* in the presence of oxygen, despite possessing an N-terminal MC. *SUB1C* lacks a NH₂-MC terminus and is stable in the cell-free system. This led to the hypothesis that *SUB1A* regulation is uncoupled from Cys-Arg/NERP.

An alternative hypothesis is that SUB1A is a poor substrate of Cys-Arg/NERP. Yet when *35S:FLAG-SUB1A* was expressed in *Arabidopsis*, the N-terminally FLAG-tagged protein appeared to be degraded in a proteasome-dependent manner, as demonstrated by the dramatic increase in FLAG-SUB1A detected in seedlings treated with the proteasome inhibitor MG-132 as compared to mock treated plants [42]. Thus, SUB1A may be unstable even when its native N-terminus is blocked from Cys-Arg modification by addition of an epitope tag.

The ectopic expression of *35S:FLAG-SUB1A* did not confer submergence tolerance to rosette-stage *Arabidopsis*, yet it recapitulated several phenotypes seen in response to submergence in Sub1 rice [42]. These phenotypes included the constitutive elevation of *ADH1* mRNA, increased ABA and decreased GA sensitivity, and modulation of two genes associated with floral induction. Ectopic expression of *35S:FLAG-SUB1A* and *35S:FLAG-SUB1C* was also associated with rosette leaf phenotypes. These findings support the hypothesis that SUB1A influences transcription in *Arabidopsis*. Consistent with this, chromatin immunopurification-sequencing (ChIP-seq) performed with *35S:FLAG-SUB1A* ectopically expressed in *Arabidopsis* identified regions with the promoters of *PCO2*, *HYPOXIA RESPONSE ATTENUATOR 1 (HRA1)*, and *LOB DOMAIN-CONTAINING PROTEIN 41 (LBD41)* as SUB1A binding sites (Pena-Castro, unpublished). Strikingly, *PCO2* and *HRA1* negatively regulate low oxygen responses by promoting ERFVII turnover or limiting ERFVII ability to promote gene transcription [17,43,44].

The *Arabidopsis* ERFVIIs directly regulate the transcription of about 25 of the 49 so called core hypoxia responsive genes (HRGs) that are upregulated across cell-types. This is mediated through an evolutionarily conserved *cis*-element called the hypoxia-responsive promoter element (HRPE) [45]. The constitutively expressed ERFVII RELATED TO APETALA2 2/3/12 (RAP2.2/3/12) were demonstrated to transactivate HRG promoters containing the HRPE as well as a synthetic HRPE in a protoplast transactivation assay. Direct interaction between RAP2.2 and RAP2.12 with HRPE containing promoters was demonstrated *in vivo* through quantitative PCR of chromatin obtained by immunoprecipitation (ChIP), demonstrating the ability of these TFs to specifically bind the HRPE. Other ChIP-qPCR results have revealed RAP2.3 interaction with subsets of genes containing GCC-box like and EBP box motifs, revealing that ERFVII regulation is not relegated to HRPE containing genes, and that ERFVII regulation affects other biological processes [46,47]. Despite the limited understanding of direct ERFVII interactions, genome-wide binding dynamics by ChIP-seq have not been resolved for any ERFVII in *Arabidopsis*. Genome-wide binding profiles for any of the SUB1A or other SUB1 family ERFVIIs in rice are similarly unresolved, due to low abundance when N-terminally tagged *SUB1A* even when the gene is constitutively expressed, and mRNA levels are highly elevated (Fukao and Bailey-Serres, unpublished).

Here, we further explore the turnover of SUB1A and analyze the DNA targets of Cys-Arg/NERP-resistant versions of HRE2, SUB1A and SUB1C in

Arabidopsis. We find that SUB1A levels increase in the *prt6* mutant background, indicating that its stability is influenced by the Cys-Arg/NERP. We provide evidence through chromatin immunopurification-sequencing (ChIP-seq) of enriched binding of HRE2 and SUB1A/C to promoters of the most highly upregulated hypoxia-responsive genes. SUB1A/C bound 5' of the transcription start site (TSS) of many genes upregulated by hypoxia, but also at high levels within the transcribed regions of upregulated genes under non-stressed growth conditions, whereas HRE2 bound primarily within 500 bp 5' of the TSS of upregulated genes and within the transcribed regions of downregulated genes under hypoxia. These observations suggest that these ERFVIs may interact with DNA as well as chromatin-associated proteins or possibly RNAPII.

3.3. Materials and methods

3.3.1. Genetic material

The following *Arabidopsis thaliana* Col-0 genotypes were used: p35S:His₆FLAG-SUB1A and p35S:His₆FLAG-SUB1C [42]; p35S:SUB1A-3XFLAG, p35S:SUB1C-3XFLAG, p35S:SUB1A-3XFLAG *prt6*, and p35S:SUB1C-3XFLAG *prt6*. The N-terminal tag was M(H)₆(G)₃DYKDDDDK(G)₇. The C-terminally tagged constructs were identical to N-terminally tagged constructs, with the exception that the SUB1A and SUB1C cDNAs were recombined into pGATA-FH [39] to place the sequence (G)₇DYKDDDDK(G)₃(H)₆, at the the C-

terminus of the protein. The *prt6-1* allele was introduced by crossing. Confirmed homozygous genotypes were used for all experiments.

3.3.2. Growth and Treatment Conditions

Arabidopsis seeds were surface sterilized by incubation in 70% (v/v) EtOH for 5 min, followed by incubation in 20% (v/v) bleach, 0.01% (v/v) TWEEN-20, followed by three washes in ddH₂O for 5 min, in triplicate. Sterilized seeds were placed onto 1x MS media (1.0x Murishige Skoog (MS) salts, 0.4% (w/v) Phytigel (Sigma-Aldrich), and 1% (w/v) Suc, pH 5.7) in 9 cm² Petri dishes and stratified by incubation at 4°C for 3 d in complete darkness. Following stratification, plates were placed vertically into a growth chamber (Percival) with 16h light / 8h dark cycle at ~120 μmol photons·s⁻¹·m⁻², at 23 °C for 7 d.

3.3.3. Seedling Treatments

For hypoxic stress, seedlings were removed from the growth chamber at Zeitgeber time (ZT) 16 and were subjected to hypoxic stress in sealed chambers into which humidified argon gas was passed at a rate of 3.33 mL / sec, in complete darkness for 2 h at 24 °C. The chamber set-up was as described by [66]. Oxygen partial pressure in the chamber was measured with the NeoFox Sport O₂ sensor and probe (Ocean Optics). Stable hypoxia (1% O₂) was achieved within 15 min of the initiation of treatment. Control samples were placed in an identical chamber that was open to ambient air under the same light

and temperature conditions. For MG-132 treatment, the roots of seedlings were flooded with 10 mL 100 μ M Calpain inhibitor IV (American Peptide), 1% (v/v) DMSO. The solution was not removed when seedlings were transferred to chambers for the non-stress (mock) and hypoxic stress treatments. Tissue was rapidly harvested into liquid N₂ and stored at -80 °C.

3.3.4. Immunopurification of protein

Seedlings were grown on Petri dishes and treated as described above. Total protein was extracted from 500 μ l packed pulverized tissue thawed to 4°C in 1 mL of extraction buffer (50 mM Tris-HCl, pH 7.5, 2.5 mM EDTA, pH 8.0, 150 mM NaCl, 10% (v/v) glycerol, 0.1% (v/v) IGEPAL, 1 mM DTT, 25 mM beta-glycerophosphate, 1X Plant Protease Inhibitor Cocktail [Sigma]). The extract was filtered through one layer of Miracloth (Calbiochem, La Jolla, CA) and centrifuged at 16,000g for 10 min at 4°C. The concentration of the supernatant protein was determined by Bradford assay with a bovine serum albumin standard [67]. Equal protein concentrations were normalized to 1 mL with extraction buffer. Per sample, 20 μ L Anti-FLAG M2 magnetic beads (Sigma) were pre-washed in extraction buffer and added to the normalized protein extract. Samples were rocked for 2 h at 4°C. The beads were magnetically collected and the supernatant was aspirated and washed three times with 1 mL of extraction buffer for 5 min at 4°C with rocking. Following the final wash, the supernatant was aspirated and the immunoprecipitated protein was eluted in 100 μ L of extraction

buffer containing 400 ng/ μ L 3X FLAG peptide (Sigma) for 30 min at 4°C with rocking. Following incubation, the beads were magnetically collected and the supernatant containing the eluted proteins was transferred to a new tube. The eluted fraction was then concentrated by adding 5 μ L StrataClean (Agilent) and vortexing for 1 min. The concentrated protein was then collected by centrifugation at 2,000g for 1 min at 4°C, after which the supernatant was aspirated and the concentrated protein fraction was re-suspended in 10 μ L of 2x Laemmli buffer (4% (w/v) SDS, 20% (v/v) glycerol, 10% (v/v) 2-mercaptoethanol, 0.004% (w/v) bromophenol blue, 0.125 M Tris-HCl, pH 6.8).

3.3.5. SDS-PAGE and Immunoblot Analysis

Immunoprecipitated samples were electrophoretically separated by SDS-PAGE on 12% (w/v) polyacrylamide gels and transferred to a nitrocellulose membrane (GE Healthcare Biosciences). Membranes were blocked with 5% (w/v) skim milk in PBST (3.2 mM Na_2HPO_4 , 0.5 mM KH_2PO_4 , 1.3 mM KCl, 135 mM NaCl, pH 7.4, 0.1% (v/v) TWEEN-20) for 1 h at room temperature while rocking. Membranes were washed three times in PBST and incubated with a 1:1000 dilution of anti-FLAG HRP (Sigma) for 1 h at room temperature while rocking. Membranes were washed three times in PBST for 5 min at room temperature. Visualization of immuno-interaction was by use of Luminata Crescendo Western HRP substrate (Millipore) and exposure to X-ray film.

3.3.6. Chromatin Immunopurification (ChIP)

ChIP was performed according to [68] with minor modifications. Seedlings were grown as described above were pre-treated with 10 mL of 100 μ M Calpain inhibitor IV (MG-132; American Peptide) and 1% (v/v) DMSO for 2 h prior to the hypoxia treatment. Following hypoxia treatment, seedlings were immediately cross-linked in 1% (v/v) formaldehyde nuclei purification buffer (NPB: 20 mM MOPS, pH 7.0, 40 mM NaCl, 90 mM KCl, 2 mM EDTA, 0.5 mM EGTA) in a dessicator under house vacuum for 10 min. The reaction was quenched by addition of 1.875 mL 5 M glycine to reach a concentration of 125 mM followed by vacuum infiltration for 5 min. After 3 rapid washes in 30 mL ddH₂O, seedlings were blotted dry and pulverized under liquid N₂. To isolate nuclei, 0.5 g tissue was thawed to 4°C in 10 mL NPB that additionally contained 0.5 mM spermidine, 0.2 mM spermine, and 1X Plant Protease Inhibitor Cocktail (Sigma-Aldrich P9599). Nuclei were pelleted by centrifugation in 4°C at 1200g for 10 min, resuspended in 120 μ L NPB, and lysed by the addition of 120 μ L 2X nuclei lysis buffer (NLB: 100 mM Tris, pH 8.0, 20 mM EDTA, 2% [w/v] SDS, and 2X Plant Protease Inhibitor Cocktail) by vortexing for 2 min at 23-25 °C. The chromatin was sheared into 200 to 600 bp fragments by sonication (Diagenode, Denville, NJ) with 40 cycles of 30 s ON and 30 s OFF at 4°C. The sample was cleared by centrifugation at 16,000g at 4°C for 2 min and the supernatant was diluted ten-fold with dilution buffer (DB: 16.7 mM Tris, pH 8.0, 167 mM NaCl, 1.1% (v/v) Triton X-100, 1.2 mM EDTA). The chromatin fraction was precleared by

incubation with uncoupled Protein G Dynabeads (ThermoFisher) for 30 min followed by collection of the supernatant. For SUB1A, SUB1C and HRE2, 1 mL of the input chromatin was incubated with 3 μ L of anti-FLAG (F1804, Sigma) overnight while rocking at 4°C. Protein G Dynabeads (30 μ L) were washed in DB, added to the chromatin fraction and allowed to incubate for 2 h while rocking at 4°C. Beads were magnetically captured and washed sequentially in 1 mL for 5 min with four buffers: low NaCl₂ wash buffer (20 mM Tris, pH 8.0, 150 mM NaCl, 0.1% [w/v] SDS, 1% [v/v] Triton X-100, 2 mM EDTA), high NaCl₂ wash buffer (20 mM Tris, pH 8.0, 500 mM NaCl₂, 0.1% [w/v] SDS, 1% [v/v] Triton X-100, 2mM EDTA), LiCl wash buffer (10 mM Tris, pH 8.0, 250 mM LiCl, 1% [w/v] sodium deoxycholate, 1% [v/v] Nonidet P-40, 1 mM EDTA), and standard TE buffer (10 mM Tris, pH 8.0, 1 mM EDTA). The beads were then washed twice with 10 mM Tris, pH 8.0 and resuspended in 25 μ L of tagmentation reaction mix (10 mM Tris, pH 8.0, 5 mM MgCl₂, 10% [w/v] dimethylformamide) containing 1 μ L of Tagment DNA Enzyme (NExtera DNA Sample Prep Kit, Illumina) and incubated at 37°C for 1 min. Beads were washed twice with low NaCl₂ wash buffer and then once in standard TE buffer. The chromatin was eluted from the beads by heating for 15 min at 65°C in elution buffer (EB: 100 mM NaHCO₃ and 1% [w/v] SDS) and reverse cross-linked by the addition of 20 μ L 5 M NaCl and incubation at 65°C overnight. Following reverse cross-linking, 0.8 units Proteinase K (New England Biolabs) was added and the sample was incubated at 55°C for 15 min. The final

tagged CHIP-DNA sample was purified using Qiagen MinElute columns according to the manufacturer's instructions and eluted with 14 μ L of EB.

3.3.7. Library Preparation

ChIPmentation library preparation for short-read sequencing (ChIP-seq) was performed according to [69], with minor modifications. Final library enrichment was performed in a 50 μ L reaction containing 12 μ L CHIP DNA, 0.75 μ M primers, and 25 μ L 2X NEBNext PCR Master Mix. To determine the appropriate amplification cycle number, a qPCR reaction was performed on 1 μ L of tagmented CHIP DNA in a 10 μ L reaction volume containing 0.15 μ M primers, 1X SybrGreen (ThermoFisher), and 5 μ L 2X NEBNext PCR Master Mix (New England Biolabs) with the following program: 72°C for 5 min, 98°C for 30 s, 24 cycles of 98°C for 10 s, 63°C for 30 s, 72°C for 30 s, and a final elongation at 72°C for 1 min. Libraries were amplified for n cycles, where n is equal to the rounded up Cq value determined in the qPCR reaction. Amplified libraries were purified and size selected using SPRI AMPure XP beads (Beckman). AMPure XP beads were added at a 0.7:1.0 bead to sample ratio, and the remaining DNA was recovered by the addition of AMPure XP beads at a 2.0:1.0 bead to sample ratio and eluted in 13 μ L of EB. Quantification of the final libraries was performed with Quant-iT PicoGreen (ThermoFisher), and library fragment distribution was evaluated by use of the the Agilent 2100 Bioanalyzer using the high sensitivity

DNA chip. Final libraries were multiplexed to >5 nM final concentration and sequenced on the HiSeq 3000/4000 at the UC Davis DNA Technologies Core.

Julian Peña Castro constructed CHIP multiplex DNA libraries according to [70], which includes an amplification step. CHIP was performed on tissue treated in the same manner and immunopurified according to [71], including Col-0. Control samples included a Col-0 CHIP sample and a Col-0 genomic DNA sample. Four pooled libraries were barcoded and sequenced by synthesis in single-read format following manufacturer protocols (Illumina) at the Genomics Core Facility, University of California Riverside.

3.3.8. Bioinformatic Analyses

Bioinformatic analyses performed for SUB1A and SUB1C ChIP-seq datasets was identical to the analyses performed for HRE2 ChIP-seq data in Chapter 2

3.4. Results

3.4.1. SUB1A accumulation is promoted in the *proteolysis 6* mutant that is deficient in oxygen-dependent N-end rule mediated degradation *in planta*

To test the hypothesis that SUB1A is not a substrate of oxygen-dependent Cys-Arg/NERP regulation, the accumulation of C-terminally tagged SUB1A was evaluated using *Arabidopsis* lines expressing *p35S:SUB1A-3xFLAG-6xHis* in the

wildtype Col-0 and the *prt6* mutant background. We first confirmed by qRT-PCR that *SUB1A-FLAG* transcript abundance was indistinguishable in extracts of 7-d-old seedlings of both genotypes (Fig. 1a). Then, SDS-soluble protein from the same tissue was used for SUB1A-FLAG immunopurification with an anti-FLAG antibody, followed by SDS-PAGE fractionation and immunoblot detection with the same antiserum. In *p35S:SUB1A-3xFLAG-6xHis* Col-0 seedlings, SUB1A-FLAG protein was undetectable (Fig. 1b). By contrast, low levels of a doublet of FLAG-tagged protein with an apparent molecular mass of 37 kDa accumulated in *p35S:SUB1A-3xFLAG-6xHis prt6* seedlings. The calculated molecular mass of FLAG-tagged SUB1A is 34.2 kDa. We also explored whether inhibition of the proteasome enhanced accumulation of C-terminally tagged SUB1A, as reported for N-terminally tagged SUB1A [42]. Treatment of seedlings with MG-132 enhanced levels of the 37 kDa SUB1A-FLAG in both Col-0 and *prt6* background. When MG-132 was used a second FLAG-tagged protein of ~55 kDa was detected in both genetic backgrounds. The increase in this protein was proportional to the level of the 37 kDa protein. The presence of the doublet and higher molecular mass isoforms indicates that SUB1A may be post-translationally modified or may form stable complexes with other proteins. To determine if SUB1A-FLAG levels are modulated by oxygen availability, the abundance and apparent molecular mass of this protein was evaluated in 7-d-old seedlings treated under non-stress (+ O₂) hypoxic stress (- O₂) conditions for 2 h, in the presence or absence of MG-132. This revealed higher SUB1A-FLAG

accumulation in aerated seedlings, which was promoted by the proteasome inhibitor without any change in transcript accumulation (Fig 1c, d). These analyses confirmed that SUB1A accumulation is influenced by the Cys-Arg/NERP E3 ligase PRT6, proteasome activity and oxygen availability when ectopically expressed in seedlings of *Arabidopsis*.

3.4.2. Genome-wide investigation of SUB1A and SUB1C binding sites

Preliminary experiments determined that levels of chromatin associated with ERFVIs is very low. Two approaches to compensate for low abundance input into a ChIP-seq library construction pipeline are the (a) amplification of the DNA of the purified immunoprecipitated chromatin prior to library construction or (b) use of Tn5 insertion to integrate an adapter that facilitates library construction. Here, both methods of low input ChIP-seq library preparation were performed, with use of Tn5 (ChIPmentation) yielding results without evidence of amplification bias. The greater ChIP-seq yields from ChIPmentation [48] may be attributed to fewer cleanup and purification steps, that are inherently associated with sample loss. As ChIPmentation relies on Tn5 insertion into any region of the immunopurified DNA that is accessible (*i.e.*, not bound by a protein or nucleosome). These two strategies yield very similar peaks for histone marks and transcription factors [48].

ChIP-Seq was performed to compare and contrast the binding targets of SUB1A, SUB1C, and HRE2 when each was expressed under the control of a

35S promoter in *Arabidopsis* seedlings. The SUB1A/C constructs were N-terminally FLAG-tagged and the HRE2 construct encoded the native NH₂-MC ERFVII with a C-terminal HA tag. Thus, in all cases turnover by NERP was not possible. Preliminary experiments determined that SUB1A/C and HRE2 protein levels under non-stress and hypoxic stress conditions were insufficient for capture of sufficient chromatin for ChIP unless seedlings were pre-treated with MG-132. Therefore, the ChIP was carried out on seedlings that were pretreated for 2 h with 100 μ M MG-132 prior to the non-stress control or 2 h hypoxic-stress treatment. Samples were subsequently crosslinked with formaldehyde and ChIP was performed. The SUB1A/C ChIP-seq datasets for the non-stress conditions were independently generated by Julian Peña-Castro by use of the library amplification method. The SUB1A/C and HRE2 ChIP-seq for hypoxic stress tissue was generated by use of the ChIPmentation method. HRE2 binding was only evaluated in hypoxic stressed samples as this is a hypoxia-upregulated TF [15,49]. All samples yielded >5 million reads that mapped to the *Arabidopsis* genome.

The mapping of ChIP-seq reads to the genome identified extensive binding of the three ERFVIIs to genic regions with a threshold of RPKM > 5 ($n > 15,600$). Because the high number of reads could reflect association of these TFs with histones or other chromatin-associated proteins, we compared the genome-wide read distribution of these TFs to the regions associated with modified histone H3s, H2A.Z and RNAPII with the Ser2P modification, as defined

with seedlings grown and treated in the same experimental system (Chapter 2). This comparison was accomplished by use of t-Distributed Stochastic Neighbor Embedding (t-SNE) analysis and provided a number of insights (Fig. 2). First, the SUB1A and SUB1C CHIP-seq data grouped together under non-stress and stress conditions (Fig. 3a, b), indicating similar binding of both factors to chromatin. Second, the binding of these TFs to chromatin was altered by hypoxia (Fig. 3c, d). Looking more closely, the RPKM values for binding of SUB1A/C to the genic regions of HRGs was highly similar under the two conditions (Pearson's correlation: non-stress, $R = 0.95$; hypoxic stress, $R = 0.88$). Third, HRE2 binding to chromatin grouped separately from that of SUB1A and SUB1C but near all RNAPII samples in the t-SNE analysis (Fig. 2). When only considering the HRGs, there was a modest correlation between HRE2 and SUB1A/C binding under the two conditions ($R = 0.45$; $R = 0.58$) (Fig. d,e).

At the global scale, a peak in SUB1A and SUB1C reads was present within 500 bp 5' of the TSS under non-stress conditions and became more associated with the gene body region in response to hypoxia (Fig. 4a). HRE2 binding under hypoxia was also generally enriched within gene bodies. Next, peak calling was performed using HOMER to better define the regions of TF binding relative to annotated genes (Fig. 4b). SUB1A and SUB1C peaks predominated 5' of the TSS and 3' of the TES of genes under non-stress conditions and hypoxic stress conditions. In response to hypoxia, both TFs displayed a shift in binding into the gene body. The profile of the location of

peaks of these two TFs was remarkably similar under both conditions. By contrast, HRE2 binding under hypoxia was both highly enriched just 5' of the TSS and as a broad peak between the TSS and TES. As observed for both SUB1A and SUB1C, read number dropped precipitously at the TES and then rose gradually in the 3' genic region. These results suggest that regions bound by SUB1A and SUB1C may be similar and altered in response to hypoxic stress.

To investigate the relationship between location of ERFVII binding and gene transcription, binding profiles across genic regions were generated for three subgroups of genes: the 49 HRGs (Mustroph et al., 2009), the 216 genes found to co-regulated at the level of RNAPII-Ser2P association, nuclear, polyadenylated and polysomal RNA accumulation (Chapter 2) and the hypoxia down-regulated genes (\log_2 fold change in polyA⁺ mRNA <1, $p < 0.05$) (Chapter 2) (Fig. 5a-c). SUB1A and to a lesser extent SUB1C binding was enriched within the promoter region of the HRGs under non-stress conditions, with a rise in association within the gene body region under hypoxic stress (Fig. 5a). HRE2 binding was enriched near the TSS of the HRGs. The binding of these TFs to individual genes confirmed these patterns but also illustrated the gene-specific nature of these interactions (Fig 5e). For example, the core HRGs *ADH1*, *LBD41* and *PCO2* all showed pronounced 5' HRE2 binding (Fig. 6a-c). Of these three genes, only *LBD41* and *PCO2* displayed a clear peak in SUB1A and SUB1C binding in their 5' flanking region under control conditions. The binding of SUB1A was also evident in the 3' regions of these genes. In response to hypoxic stress,

SUB1A/C binding was pronounced along the body of all three HRGs.

Interestingly, HRE2 demonstrated the strongest enrichment in promoter region binding for many HRGs (Fig. 5d). The 5' binding coincided with the hypoxia-inducible region of open chromatin and upregulation from RNAPII-SerP engagement through translation in Col-0 (Fig. 6a-c). Notably, 1,040 of 1,804 of the genes with a peak 5' of the TSS for HRE2 also had a peak for SUB1A. Binding of SUB1C was generally lower, but detectable in 226 of the 1,804 genes bound by HRE2 and SUB1A.

Extending the analysis to the 216 co-regulated HRGs revealed a different pattern of binding for HRE2, SUB1A and SUB1C (Fig. 5b and f; 6d-e). SUB1A and SUB1C binding was highly enriched within the body of these genes particularly under non-stress conditions, as opposed to HRE2 binding, where peaks were evident in the promoter of a subset of genes as shown by comparison across *EXORDIUM-LIKE1* and *CALMODULIN-LIKE 12/TOUCH3* (Fig 6). By contrast to the HRGs, the 5' peak was lower and the binding within the gene body was greater. The distinction between the binding profiles of the 49 HRGs and the 216 co-regulated HRGs (containing 37 core HRGs) could reflect differences in regulation between subsets of hypoxia-inducible genes as well as differences in the mode of binding to chromatin.

To complete this survey we generated binding profiles for the 297 genes that were significantly down-regulated at the polyA⁺ mRNA level in response to hypoxic stress (Chapter 2). Overall, the levels of binding of the three ERFVIs to

these genes was significantly lower than for the upregulated genes (Fig. 5c and f). Intriguingly, SUB1A bound to the 5' and/or 3' portions of a number of these genes under non-stress conditions, whereas SUB1C binding was limited. In response to hypoxic stress, levels of binding to the gene body region increased. By contrast to the other two gene groups examined, there was no peak in HRE2 association within the promoter region, but there was association within the gene bodies of the down-regulated genes. Together, these results demonstrate that binding profiles of SUB1A and SUB1C are dynamically regulated in response to hypoxic stress, with respect to binding to chromatin regions of both the promoter and transcribed regions of genes. HRE2 primarily bound to promoters of up-regulated genes and displayed occupancy along the transcribed regions of both up and down-regulated genes.

3.5. Discussion

The major finding of this study is that the stability and binding of rice SUB1A and SUB1C to chromatin is regulated when ectopically expressed in seedlings of *Arabidopsis*. Previously, SUB1A was distinguished from HRE2 and the other four ERFVIs of *Arabidopsis* by its resilience to Cys-Arg/NERP in a cell-free transcription and translation system, despite the conservation of the CVII-1 motif at its N-terminus [15]. Mutation of the N-terminus of the *Arabidopsis* ERFVIs, from NH₂-MC to NH₂-MA, is sufficient for their stabilization in the *in vitro* system and *in planta* unless the Cys-Arg/NERP is disrupted by mutation of a key

component such as the E3 ligase PRT6 [15,16]. By use of ectopic expression of MC-SUB1A with a C-terminal FLAG tag in *Arabidopsis* we determined its accumulation is increased in *prt6* seedlings. SUB1A-FLAG is also shown to be highly unstable under control and stress conditions due to proteasomal activity.

3.5.1. SUB1A accumulation is highly unstable and influenced by the Cys-Arg/NERP and other factors when ectopically expressed in *Arabidopsis*

These *in planta* results contrast with the reproducible observation that SUB1A is not an *in vitro* NERP target [15,50]. This could be due to the presence of factors or protein-protein interactions in *Arabidopsis* that are absent in the rabbit reticulocyte *in vitro* system. First, SUB1A-FLAG expressed in *Arabidopsis* may be posttranslationally modified or interact with other proteins in a manner that exposes the N-terminus or ubiquitylation site for Cys-Arg/NERP-mediated degradation. The interacting proteins could include Cys-Arg/NERP machinery absent from the *in vitro* system, TFs or other proteins. Intriguingly, SUB1A that is tagged with His₆-FLAG at its N-terminus or 3xFLAG at its C-terminus displays distinctions in apparent molecular mass that differ from the calculated mass of the tagged protein (33.0 and 34.2 kDa, respectively). Immunoblot analysis of SUB1A-FLAG resolved proteins with apparent molecular masses of 50 and 37 kDa (Fig. 1 c, d), whereas FLAG-SUB1A migrated with an apparent molecular mass of 46 kDa [42]. SUB1A reportedly is post-translationally phosphorylated by MAP kinase 3 in rice [51]. The SUB1A interactome defined by yeast 2-hybrid

analysis includes at least one putative transcription factor of rice [52]. ERFVII additionally interact with other TFs, a chromatin remodeler and membrane associated proteins in *Arabidopsis* [16,32,43,46]. The observed variation in apparent molecular mass of SUB1A-FLAG is suggestive of posttranslational modifications including phosphorylation or ubiquitylation (*i.e.*, the doublet at 37 kDa and higher molecular mass isoform at 50 kDa), although the latter typically results in multiple higher molecular mass forms. The 50 kDa isoform could reflect a stable interaction with another protein that is not dissociated by standard SDS-PAGE methods. This is not unusual for homo- and heterodimeric interactions of transcription factors. These interactions could also contribute to the pattern of SUB1A accumulation. For example, if the interaction is with a NERP-regulated *Arabidopsis* ERFVII, stabilization of that protein with MG-132 or in the *prt6* background could enhance accumulation of SUB1A. The variation in SUB1A levels and electrophoretic migration might also be related to the recently discovered pathway of selective autophagy that is integrated upstream of PRT6 in the Cys-Arg/NERP [53].

We also observed higher SUB1A-FLAG accumulation under non-stress conditions, which is counterintuitive if its stability is controlled by the oxygen or NO-requiring Cys-Arg/NERP. Based on the pronounced effect of inhibition of the proteasome on accumulation of N- or C-terminally tagged SUB1A under both non-stress and hypoxic stress conditions it is clear this protein is highly unstable *in vivo* in *Arabidopsis*. This is consistent with the low abundance of SUB1A in rice

expressing *pZmUBI1:TAP-SUB1A* at sufficient levels to provide submergence tolerance (T. Fukao and J. Bailey-Serres, unpublished). We propose that the decline in abundance of SUB1A-FLAG under hypoxia could reflect the ~50% global reduction in protein synthesis in *Arabidopsis* seedlings exposed to hypoxic stress for 2 h [54–56]. A preliminary analysis confirmed that *SUB1A-FLAG* mRNA levels decreased in polysomes following 2 h of hypoxic stress in *35S:SUB1A-FLAGHis₆* seedlings despite unchanged levels of *SUB1A-FLAG* mRNA (data not shown).

These findings demonstrate that SUB1A accumulation is influenced by the E3 ligase PRT6 and proteasomal activity, but additional research is required to better understand the observed variations in SUB1A electrophoretic mobility and their relationship to function and turnover in a physiological context. *Arabidopsis* provides a platform for such studies, but ultimately evaluation in rice is needed.

3.5.2. SUB1A and SUB1C have conserved targets of chromatin binding that can overlap with binding of the endogenous hypoxia-induced HRE2 in *Arabidopsis* seedlings

This study revealed that SUB1A and SUB1C bind to similar regions of the *Arabidopsis* genome and that their binding is influenced by hypoxic stress (Fig. 2. a-d; Fig. 6). The promoter regions of the 49 HRGs displayed peaks of SUB1A and SUB1C binding under non-stress conditions. These were largely absent under hypoxic stress, with the association shifted into the transcribed regions of

these genes. Nonetheless, for some genes the binding of SUB1A and SUB1C within promoters overlapped with that of HRE2 under hypoxic stress (Fig. 6; *LBD41*, *PCO2*). The 216 genes that display concerted co-expression from Ser2P to translation defined in Chapter 2 (including 37 HRGs) showed a prevalence of SUB1A and SUB1C binding within their transcribed region under both non-stress and hypoxic stress conditions (Fig. 5 a, b). HRE2 binding in gene bodies was evident on these genes but to a lesser extent. Contrastingly, HRE2 binding showed increased prevalence within the gene bodies of down-regulated genes under hypoxia. The binding of these constitutively expressed and MG-132 stabilized TFs in promoter regions of HRGs is consistent with a role in transcriptional regulation, whereas the binding within transcribed regions is more enigmatic. These results hint that the ERFVIs are multifunctional. This could be driven by conditionally influenced dynamics in post-translational modifications or protein-protein interactions.

Although not frequently reported, binding of TFs within gene bodies of target genes has been demonstrated for other TFs. In mammals, CCCTC-binding factor (CTCF) is an insulator TF that facilitates enhancer interactions that can lead to either activation or repression of target genes [57]. CTCF functions in the formation of chromatin loops that are thought to facilitate efficient transcription through the reuse of RNAPII following transcriptional termination. CTCF has been found to interact with various proteins, including: other TFs, histone modifying enzymes, and chromatin remodelers. CTCF is additionally

regulated in a cell-type specific manner, which may be attributed to the wide range of CTCF protein interactions and functions [58]. Reflective of its varied roles in transcriptional and chromatin regulation, CTCF is predominantly associated with gene bodies and intergenic regions (42%, 42%), with relatively limited association with promoter regions of genes (16%). Mammalian PRDI-BF1 and RIZ homology domain containing 5 (Prdm5) also binds to gene bodies. Similar to CTCF, Prdm5 is associated with both transcriptional activation and repression, as well as cell-type specific expression [59,60]. Prdm5 binding is most strongly associated within gene bodies (39%), promoter (29%) and upstream regions (14%). In contrast to CTCF, Prdm5 association within gene bodies is attributed to its role in the maintenance of transcriptional elongation. Prdm5 directly interacts with RNAPII, with decreased levels of RNAPII observed within gene bodies in the absence of Prdm5. Together, CTCF and Prdm5 demonstrate distinct roles for TF binding within gene bodies of target genes. Finally, mammalian HIF1 α , mentioned previously for its oxygen-regulated turnover, is known to modulate transcription as well as chromatin accessibility [61] and histone post-translational modification [62] via interactions with chromatin remodelers and histone modifying enzymes. These interactions would be anticipated to increase association of HIF1 α within transcribed regions.

There is growing evidence that SUB1A and other ERFs interact with proteins that bind to promoter and other genomic regions. A yeast two-hybrid screen for SUB1A and SUB1C interactors of rice identified two common

interactors and numerous protein-specific interactors [52]. One SUB1A/C interactor, SUB1A binding protein 18 (SAB18) is closely related to *Arabidopsis* *HRA1*, a hypoxia inducible Trihelix-domain TF encoded by an HRG that negatively regulates transcription of many of the 49 HRGs by controlling the function of at least the constitutively expressed ERFVII RAP2.12 in *Arabidopsis* [43,44]. This attenuation function may be driven by protein-protein interactions as HRA1 binds to only a handful of promoter regions under hypoxia based on ChIP-seq data from seedlings produced in the same system as this dataset ([43,44]). HRA1 and SAB18 contain a Swi3, Ada2, N-Cor, and TFIIIB (SANT) domain, known to function in chromatin remodeling and the post-translational modification of histones in other organisms [63]. Intriguingly, the *Arabidopsis* ERFVIIs RAP2.2, RAP2.3, and RAP2.12 physically interact with the SWI/SNF chromatin remodeler *BRAHMA* (*BRM*) in yeast 2-hybrid and bimolecular fluorescence complementation assays, with pleiotropic phenotypes observed in higher order *erfvii brm* mutants [32]. These results hint that ERFVIIs may influence the activity of chromatin remodelers. Interaction with a chromatin modifying enzyme specifically in hypoxic stress could explain the observation of SUB1A/C association within gene bodies of target genes.

Altogether, the results of this study demonstrate that when heterologously and constitutively synthesized in *Arabidopsis*, SUB1A protein abundance is limited by the proteasome and is influenced by Cys-Arg/NERP activity and hypoxic stress. This is in contrast to *in vitro* findings, suggesting that *in planta*

dynamics associated with SUB1A stability are more complex. Additionally, genome-wide *in planta* chromatin binding profiles revealed a strong similarity in SUB1A and SUB1C binding of promoter and transcribed regions, the latter akin to distributions of histone modifying enzymes and chromatin remodelers. These results can be explained by the possible interaction of SUB1A/C with chromatin modifying complexes in a hypoxia-dependent manner. A preliminary proteomic assessment of proteins that are co-immunopurified with SUB1A-FLAG showed significant association with histone H4, H2A, and H2A.X (data not shown, unpublished). Although the immunopurification method used was not ChIP, the co-purification of SUB1A and histones was not unexpected. However, not all histone subunits were recognized among the co-purified proteins. Further molecular studies are required to validate the hypothesis that the SUB1s participate in processes other than transcriptional activation. A first step towards understanding this would be to comparatively profile chromatin accessibility and histone modifications in SUB1A/C and HRE overexpression lines (*i.e.*, H3K9Ac, H3K4me3), coupled with RNA-seq analysis under the two conditions. The availability of other *Arabidopsis* ERFVII overexpression and mutants would prove valuable for further study. If evidence of differential histone modifications mutants of specific histone modification enzymes can be tested at phenotypic, epigenetic and transcriptomic levels. If chromatin accessibility is distinctly regulated in these lines, this can be further evaluated by SUB1A/C binding and function in mutant backgrounds for remodelers such as BRAHMA.

The observation that SUB1A and SUB1C binding is associated with promoter regions of target genes in control conditions, whereas binding migrates into transcription units of genes is similar to binding dynamics of CTCF and Prmd5. These TFs are associated with an array of gene regulatory functions and promote both transcriptional activation and repression, based on the presence of interacting proteins. It is enticing to hypothesize that the SUB1s are similarly capable of orchestrating varied gene regulatory activities. Support for this hypothesis may be evidenced from the identification that the *SUB1A-1* allele specifically confers submergence tolerance to rice. In submergence intolerant rice cultivars, the presence of *SUB1A-2*, *SUB1B*, and *SUB1C* is not sufficient to confer the quiescence survival strategy. *SUB1A-1* contains a MPK phosphorylation domain that is absent in the *SUB1A-2* allele [33,51]. It is possible that SUB1A phosphorylation or other post-translational modifications facilitate protein-protein interactions not achieved by SUB1A-2, SUB1B, or SUB1C. The ability of SUB1A-1 to interact with evolutionarily conserved partners would be consistent with the findings that SUB1A-1 binding is dynamically regulated in *Arabidopsis*. Yet an equally possible alternative hypothesis is that *SUB1A-1* and *SUB1A-2* are functionally equivalent but provide different levels of protection from submergence due to the timing, level, or location of their expression [33,34,64]. The similarity in SUB1A and SUB1C binding is also notable. These proteins possess all of the same conserved motifs found in ERFVIIIs, with the exception of the absence of the N-terminal domain associated

with Cys-Arg/NERP regulation [15,19], yet the proteins only share 77% amino acid similarity [33]. The challenging question remains whether SUB1A and SUB1C chromatin binding and activities are indeed similar within rice plants under submergence, as indicated when heterologously expressed in *Arabidopsis*.

The present findings suggest that regulation of SUB1A accumulation and function is multifaceted. The possibility that this factor influences the chromatin landscape may help to explain why the addition of SUB1A to a rice cultivar is sufficient to influence myriad aspects of the response to submergence and desubmergence recovery [34,35,40,41,65]. Future studies should proceed towards direct monitoring of SUB1A function in regulation of the epigenome and transcriptome dynamics in rice, despite the challenges associated with the high instability and low abundance of this agriculturally relevant protein.

3.6. Acknowledgements

Julian Peña-Castro and Seung Cho Lee provided unpublished SUB1 data and genetic resources that both stimulated and enabled these experiments. We would also like to acknowledge Erin Brinton for her validation of prior SUB1A, SUB1B SUB1C stability findings in the *in vitro* transcription and translation assay. This work was supported by U.S. National Science Foundation (Grant Nos. IOS-1121626, IOS-1238243 and MCB-1716913) and the U.S. Department of Agriculture, National Institute of Food and Agriculture - Agriculture and Food Research Initiative (Grant No. 2011-04015) to J.B.-S.

Figure 3.1. Rice SUB1A and SUB1C are unstable proteins when constitutively expressed in *Arabidopsis*. **a.** Western immunoblot detection of p35S:SUB1A-FLAG and p35S:SUB1C-FLAG in *Arabidopsis* Col-0 background. p35S:SUB1A-FLAG transcript accumulation is similar in **b.** Col-0 and *prt6* genetic backgrounds and **d.** in response to hypoxic stress. Transcript accumulation was normalized to *PP2A*. Mean values from two biological replicates with two technical replicates \pm standard error are depicted. SUB1A-FLAG accumulation is limited by PROTEOLYSIS 6 (PRT6), proteasomal activity, and hypoxic stress when ectopically expressed in *Arabidopsis*. **c.** Western immunoblot with anti-FLAG antiserum of anti-FLAG immunoprecipitated protein isolated from seedling extracts of wildtype (Col-0), a transgenic expressing C-terminally epitope tagged SUB1A (35S:SUB1A-FLAG) in the wildtype or *prt6* mutant (35S:SUB1A-FLAG *prt6*). **e.** Western immunoblot of anti-FLAG immunoprecipitated protein isolated from Col-0, 35S:SUB1A-FLAG. Plate-grown 7-d-old seedlings were mock treated (-) or treated with 100 μ M MG-132 (+) to inhibit proteasome activity for 2 h under normoxia (+O₂) or hypoxia (-O₂). Proteins were separated by 12% SDS-PAGE. Detection with anti-FLAG identified SUB1A protein migration at 37 and ~55 kDa. The predicted molecular mass of SUB1A-FLAG is 34.2 kDa.

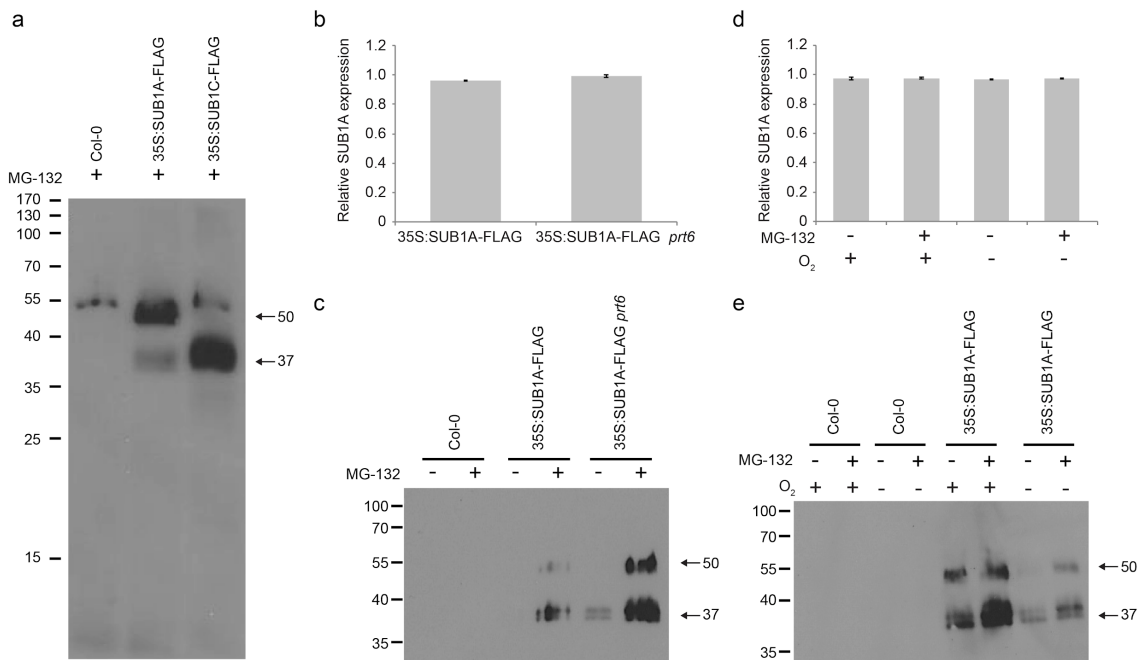


Figure 3.2. Global-scale evaluation of genomic regions bound by the ERFVII transcription factors SUB1A, SUB1C and HRE2 in *Arabidopsis* seedlings reveals a high similarity between the binding of SUB1s under non-stress (NS) and hypoxic stress (HS) conditions. t-Distributed Stochastic Neighbor Embedding (t-SNE) of chromatin immunopurification-sequencing (ChIP-seq) outputs including three ERFVII transcription factors, H2A.Z binding, Histone H3 modifications and Ser2P engagement (Chapter 2). All samples for transcription factor ChIP-seq were performed on seedlings pre-treated with MG-132 for 2 h. Samples for histone readouts were not. Genic regions bound by ectopically expressed SUB1A-FLAG and SUB1C-FLAG group under control (2NS) and hypoxic-stress conditions. Genic regions bound by C-terminally tagged HRE2 under hypoxic stress group with regions with the H3K14ac mark.

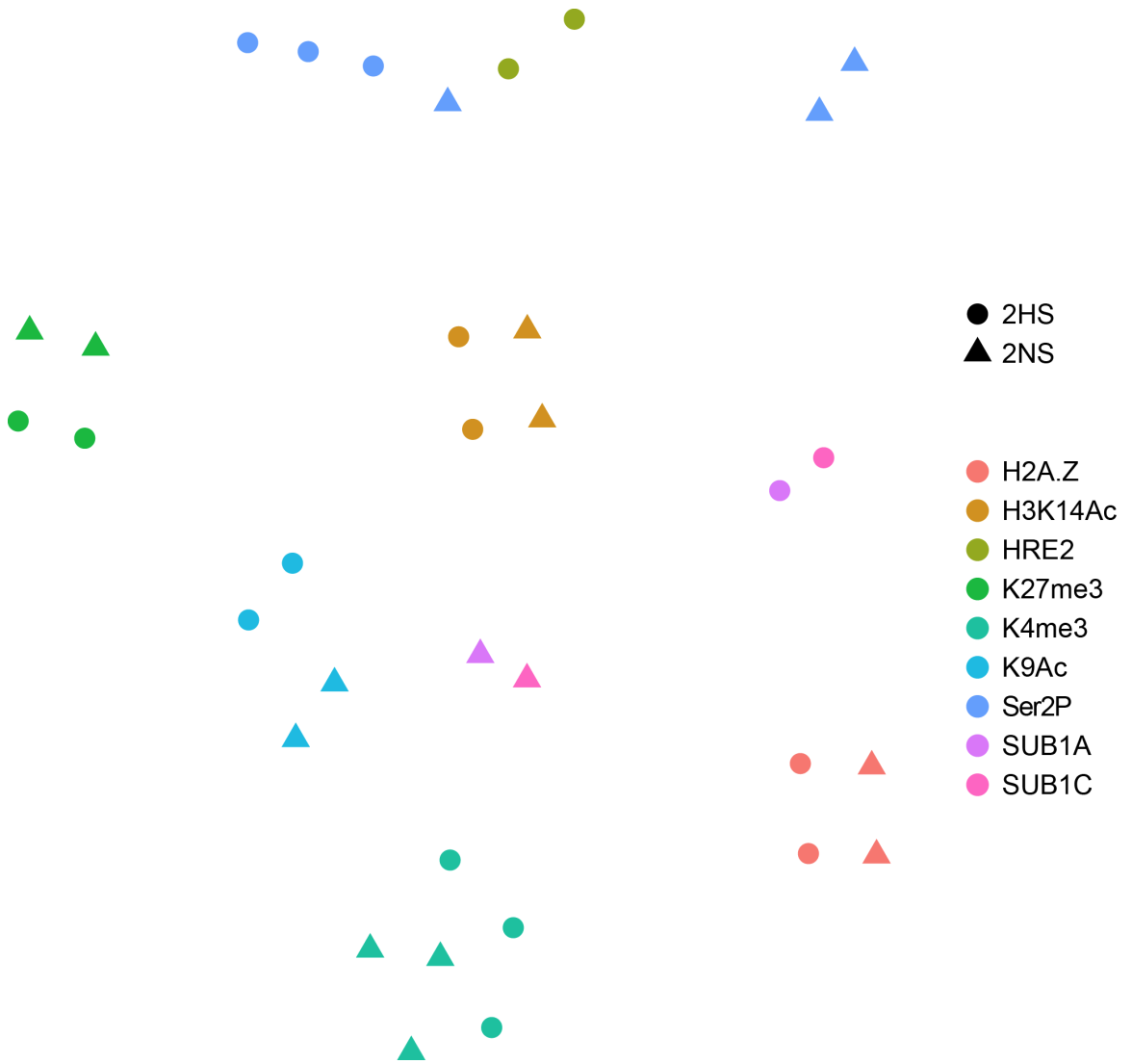


Figure 3.3. Scatterplot of reads (per kilobase per million reads; RPKM) values along gene bodies for SUB1A and SUB1C binding under **a.** non-stress (NS) and **b.** hypoxic stress (HS). RPKM values along gene bodies were compared in NS and HS for **c.** SUB1A and **d.** SUB1C. RPKM values were also compared between HRE2 and **e.** SUB1A and **f.** SUB1C. All genes with RPKM > 5 for either protein were plotted. Yellow dots correspond to the 49 core hypoxia response genes. The genome wide Pearson correlation coefficient is depicted as a blue line and indicated in black text. The Pearson correlation coefficient for the 49 HRGs is displayed as orange text.

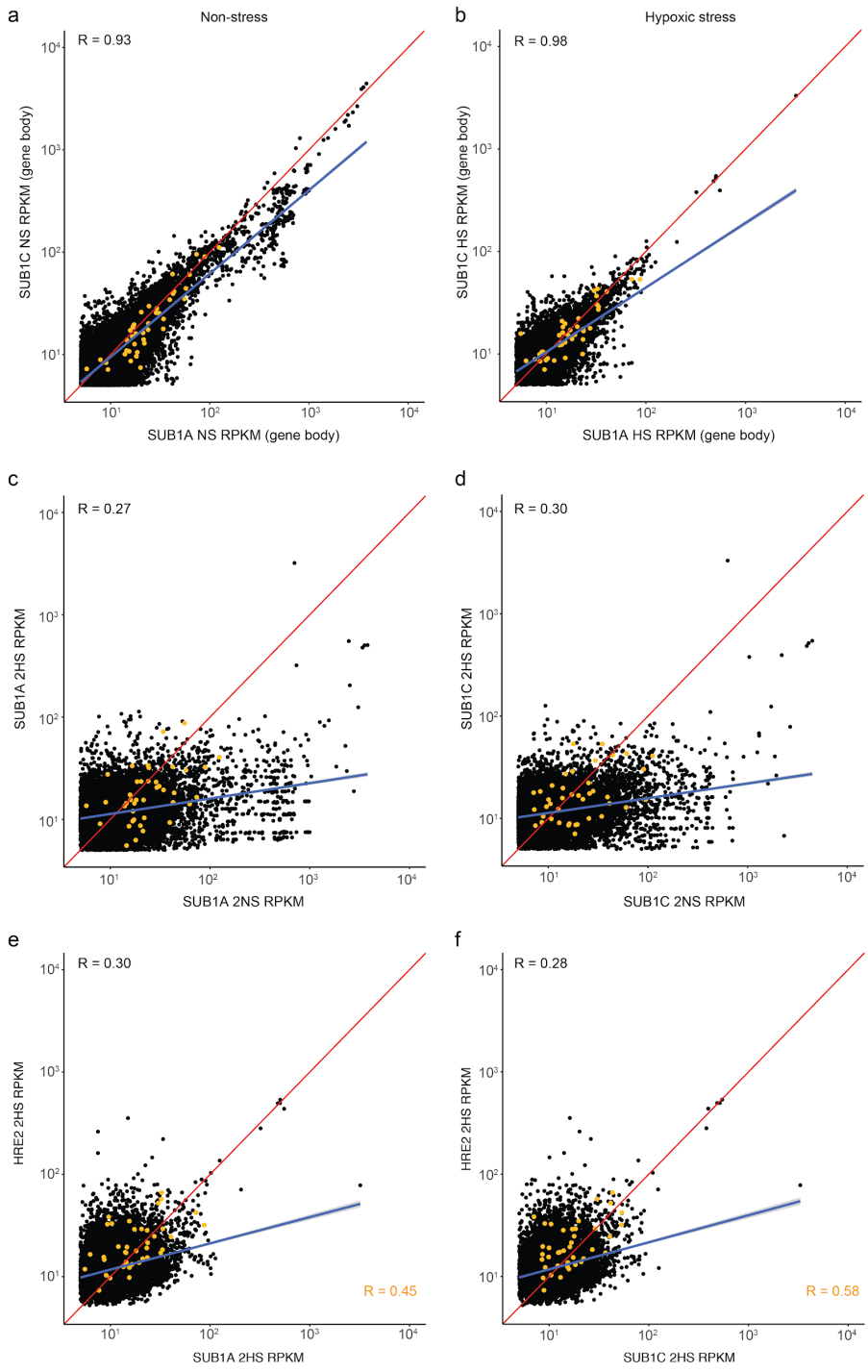


Figure 3.4. Genome-wide distribution of SUB1A and SUB1C binding sites (peaks) and read distribution is influenced by oxygen availability. **a.** Profiles of genome-wide binding of SUB1A and SUB1C to genic regions (n=27,457). Reads are plotted from 1 kb upstream of the transcription start site (TSS) to 1 kb downstream of the transcription end site (TES) of all annotated protein-coding genes. The average signal is displayed on the y-axis for each dataset. **b.** Genomic distribution of peaks identified using the peak calling software HOMER on defined genomic features for each condition (non-stress, NS; hypoxic stress, HS) and dataset (SUB1A, SUB1C, HRE2). Percentage of reads are shown relative to their position upstream or downstream of the transcription start site (TSS) as percentage values.

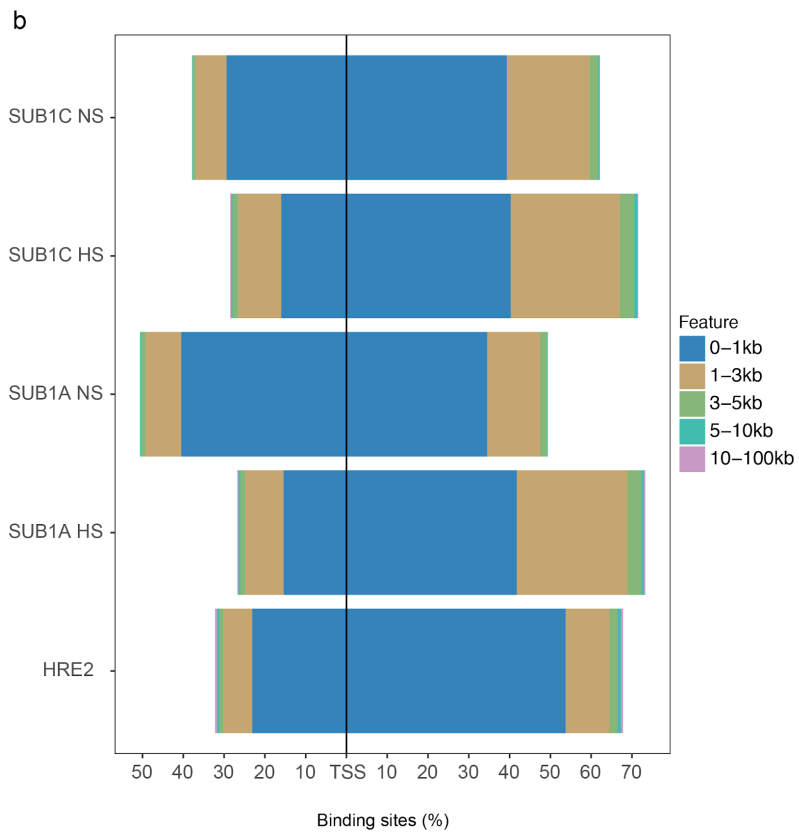
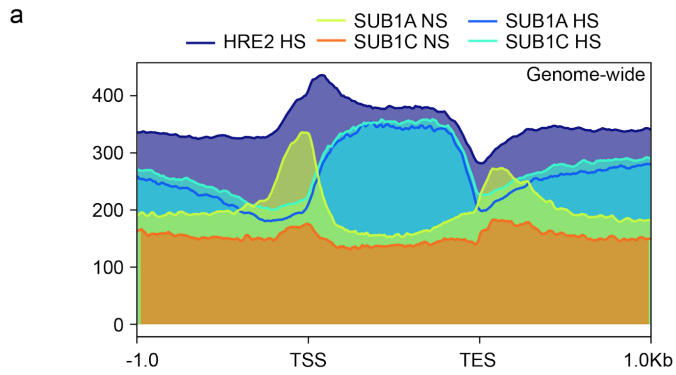


Figure 3.5. Binding profile along genic regions of three ERFVIIIs under non-stress (NS) and hypoxic stress conditions (HS) in *Arabidopsis* seedlings. Binding profiles are depicted **a.** for the core hypoxia response genes upregulated across cell-types (HRGs; n=49); **b.** for all genes coordinately upregulated by hypoxic stress based on RNAPII-Ser2P, nuclear RNA, polyA⁺ and polysome-associated RNA (co-regulated HRGs; n=216), which include 37 core HRGs; and **c.** for the significantly downregulated polyA⁺ mRNAs (n=297). Data are plotted from 1 kb upstream of the transcription start site (TSS) to 1 kb downstream of the transcription end site (TES) of all annotated protein-coding genes. Upper panel: the signal is displayed on the y-axis. Lower panel: the orange bar at the bottom of each heat map represents the transcribed region and the signal scale is indicated to the right of each heat map.

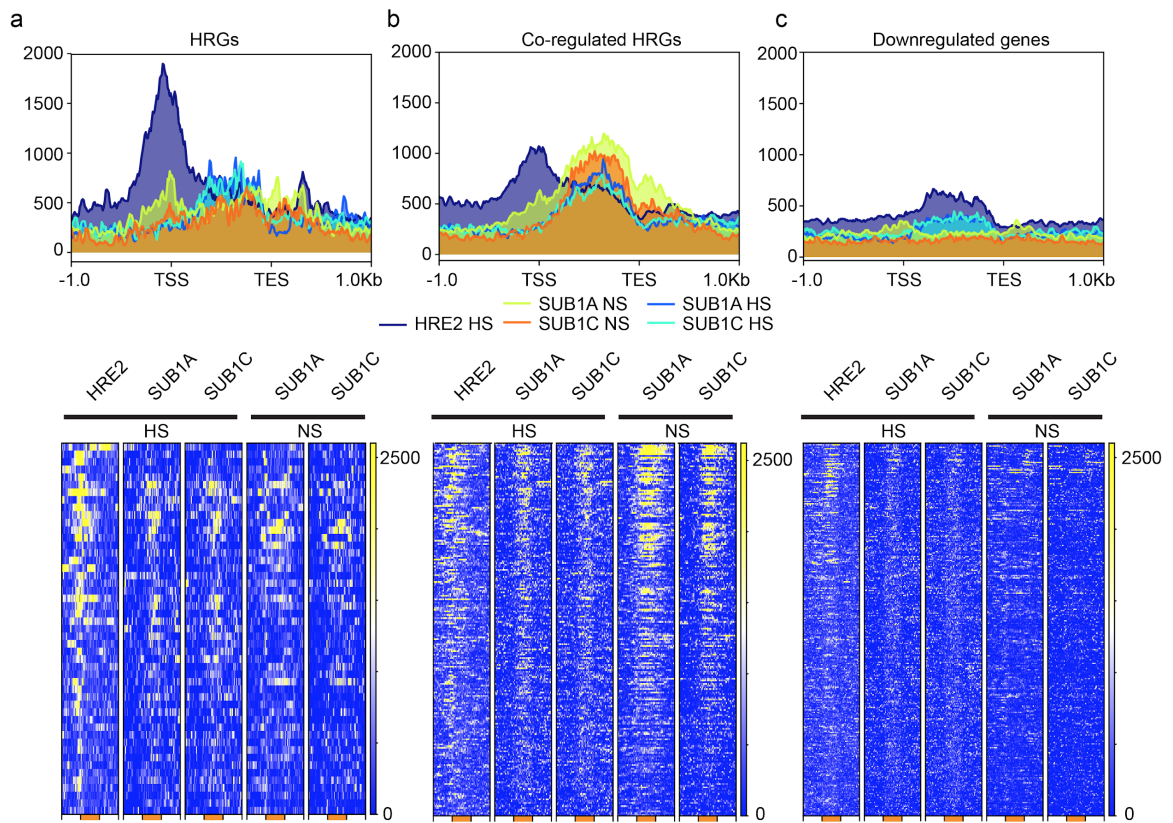
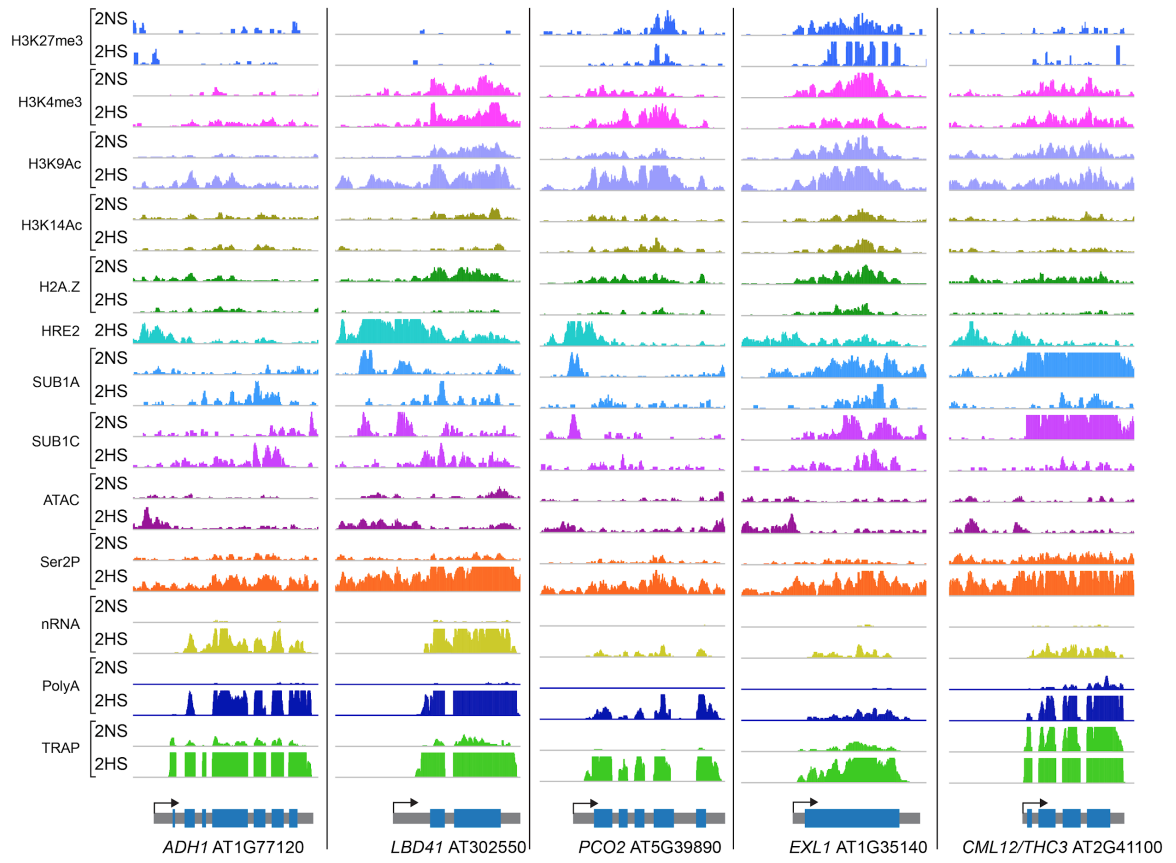


Figure 3.6. Genome browser view of normalized read coverage on selected genes for HRE2, SUB1A and SUB1C, as well as histone, RNAPII, and three distinct RNA outputs (Chapter 2) for 2NS and 2HS samples. The maximum read scale value used for chromatin and RNA outputs is the same for individual genes. Transcription unit is shown in grey with the TSS marked with an arrow.



3.7. References

1. Bailey-Serres J, Fukao T, Gibbs DJ, Holdsworth MJ, Lee SC, Licausi F, et al. Making sense of low oxygen sensing. *Trends Plant Sci.* 2012;17:129–38.
2. Voeselek LACJ, Bailey-Serres J. Flood adaptive traits and processes: an overview. *New Phytol.* 2015;206:57–73.
3. Bailey-Serres J, Voeselek LACJ. Flooding stress: acclimations and genetic diversity. *Annu Rev Plant Biol.* 2008;59:313–39.
4. Lee SC, Mustroph A, Sasidharan R, Vashisht D, Pedersen O, Oosumi T, et al. Molecular characterization of the submergence response of the *Arabidopsis thaliana* ecotype Columbia. *New Phytol.* 2011;190:457–71.
5. Vashisht D, Hesselink A, Pierik R, Ammerlaan JMH, Bailey-Serres J, Visser EJW, et al. Natural variation of submergence tolerance among *Arabidopsis thaliana* accessions. *New Phytol.* 2011;190:299–310.
6. Fukao T, Bailey-Serres J. Plant responses to hypoxia – is survival a balancing act? *Trends Plant Sci.* 2004;9:449–56.
7. Considine MJ. Oxygen, Energy, and Light Signalling Direct Meristem Fate. *Trends Plant Sci.* 2018;23:1–3.
8. Schmidt RR, Weits DA, Feulner CFJ, van Dongen JT. Oxygen Sensing and Integrative Stress Signaling in Plants. *Plant Physiol.* 2018;176:1131–42.
9. Loreti E, Valeri MC, Novi G, Perata P. Gene Regulation and Survival under Hypoxia Requires Starch Availability and Metabolism. *Plant Physiol.* 2018;176:1286–98.
10. Li F, Vierstra RD. Autophagy: a multifaceted intracellular system for bulk and selective recycling. *Trends Plant Sci.* 2012;17:526–37.
11. Kim J, Lee H, Lee HN, Kim S-H, Shin KD, Chung T. Autophagy-related proteins are required for degradation of peroxisomes in *Arabidopsis* hypocotyls during seedling growth. *Plant Cell.* 2013;25:4956–66.
12. Sakuraba Y, Lee S-H, Kim Y-S, Park OK, Hörtensteiner S, Paek N-C. Delayed degradation of chlorophylls and photosynthetic proteins in *Arabidopsis* autophagy mutants during stress-induced leaf yellowing. *J Exp Bot.* 2014;65:3915–25.

13. Hirota T, Izumi M, Wada S, Makino A, Ishida H. Vacuolar Protein Degradation via Autophagy Provides Substrates to Amino Acid Catabolic Pathways as an Adaptive Response to Sugar Starvation in *Arabidopsis thaliana*. *Plant Cell Physiol* [Internet]. 2018; Available from: <http://dx.doi.org/10.1093/pcp/pcy005>
14. Semenza GL. , and the 3 PHDs: HIF-1, O Minireview How Animal Cells Signal Hypoxia to the Nucleus. *Cell*. 2001;107:1–3.
15. Gibbs DJ, Lee SC, Isa NM, Gramuglia S, Fukao T, Bassel GW, et al. Homeostatic response to hypoxia is regulated by the N-end rule pathway in plants. *Nature*. 2011;479:415–8.
16. Licausi F, Kosmacz M, Weits DA, Giuntoli B, Giorgi FM, Voeselek LACJ, et al. Oxygen sensing in plants is mediated by an N-end rule pathway for protein destabilization. *Nature*. 2011;479:419–22.
17. Weits DA, Giuntoli B, Kosmacz M, Parlanti S, Hubberten H-M, Riegler H, et al. Plant cysteine oxidases control the oxygen-dependent branch of the N-end-rule pathway. *Nat Commun*. 2014;5:3425.
18. White MD, Klecker M, Hopkinson RJ, Weits DA, Mueller C, Naumann C, et al. Plant cysteine oxidases are dioxygenases that directly enable arginyl transferase-catalysed arginylation of N-end rule targets. *Nat Commun*. 2017;8:14690.
19. Nakano T, Suzuki K, Fujimura T, Shinshi H. Genome-wide analysis of the ERF gene family in *Arabidopsis* and rice. *Plant Physiol*. 2006;140:411–32.
20. Licausi F, Ohme-Takagi M, Perata P. APETALA2/Ethylene Responsive Factor (AP2/ERF) transcription factors: mediators of stress responses and developmental programs. *New Phytol*. 2013;199:639–49.
21. van Dongen JT, Licausi F. Oxygen sensing and signaling. *Annu Rev Plant Biol*. 2015;66:345–67.
22. Kosmacz M, Parlanti S, Schwarzländer M, Kragler F, Licausi F, Van Dongen JT. The stability and nuclear localization of the transcription factor RAP2. 12 are dynamically regulated by oxygen concentration. *Plant Cell Environ*. Wiley Online Library; 2015;38:1094–103.
23. Licausi F. Molecular elements of low-oxygen signaling in plants. *Physiol Plant*. 2013;148:1–8.

24. Bui LT, Giuntoli B, Kosmacz M, Parlanti S, Licausi F. Constitutively expressed ERF-VII transcription factors redundantly activate the core anaerobic response in *Arabidopsis thaliana*. *Plant Sci*. 2015;236:37–43.
25. Giuntoli B, Perata P. Group VII Ethylene Response Factors in *Arabidopsis*: Regulation and Physiological Roles. *Plant Physiol*. 2018;176:1143–55.
26. Voeselek LAC, Bailey-Serres J. Hypoxia and development: Air conditional. *Nat Plants*. 2015;1:15095.
27. Abbas M, Berckhan S, Rooney DJ, Gibbs DJ, Vicente Conde J, Sousa Correia C, et al. Oxygen sensing coordinates photomorphogenesis to facilitate seedling survival. *Curr Biol*. 2015;25:1483–8.
28. Paul MV, Iyer S, Amerhauser C, Lehmann M, van Dongen JT, Geigenberger P. Oxygen Sensing via the Ethylene Response Transcription Factor RAP2.12 Affects Plant Metabolism and Performance under Both Normoxia and Hypoxia. *Plant Physiol*. 2016;172:141–53.
29. Considine MJ, Diaz-Vivancos P, Kerchev P, Signorelli S, Agudelo-Romero P, Gibbs DJ, et al. Learning To Breathe: Developmental Phase Transitions in Oxygen Status. *Trends Plant Sci*. 2017;22:140–53.
30. Giuntoli B, Shukla V, Maggiorelli F, Giorgi FM, Lombardi L, Perata P, et al. Age-dependent regulation of ERF-VII transcription factor activity in *Arabidopsis thaliana*. *Plant Cell Environ* [Internet]. Wiley Online Library; 2017; Available from: <http://onlinelibrary.wiley.com/doi/10.1111/pce.13037/full>
31. Eysholdt-Derzsó E, Sauter M. Root Bending Is Antagonistically Affected by Hypoxia and ERF-Mediated Transcription via Auxin Signaling. *Plant Physiol*. 2017;175:412–23.
32. Vicente J, Mendiondo GM, Movahedi M, Peirats-Llobet M, Juan Y-T, Shen Y-Y, et al. The Cys-Arg/N-End Rule Pathway Is a General Sensor of Abiotic Stress in Flowering Plants. *Curr Biol*. 2017;27:3183–90.e4.
33. Xu K, Xu X, Fukao T, Canlas P, Maghirang-Rodriguez R, Heuer S, et al. Sub1A is an ethylene-response-factor-like gene that confers submergence tolerance to rice. *Nature*. 2006;442:705–8.
34. Fukao T, Xu K, Ronald PC, Bailey-Serres J. A variable cluster of ethylene response factor--like genes regulates metabolic and developmental acclimation responses to submergence in rice. *Plant Cell. Am Soc Plant Biol*; 2006;18:2021–34.

35. Fukao T, Bailey-Serres J. Submergence tolerance conferred by Sub1A is mediated by SLR1 and SLRL1 restriction of gibberellin responses in rice. *Proc Natl Acad Sci U S A*. 2008;105:16814–9.
36. Hattori Y, Nagai K, Furukawa S, Song X-J, Kawano R, Sakakibara H, et al. The ethylene response factors SNORKEL1 and SNORKEL2 allow rice to adapt to deep water. *Nature*. 2009;460:1026–30.
37. Kuroha T, Nagai K, Kurokawa Y, Nagamura Y, Kusano M, Yasui H, et al. eQTLs Regulating Transcript Variations Associated with Rapid Internode Elongation in Deepwater Rice. *Front Plant Sci*. 2017;8:1753.
38. Minami A, Yano K, Gamuyao R, Nagai K, Kuroha T, Ayano M, et al. Time-Course Transcriptomics Analysis Reveals Key Responses of Submerged Deepwater Rice to Flooding. *Plant Physiol*. 2018;176:3081–102.
39. Muroph A, Lee SC, Oosumi T, Zanetti ME, Yang H, Ma K, et al. Cross-kingdom comparison of transcriptomic adjustments to low-oxygen stress highlights conserved and plant-specific responses. *Plant Physiol*. 2010;152:1484–500.
40. Fukao T, Yeung E, Bailey-Serres J. The submergence tolerance gene SUB1A delays leaf senescence under prolonged darkness through hormonal regulation in rice. *Plant Physiol*. 2012;160:1795–807.
41. Locke AM, Barding GA Jr, Sathnur S, Larive CK, Bailey-Serres J. Rice SUB1A constrains remodelling of the transcriptome and metabolome during submergence to facilitate post-submergence recovery. *Plant Cell Environ*. Wiley Online Library; 2018;41:721–36.
42. Peña-Castro JM, van Zanten M, Lee SC, Patel MR, Voesenek LAJC, Fukao T, et al. Expression of rice SUB1A and SUB1C transcription factors in *Arabidopsis* uncovers flowering inhibition as a submergence tolerance mechanism. *Plant J*. Blackwell Publishing Ltd; 2011;67:434–46.
43. Giuntoli B, Lee SC, Licausi F, Kosmacz M, Oosumi T, van Dongen JT, et al. A trihelix DNA binding protein counterbalances hypoxia-responsive transcriptional activation in *Arabidopsis*. *PLoS Biol*. 2014;12:e1001950.
44. Giuntoli B, Licausi F, van Veen H, Perata P. Functional Balancing of the Hypoxia Regulators RAP2.12 and HRA1 Takes Place *in vivo* in *Arabidopsis thaliana* Plants. *Front Plant Sci*. 2017;8:591.

45. Gasch P, Fundinger M, Müller JT, Lee T, Bailey-Serres J, Mustroph A. Redundant ERF-VII transcription factors bind an evolutionarily-conserved cis-motif to regulate hypoxia-responsive gene expression in *Arabidopsis*. *Plant Cell* [Internet]. American Society of Plant Biologists; 2015; Available from: <http://www.plantcell.org/content/early/2015/12/14/tpc.15.00866>
46. Marín-de la Rosa N, Sotillo B, Miskolczi P, Gibbs DJ, Vicente J, Carbonero P, et al. Large-scale identification of gibberellin-related transcription factors defines group VII ETHYLENE RESPONSE FACTORS as functional DELLA partners. *Plant Physiol.* 2014;166:1022–32.
47. Gibbs DJ, Md Isa N, Movahedi M, Lozano-Juste J, Mendiondo GM, Berckhan S, et al. Nitric oxide sensing in plants is mediated by proteolytic control of group VII ERF transcription factors. *Mol Cell.* 2014;53:369–79.
48. Schmidl C, Rendeiro AF, Sheffield NC, Bock C. ChIPmentation: fast, robust, low-input ChIP-seq for histones and transcription factors. *Nat Methods.* 2015;12:963–5.
49. Mustroph A, Zanetti ME, Jang CJH, Holtan HE, Repetti PP, Galbraith DW, et al. Profiling translomes of discrete cell populations resolves altered cellular priorities during hypoxia in *Arabidopsis*. *Proc Natl Acad Sci U S A.* 2009;106:18843–8.
50. Brinton EK. Flooding Responses in *Zea mays* ssp. *mays*: Genetic Variation and Molecular Characterization. University of California, Riverside; 2015.
51. Singh P, Sinha AK. A Positive Feedback Loop Governed by SUB1A1 Interaction with MITOGEN-ACTIVATED PROTEIN KINASE3 Imparts Submergence Tolerance in Rice. *Plant Cell.* 2016;28:1127–43.
52. Seo Y-S, Chern M, Bartley LE, Han M, Jung K-H, Lee I, et al. Towards establishment of a rice stress response interactome. *PLoS Genet.* 2011;7:e1002020.
53. Yoo YD, Mun SR, Ji CH, Sung KW, Kang KY, Heo AJ, et al. N-terminal arginylation generates a bimodal degron that modulates autophagic proteolysis. *Proc Natl Acad Sci U S A* [Internet]. 2018; Available from: <http://dx.doi.org/10.1073/pnas.1719110115>
54. Branco-Price C, Kaiser KA, Jang CJH, Larive CK, Bailey-Serres J. Selective mRNA translation coordinates energetic and metabolic adjustments to cellular oxygen deprivation and reoxygenation in *Arabidopsis thaliana*. *Plant J. Wiley Online Library;* 2008;56:743–55.

55. Sorenson R, Bailey-Serres J. Selective mRNA sequestration by OLIGOURIDYLATE-BINDING PROTEIN 1 contributes to translational control during hypoxia in Arabidopsis. *Proc Natl Acad Sci U S A*. 2014;111:2373–8.
56. Juntawong P, Girke T, Bazin J, Bailey-Serres J. Translational dynamics revealed by genome-wide profiling of ribosome footprints in Arabidopsis. *Proc Natl Acad Sci U S A*. 2014;111:E203–12.
57. Holwerda SJB, de Laat W. CTCF: the protein, the binding partners, the binding sites and their chromatin loops. *Philos Trans R Soc Lond B Biol Sci*. 2013;368:20120369.
58. Lee B-K, Bhinge AA, Battenhouse A, McDaniel RM, Liu Z, Song L, et al. Cell-type specific and combinatorial usage of diverse transcription factors revealed by genome-wide binding studies in multiple human cells. *Genome Res*. 2012;22:9–24.
59. Hohenauer T, Moore AW. The Prdm family: expanding roles in stem cells and development. *Development*. 2012;139:2267–82.
60. Galli GG, Honnens de Lichtenberg K, Carrara M, Hans W, Wuelling M, Mentz B, et al. Prdm5 regulates collagen gene transcription by association with RNA polymerase II in developing bone. *PLoS Genet*. 2012;8:e1002711.
61. Buck MJ, Raaijmakers LM, Ramakrishnan S, Wang D, Valiyaparambil S, Liu S, et al. Alterations in chromatin accessibility and DNA methylation in clear cell renal cell carcinoma. *Oncogene*. 2014;33:4961–5.
62. Chervona Y, Costa M. The control of histone methylation and gene expression by oxidative stress, hypoxia, and metals. *Free Radic Biol Med*. 2012;53:1041–7.
63. Boyer LA, Latek RR, Peterson CL. The SANT domain: a unique histone-tail-binding module? *Nat Rev Mol Cell Biol*. 2004;5:158–63.
64. Singh N, Dang TTM, Vergara GV, Pandey DM, Sanchez D, Neeraja CN, et al. Molecular marker survey and expression analyses of the rice submergence-tolerance gene SUB1A. *Theor Appl Genet*. 2010;121:1441–53.
65. Fukao T, Yeung E, Bailey-Serres J. The Submergence Tolerance Regulator SUB1A Mediates Crosstalk between Submergence and Drought Tolerance in Rice. *Plant Cell*. 2011;23:412–27.

66. Branco-Price C, Kaiser KA, Jang CJH, Larive CK, Bailey-Serres J. Selective mRNA translation coordinates energetic and metabolic adjustments to cellular oxygen deprivation and reoxygenation in *Arabidopsis thaliana*. *Plant J*. 2008;56:743–55.
67. Bradford MM. A rapid and sensitive method for the quantitation of microgram quantities of protein utilizing the principle of protein-dye binding. *Anal Biochem*. 1976;72:248–54.
68. Deal RB, Henikoff S. A simple method for gene expression and chromatin profiling of individual cell types within a tissue. *Dev Cell*. 2010;18:1030–40.
69. Schmidl C, Rendeiro AF, Sheffield NC, Bock C. ChIPmentation: fast, robust, low-input ChIP-seq for histones and transcription factors. *Nat Methods*. 2015;12:963–5.
70. Lefrançois P, Euskirchen GM, Auerbach RK, Rozowsky J, Gibson T, Yellman CM, et al. Efficient yeast ChIP-Seq using multiplex short-read DNA sequencing. *BMC Genomics*. 2009;10:37.
71. Saleh A, Alvarez-Venegas R, Avramova Z. An efficient chromatin immunoprecipitation (ChIP) protocol for studying histone modifications in *Arabidopsis* plants. *Nat Protoc*. 2008;3:1018–25.

Chapter 4

General conclusions

A rapid or severe decline in cellular oxygen content (hypoxia) presents an abiotic stress that drastically limits the efficiency in cellular ATP production through aerobic respiration and limits plant growth and ultimately challenges survival. Hypoxia can be a consequence of changes in the external environment, such as flooding, or intrinsic to a developmental zone such as a meristem with high metabolic activity. In response to external hypoxia, the progression to controlled anaerobic metabolism is associated with stabilization of group VII ethylene responsive factor (ERFVII) transcription factors associated with upregulation of genes encoding enzymes required for anaerobic metabolism (*i.e.*, ADH1, PDC1), as well as proteins associated with curtailment of ERFVII activity (PLANT CYSTEINE OXIDASE 1/2 (PCO1/2), HYPOXIA RESPONSE ATTENUATOR1 (HRA1)). Whereas HRA1 restricts transcriptional activation by ERFVIIs, the PCOs are oxygen-dependent enzymes that catalyze the modification of ERFVIIs that leads to their turnover by the proteasome [1,2]. Hypoxia is also a component of normal plant development, acting as a cue to stabilize constitutively synthesized ERFVIIs that function in apical hook maintenance, de-etiolation, root bending, and likely other processes in *Arabidopsis* [3,4]. The process of ERFVII stabilization/destabilization by low oxygen availability may be the plant's [2,5–7].

Plant strategies to minimize energy consumption to endure periods of energy deficiency, such as transient hypoxia, include selective mRNA translation. *Arabidopsis* seedlings display a ~50% reduction in cellular ATP content that is matched by a similar reduction in translational activity under hypoxia relative to non-stress conditions, as mRNA translation is an energy intensive process [8,9]. This is likely an indirect response to hypoxia mediated through the low energy signaling network involving the conserved sucrose-non-fermenting-1-related protein kinase-1 and target of rapamycin kinases [10]. Yet, the translational response does not affect all mRNAs similarly. Translation of most of the highly hypoxia-induced mRNAs is maintained whereas many mRNAs are routed to translationally inactive cytoplasmic ribonucleoprotein complexes until reaeration. Hypoxic stress also promotes intron retention and modulates the functional role of upstream open reading frames on the translation of downstream coding regions [9]. These findings of post-transcriptional regulation [11], particularly the pronounced homodirectional elevation and selective translation of the 49 core hypoxia responsive gene (HRG) mRNAs, led to the hypothesis that nuclear processes may predispose HRGs for effective expression from transcription through translation. This hypothesis was a major motivation for this dissertation research.

To investigate this hypothesis at the global scale, regulation within the nucleus was profiled at the level of chromatin and nuclear RNA of *Arabidopsis thaliana* seedlings (Chapter 2), taking advantage of a number of high-resolution

next-generation sequencing technologies (Chapter 1). From these experiments, it was determined that hypoxia rapidly and reversibly modulates regions of chromatin that are not bound by nucleosomes. These accessible regions were predominantly 5' and 3' of active transcription units. Hypoxia also promotes modification of the tails of Histone H3, alterations in the presence of the Histone H2 variant H2A.Z, and the binding of at least one of the five *Arabidopsis* ERFVIs. Additionally, hypoxia influenced elongation of RNA Polymerase II (RNAPII), assayed by the presence of the elongating Ser2P modified RNAPII to transcribed regions, and the detection of protein-coding gene transcripts in the nucleus. Based on the mapping of these readouts to genes, the nuclear RNA included nascent pre-mRNA undergoing transcription and co-transcriptional processing to fully processed mRNAs. This approach recognized transcripts that were nuclear-enriched or nuclear-depleted, as compared to the polyadenylated transcriptome. The results revealed that multifaceted gene regulatory responses, from chromatin to translation, occurs in response to hypoxia in *Arabidopsis*. In revelation of these additional levels of gene regulation, additional processes can be investigated to yield a more comprehensive roadmap of gene regulation.

Chromatin regulation occurs via the activity of chromatin modifying enzymes and complexes. Based on the findings that RNAPII-Ser2P association is correlated with increased H3K9Ac and loss of H2A.Z in response to hypoxia, chromatin modifying complexes must be recruited to hypoxia regulated genes. Similar to HIF1 α regulation, it can be hypothesized that ERFVIs similarly interact

with chromatin modifying enzymes to facilitate transcriptional activation as well as epigenetic modifications. It has been reported that ERFVIIIs form homo- and hetero-dimers (Ming Che Shih, personal correspondence). Various ERFVII dimer configurations could allow for specific interactions between distinct chromatin modifying complexes. The finding that ERFVII HRE2 binding is associated within the promoter regions of hypoxia induced genes, whereas HRE2 binding occurs within gene bodies of hypoxia downregulated genes may support this interaction of differential ERFVII activity (Chapter 3, Fig. 5). Based on these findings, it can be hypothesized that ERFVIIIs can transiently lead to transcriptional activation via promoter interaction but may have long lasting regulatory effects via the recruitment of chromatin modifying enzymes to target genes. An alternative hypothesis is that ERFVII binding within gene bodies reflects interaction with RNAPII. If this is the case then these proteins could be a talisman that fosters post-transcriptional regulation that leads to efficient export and ultimately selection for translation.

The work from this study additionally demonstrated that global chromatin accessibility was affected in response to hypoxia. In response to 2 h hypoxic stress (2HS), a general increase in chromatin accessibility was observed in genic regions near the TSS and TES, with a greater increase observed following 1 h re-oxygenation (1R) following 2HS. In response to hypoxia, a global increase in chromatin accessibility, if associated with productive transcription, would be counterproductive to the energy conservation processes seen for translation. A

possible explanation for the increase in chromatin accessibility is the priming of genes necessary for re-oxygenation and recovery. This is supported by the finding that subsets of genes with unchanged polyadenylated mRNA abundance are regulated within the nucleus at the levels of chromatin accessibility, RNAPII-Ser2P association, and nRNA abundance (Chapter 2, Fig. 4a, Supplemental Fig. 4; Clusters 6, 7). Another subset of genes is associated with increased RNAPII-Ser2P association but unchanged nRNA and polyadenylated RNA accumulation (Cluster 9). The poising (or priming) of recovery-specific genes for rapid transcriptional activation can further be supported by the identification of genes specifically upregulated in response to re-oxygenation, with limited dynamics observed in non-stress (2NS) and 2HS (Supplemental Fig. 8). Chromatin accessibility was additionally regulated between the end of the day and an one hour extension of night in non-stress conditions (2NS and 9NS). This is consistent with the observation that global chromatin accessibility is circadian regulated in mammalian systems [12]. Interestingly, the comparison of 9NS to 9HS revealed that prolonged hypoxia resulted in decreased chromatin accessibility. The activity of chromatin remodeling enzymes is ATP dependent, thus it can be hypothesized that the reduced chromatin accessibility is due to reduced activity of these complexes as ATP becomes extremely limited under prolonged hypoxic stress as the plant nears lethality.

This dissertation also revealed that active transcription, nuclear RNAs and the polyadenylated transcriptome are distinctly regulated under control and

stress conditions. Profiling of RNAP-Ser2P association and nRNA revealed aspects of gene regulation not apparent in the transcriptome. Despite the close relatedness of RNAPII-Ser2P association and snRNA accumulation, subsets of genes displayed distinct regulation between these two readouts of nuclear activity. For example, RNAPII-Ser2P engagement was observed without a concomitant increase in nRNA, and conversely nRNA accumulation with no apparent RNAPII-Ser2P association. It can be hypothesized that polymerase stalling and nuclear retention of mRNAs are responsible for the observed differences between RNAPII-Ser2P and nRNA, respectively. A deeper investigation of RNAPII activity may reveal polymerase dynamics modulated under hypoxic stress. Examination of other RNAPII CTD phospho-isoforms, including Ser5P, Tyr1P, and Thr4P may yield additional insights related to transcriptional initiation and repression, or promotion of transcriptional termination, respectively, that may be associated with the observed distinctions between RNAPII-Ser2P and nRNA [13]. Further dissection of transcription can be achieved through global nuclear run-on sequencing (GRO-seq). GRO-seq entails nuclear run-on transcription of isolated nuclei with use of labeled nucleotides to investigate active transcription and identify nascently transcribed RNAs. When applied to *Arabidopsis*, GRO-seq revealed a correlation between nascent transcription and steady state mRNA accumulation ($R=0.57$) [14]. A comparison between GRO-seq and the RNAPII-Ser2P and nRNA datasets generated in this study may provide greater resolution between RNAPII

engagement and termination of transcription. Yet, even with these technologies it may be difficult to resolve distinctions in elongation rate.

There remains opportunities for identification of other nuclear regulatory processes that contribute to hypoxic responses. It has been demonstrated that noncanonical alternative polyadenylation is enhanced by hypoxic stress in *Arabidopsis* [15]. The observation that alternative polyadenylation was associated with changes in mRNA stability and translation suggests that this mechanism functions as an additional level of gene regulation. Alternative splicing and retention of introns is also active during hypoxia [9]. The data generated in this study provide the opportunity to evaluate intron retention in the nRNA, polyadenylated and polysomal RNA populations under nonstress and hypoxic conditions. Might intron retention be associated with nuclear retention of pre-mRNAs prior to re-oxygenation or is primarily driving mRNA turnover via nonsense mediated decay? In mammalian cells, intron retention in response to hypoxia function to inhibit translation [16]. Thus, the combinatorial role of alternative splicing and noncanonical polyadenylation may function in concert to finely regulate hypoxia responses. Although not as well studied, there is evidence for a regulatory role of the three-dimensional organization of chromatin in gene regulation in *Arabidopsis* [17,18]. Chromosome territories within the nucleus can impact the binding of TFs and transcriptional activation of target genes. Changes in chromosomal organization occurs in response to abiotic

stresses in *Arabidopsis*, and thus may be similarly affected in response to hypoxia [19,20].

The presence of evolutionarily conserved TFs necessary for hypoxic responses may hint at the presence of additional mechanisms that facilitate successful hypoxia responses. The identification of enhanced translation of subsets of mRNAs in hypoxic stress with unchanging mRNA levels, in spite of ~50% global reduction in translation, demonstrates that genes associated with hypoxia responses are regulated distinctly from global dynamics. Thus, there remains the potential for TF specific responses that promotes efficient transcription and ultimately translation of target genes in response to stress. In yeast, it was demonstrated that in response to starvation and heat stress, promoter sequence and TF specificity allows for efficient transcription, rapid nuclear export, and efficient translation of stress responsive genes [21,22]. Additionally, the rate of transcription has a demonstrated role in mRNA regulation and fate [23].

Based on the findings of this dissertation, support for the hypothesis that transcriptional activation can be coupled with efficient post-transcriptional processes leading to productive translation under hypoxia is exemplified by the 216 co-regulated HRGs. Strong transcriptional to translational regulation was characterized by increased chromatin accessibility, enhanced H3K9Ac, and reduced H2A.Z association. Over 25% (58) of the co-regulated genes were associated with HRE2 binding within the promoter region. Enrichment of the

hypoxia responsive promoter element (HRPE) or GCC box within the promoters of the most highly co-regulated genes may be important for efficient transcription and translation. Further dissection of the hypothesized role of *cis*-element and TF specificity in efficient gene regulation could utilize synthetic promoter elements (i.e. 3xHRPE or 3xGCC box) in transgenic plants of distinct genotypes (i.e., mutant or overexpression of specific TFs) to investigate transcriptional activity and ribosome association. An outstanding question is whether the rice SUB1A and SNORKEL1/2 ERFs, which engender effective strategies for flooding tolerance, mediate epigenetic as well as transcriptional regulation. Altogether, findings of this dissertation identified intermediary gene regulatory processes within the nucleus that function in hypoxia responses. Novel distinctions in ERFVII stability and genome-wide binding dynamics were described.

Figure 4.1. Overview of histone modifications and the histone variant H2A.Z in response to short term hypoxic stress in *Arabidopsis*. The abundance of three histone modifications (H3K4me3, H3K9Ac, and H3K14Ac), and the histone variant H2A.Z along the gene unit is depicted for three subsets of genes: genes induced by hypoxia with increased polyA mRNA accumulation, poised genes induced within the nucleus with unchanged polyA mRNA accumulation, and downregulated genes with decreased polyA mRNA accumulation in response to hypoxia.

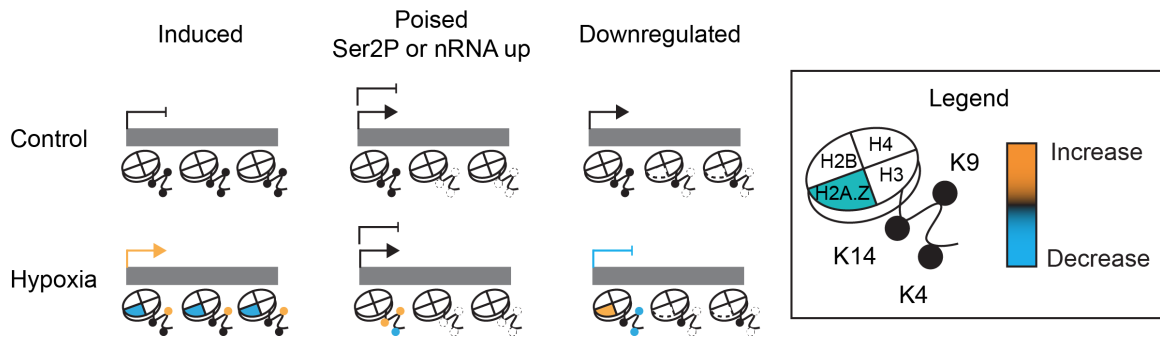
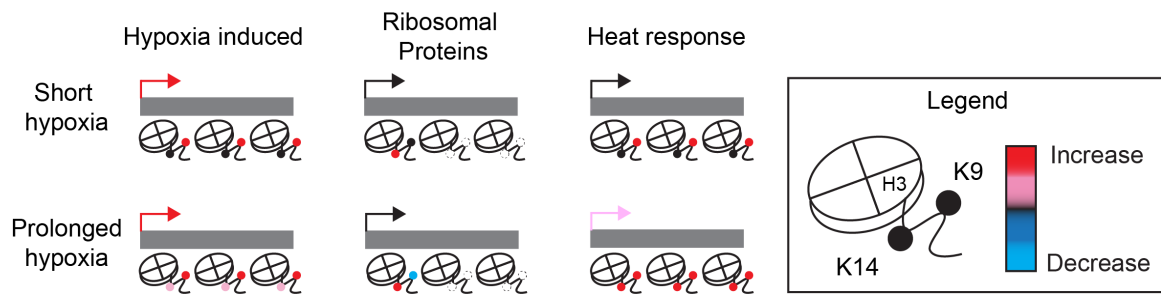


Figure 4.2. Overview of H3K9Ac and H3K14Ac dynamics in response to short and long term hypoxic stress in *Arabidopsis*. The abundance of H3K9Ac and H3K14Ac along the gene unit is depicted for three subsets of genes: genes induced by hypoxia with increased polyA mRNA accumulation, constitutively expressed Ribosomal proteins with unchanged polyA mRNA accumulation, and genes related to heat stress with unchanged polyA mRNA accumulation in response to short term hypoxia.



4.1. References

1. Weits DA, Giuntoli B, Kosmacz M, Parlanti S, Hubberten H-M, Riegler H, et al. Plant cysteine oxidases control the oxygen-dependent branch of the N-end-rule pathway. *Nat Commun.* 2014;5:3425.
2. White MD, Klecker M, Hopkinson RJ, Weits DA, Mueller C, Naumann C, et al. Plant cysteine oxidases are dioxygenases that directly enable arginyl transferase-catalysed arginylation of N-end rule targets. *Nat Commun.* 2017;8:14690.
3. Abbas M, Berckhan S, Rooney DJ, Gibbs DJ, Vicente Conde J, Sousa Correia C, et al. Oxygen sensing coordinates photomorphogenesis to facilitate seedling survival. *Curr Biol.* 2015;25:1483–8.
4. Eysholdt-Derzsó E, Sauter M. Root Bending Is Antagonistically Affected by Hypoxia and ERF-Mediated Transcription via Auxin Signaling. *Plant Physiol.* 2017;175:412–23.
5. Bailey-Serres J, Fukao T, Gibbs DJ, Holdsworth MJ, Lee SC, Licausi F, et al. Making sense of low oxygen sensing. *Trends Plant Sci.* 2012;17:129–38.
6. Kosmacz M, Parlanti S, Schwarzländer M, Kragler F, Licausi F, Van Dongen JT. The stability and nuclear localization of the transcription factor RAP2. 12 are dynamically regulated by oxygen concentration. *Plant Cell Environ. Wiley Online Library;* 2015;38:1094–103.
7. van Dongen JT, Licausi F. Oxygen sensing and signaling. *Annu Rev Plant Biol.* 2015;66:345–67.
8. Branco-Price C, Kaiser KA, Jang CJH, Larive CK, Bailey-Serres J. Selective mRNA translation coordinates energetic and metabolic adjustments to cellular oxygen deprivation and reoxygenation in *Arabidopsis thaliana*. *Plant J. Wiley Online Library;* 2008;56:743–55.
9. Juntawong P, Girke T, Bazin J, Bailey-Serres J. Translational dynamics revealed by genome-wide profiling of ribosome footprints in *Arabidopsis*. *Proc Natl Acad Sci U S A.* 2014;111:E203–12.
10. Tome F, Nägele T, Adamo M, Garg A, Marco-Illorca C, Nukarinen E, et al. The Low Energy Signaling Network. 2015.
11. Sorenson R, Bailey-Serres J. Selective mRNA Translation Tailors Low Oxygen Energetics. In: van Dongen JT, Licausi F, editors. *Low-Oxygen Stress in Plants: Oxygen Sensing and Adaptive Responses to Hypoxia.* Vienna: Springer Vienna; 2014. p. 95–115.

12. Sobel JA, Krier I, Andersin T, Raghav S, Canella D, Gilardi F, et al. Transcriptional regulatory logic of the diurnal cycle in the mouse liver. *PLoS Biol.* 2017;15:e2001069.
13. Hajheidari M, Koncz C, Eick D. Emerging roles for RNA polymerase II CTD in *Arabidopsis*. *Trends Plant Sci.* 2013;18:633–43.
14. Hetzel J, Duttke SH, Benner C, Chory J. Nascent RNA sequencing reveals distinct features in plant transcription. *Proceedings of the National Academy of Sciences.* 2016;113:12316–21.
15. de Lorenzo L, Sorenson R, Bailey-Serres J, Hunt AG. Noncanonical Alternative Polyadenylation Contributes to Gene Regulation in Response to Hypoxia. *Plant Cell* [Internet]. 2017; Available from: <http://dx.doi.org/10.1105/tpc.16.00746>
16. Brady LK, Wang H, Radens CM, Bi Y, Radovich M, Maity A, et al. Transcriptome analysis of hypoxic cancer cells uncovers intron retention in EIF2B5 as a mechanism to inhibit translation. *PLoS Biol.* 2017;15:e2002623.
17. Liu C, Weigel D. Chromatin in 3D: progress and prospects for plants. *Genome Biol.* 2015;16:170.
18. Sotelo-Silveira M, Chávez Montes RA, Sotelo-Silveira JR, Marsch-Martínez N, de Folter S. Entering the Next Dimension: Plant Genomes in 3D. *Trends Plant Sci* [Internet]. 2018; Available from: <http://dx.doi.org/10.1016/j.tplants.2018.03.014>
19. Li L, Lyu X, Hou C, Takenaka N, Nguyen HQ, Ong C-T, et al. Widespread rearrangement of 3D chromatin organization underlies polycomb-mediated stress-induced silencing. *Mol Cell.* 2015;58:216–31.
20. Probst AV, Mittelsten Scheid O. Stress-induced structural changes in plant chromatin. *Curr Opin Plant Biol.* 2015;27:8–16.
21. Zid BM, O’Shea EK. Promoter sequences direct cytoplasmic localization and translation of mRNAs during starvation in yeast. *Nature.* 2014;514:117–21.
22. Zander G, Hackmann A, Bender L, Becker D, Lingner T, Salinas G, et al. mRNA quality control is bypassed for immediate export of stress-responsive transcripts. *Nature* [Internet]. 2016; Available from: <http://dx.doi.org/10.1038/nature20572>
23. Danko CG, Hah N, Luo X, Martins AL, Core L, Lis JT, et al. Signaling pathways differentially affect RNA polymerase II initiation, pausing, and elongation rate in cells. *Mol Cell.* 2013;50:212–22.